

STRUCTURAL GEOLOGY OF THE SAN ANDREAS FAULT ZONE AT MIDDLE
MOUNTAIN, NEAR PARKFIELD, CENTRAL CALIFORNIA

by

Maurits Thayer

A Thesis Presented in Partial Fulfillment
of the Requirements for the Degree
Master of Science

ARIZONA STATE UNIVERSITY

May 2006

STRUCTURAL GEOLOGY OF THE SAN ANDREAS FAULT ZONE AT MIDDLE
MOUNTAIN, NEAR PARKFIELD, CENTRAL CALIFORNIA

by

Maurits Thayer

has been approved

March 2006

APPROVED:

_____, Chair

Supervisory Committee

ACCEPTED:

Department Chair

Dean, Division of Graduate Studies

ABSTRACT

Middle Mountain near Parkfield, CA exposes an important record of late Cenozoic evolution of the San Andreas fault (SAF) system. Detailed geologic field mapping defines the shallow structure of this active fault zone, and the resulting geometric relationships of the rock units provide insights into fault zone behavior. En echelon folds and faults deform the southwestern side, whereas SAF-parallel reverse faults and folds cut and bend the northeastern terrain. The fault zone becomes progressively wider with time. A flower structure model does not adequately characterize the shallow structure of Middle Mountain. Three reverse faults on the southwestern side strike nearly perpendicular to the SAF and probably are a manifestation of compression induced by a southwest-dipping SAF near the center of the field area. The SAF trace has migrated 2.9 kilometers northeastward through the field area. Two differentially active earthquake rupture traces along one stretch of the SAF may explain the transfer of rocks from the southwestern to the northeastern side. Uplift of Middle Mountain probably results from a complex combination of a restraining bend in SAF strike, restraining bend in SAF dip, slip along transverse faults, and upward cataclastic flow of rock units. Entombed within Pliocene sediments northeast of the SAF are flat-lying blocks of marble and granite that have a southwestern provenance and are likely large landslides that were detached from the southwestern side and transported eastward across the SAF into a low-lying elongate basin. The structural model developed for Middle Mountain can serve as an analog for pop-up oilfields. The geologic history of the area illustrates a complex interaction of tectonism and sedimentation in a place that has been undergoing simple shear deformation since the mid-Miocene.

ACKNOWLEDGMENTS

I would like to take this opportunity to thank and acknowledge people who have had a profound impact on my life and are partly responsible for the work herein. My family essentially molded me into the person I am today. My oldest brother Thorfinn served as my first role model in life and illustrated how intensity can drive a person. My middle brother Nicholas has served as both sparring partner and fiercest ally. My sister Gudrid has been my most ardent supporter and primary disciplinarian. All three are my best buds. I would like to thank my parents for instilling self-reliance and independence in an environment with plenty of room to roam. I would also like to thank my adopted family members Gerry, Ruby, and Charlie from Wyoming. All have provided support during my time at ASU and I am grateful.

I would like to thank several scientists who have impacted this work. My advisor Ramon Arrowsmith, who had the objectives of the research already conceived and outlined when I arrived at ASU in the Fall of 2003. He invariably made time in his hectic schedule to discuss the progression of my research and enthusiastically provided direction. His positive energy is truly amazing. I thank Paul Knauth for serving on my committee and teaching the most interesting geology class I have ever taken. His extensive knowledge of the earth's history and processes take on a movie-like feel during his lectures. I thank Steve Reynolds for signing up to serve on my committee at the last second and being an outstanding teacher of western Cordilleran geology. I thoroughly enjoy Steve's geologic discussions, and I do believe Steve has the best laugh in the world. I thank Steve Hickman of the USGS, Naomi Bonness of Stanford, and Sarah Draper from Utah State University for their collaboration regarding SAFOD research. I

thank Annia Fayon from the University of Minnesota for collaboration regarding present and future apatite fission-track dating of granitic rocks in my field area. Lastly, I would like to thank Art Snoke, Steve Holbrook, and Charlie Angevine from the University of Wyoming for instruction and inspiration during my undergraduate years.

I would like to thank all the Parkfield, CA landowners who granted me access to map on their land. These include the Jack Varian family, Teddy Gilbert, the Horwedel family, Dwayne Hammond, Jim Batson, the Robertson family, Sandra Santos, the Gregory family, the Thomason family, the Moore family, and the Kester family.

Several graduate students at ASU deserve a thank you. Chris Crosby and Jessica Block provided invaluable assistance regarding ARC GIS software. Jeri Young and Nathan Toke helped me with field characterization studies and provided much appreciated social interaction while staying at the hunting cabin near Parkfield. Lastly, I would like to thank the geology graduate students of ASU as a whole for making my time in Tempe an enjoyable stay.

TABLE OF CONTENTS

	Page
LIST OF TABLES.....	xii
LIST OF FIGURES.....	xiii
 CHAPTER	
1 INTRODUCTION.....	1
Motivating research themes.....	2
How is deformation distributed?.....	2
Fault geometries and densities.....	3
Folding.....	3
Cross sectional geometry: Flower structure.....	3
Fault zone evolution.....	4
Tectonic geomorphology and sedimentation in strike-slip fault zones: Rift-valley to rift-arch.....	5
Uplift.....	6
Parkfield, CA is a special place.....	7
Parkfield segment: Transition zone.....	7
Parkfield Experiment.....	8
San Andreas Fault Observatory at Depth and related research.....	8
San Andreas Fault strength.....	10
Petroleum analog.....	10
Research Statement.....	11

CHAPTER	Page
Agenda.....	11
Overview of relevant central California geology.....	11
Review of previous geological mapping in the Parkfield area.....	15
2 METHODS.....	17
Overview.....	17
Rock Descriptions and analysis.....	17
Tectonic geomorphology.....	17
Mapping.....	18
GIS compilation.....	18
Cross sections and visualization.....	20
3 RESULTS.....	22
Overview.....	22
Northeast Terrain.....	23
Rock Units.....	23
Granite/Granodiorite.....	23
Biotite schist.....	23
Marble.....	24
Monterey Formation.....	24
Etchegoin Formation.....	25
Etchegoin Conglomerate.....	25
Varian Ranch Formation.....	26
Sandstone Member.....	26

CHAPTER	Page
Breccia Member.....	26
Alluvial Fan unit.....	27
Fault Rocks.....	28
Sag Pond deposits.....	28
Landslide deposits.....	29
Granitic soil.....	29
Terrace deposits.....	29
Alluvium.....	29
Structural Geology of a Fault Zone-NE Side.....	30
Sub parallel faults.....	30
Gold Hill fault.....	30
Folding.....	31
Miscellaneous Structures.....	31
Southwest Terrain.....	32
Rock Units.....	32
Granite/Granodiorite.....	32
Volcanic Rocks.....	32
Monterey Shale.....	33
Dibblee Conglomerate Unit.....	33
Santa Margarita.....	34
Unnamed sand and gravel.....	34
Etchegoin Big Pappa.....	35

CHAPTER	Page
Paso Robles Clay Member.....	35
Paso Robles Fluvial Member.....	36
Fault Rocks.....	37
Sag Pond.....	38
Landslide.....	38
Granitic soil.....	38
Terrace.....	38
Alluvium.....	38
Structural Geology of a Fault Zone—SW Side.....	39
Sub parallel faults.....	39
En echelon folds.....	39
Transverse faults.....	40
Teddy’s Faults.....	41
Cross Section Progresssion.....	42
L-L’.....	42
K-K’.....	43
J-J’.....	43
I-I’.....	44
H-H’.....	44
G-G’.....	45
F-F’.....	46
E-E’.....	46

CHAPTER	Page
D-D'	47
C-C'	47
B-B'	48
A-A'/SAFOD.....	48
4 DISCUSSION.....	52
Fault Density.....	52
Flower Structure	53
Subhorizontal Detachments.....	54
Transverse Fault development.....	55
Fault Zone Evolution.....	57
Varying Ages.....	57
Remnant SAF.....	59
Fault Zone Sedimentation.....	60
Fault Rocks.....	62
Tectonic uplift, fluvial processes, landsliding.....	63
Uplift.....	63
Fluvial Processes.....	64
Landsliding.....	64
Slivering Ideas.....	65
Spatial and Temporal Discontinuity of the SAF Rupture Trace.....	66
Fault Zone Strength.....	68
General Regional Geology.....	69

CHAPTER	Page
Petroleum analogs and potential.....	71
Geologic History.....	73
Conclusion.....	75
REFERENCES.....	104

LIST OF TABLES

Table	Page
1. Cross section assumptions.....	76

LIST OF FIGURES

Figure	Page
1. General geologic map of California and outline of field area.....	78
2. Deformation structures in a simple shear zone.....	79
3. Flower structure model examples.....	80
4. Rift-valley and rift-arch topographic profiles.....	81
5. SAF segments in Central California.....	82
6. SAF Strength models.....	83
7. Andean-type subduction model.....	84
8. SAF evolution diagram.....	85
9. Neogene sedimentary basin formation and triple junction migration.....	86
10. Simplified geologic map of the field area.....	87
11. Fault and formation feature class attribute tables	88
12. Map of several sub parallel faults.....	89
13. Photograph of a dormant fault cutting Tm and Te.....	90
14. Gold Hill Fault.....	91
15. Folding near Gold Hill fault.....	92
16. Middle Mountain syncline and Tusg fault.....	93
17. Large Transverse fault.....	94
18. Picture of active transverse fault.....	95
19. Teddy's Faults.....	96
20. Density map and graphs.....	97
21. SAF calculations overlying a DEM.....	98

Figure	Page
22. Migrating flower structure model.....	99
23. Ductile middle crust model.....	100
24. Unconformity within the Varian Ranch formation.....	101
25. Slide Block and L-shaped thrust models.....	102
26. SAF Rupture discontinuities.....	103

CHAPTER 1

INTRODUCTION

Geologic mapping of fault zones at large scale ($>1:10,000$) provides important documentation of the geometries of the blocks and faults that comprise such zones. In addition, it defines the rock units and the geologic history of the area. From these data, important inferences about the distribution of deformation within fault zones and their evolution can be made.

The San Andreas Fault (SAF) in California is the most studied fault in the world, but much of the past geologic mapping is regional in scale and did not clearly document the kilometer-scale movement of crustal blocks within the fault zone. Fault zones within the SAF are convoluted due to the abundance of secondary faults and folds formed by simple shear. Recent geodetic surveys suggest that total right-lateral deformation rates increase with distance laterally away from the SAF in central California (Titus, et al, 2005). Therefore structures adjacent to the main SAF accommodate more deformation than previously thought, and these secondary faults cause deformation to be an interactive system rather than a single master transform fault.

In order to further understand the shallow crustal deformation along one portion of the SAF, I conducted detailed 1:6000-scale geologic field mapping during the 2004 and 2005 field seasons in order to more completely characterize the geologic structure with an emphasis on the fault geometries. From this information I am able to assess the shallow structure, distribution of deformation, kilometer-scale crustal block movements, fault zone development and migration, and provide insights into fault strength.

Furthermore, the geologic history encompassing tectonic uplift, localized sedimentation, and erosional degradation has been established. The regional location of the study area is shown in Figure 1 and the final map product is shown in Plate 1 and serial cross sections in Plate 2.

Motivating research themes

How is deformation distributed?

The idea that a single transform fault accommodates the plate motion between the rigid North American and Pacific plates is too simplistic when one looks closely at the SAF system (Wakabayashi, 1999; Dickinson et al, 2005). Atwater and Stock (1998) cite diffuse seismicity patterns and geologic reconstructions in the western US to suggest that the entire western region of North America may act as a wide, soft boundary between the Pacific and North American plates. In addition, other studies conclude that 25-30% of the relative Pacific and North American motion is accommodated in the Basin and Range geologic province, several hundred kilometers east of the SAF (Minster and Jordan, 1987; Wallace, 1990).

The SAF is often described by a single master fault or trace. Again this is too simplistic a view. Lithostatic stress increases with depth (Davis and Reynolds, 1996) and constrains deformation into a narrow layer as imaged from exhumed faults elsewhere in California (Chester et al, 1993; Chester and Chester, 1998). In the opposite sense then, lithostatic stress decreases near the surface and the zone of deformation apparently widens accordingly. In the shallow crust, the SAF is a discrete zone of numerous faults (including the active fault surface) and folds constituting a 0.5-3 kilometer wide fault

zone in which blocks have been shuffled and warped in a bewildering manner (e.g., Dickinson, 1966). Figure 2 shows the geometric layout of secondary faults and folds in a strike-slip simple shear zone and links them to the principal strain directions (Sylvester and Smith, 1976). Reverse faults and folds thus should strike obliquely (40°) to the principal displacement zone (PDZ) and accommodate crustal deformation.

Fault geometries and densities

Fault geometries and densities change markedly throughout a fault zone. Faults do not exist infinitely through a medium, but rather exhibit segmented and elliptical tipline geometries (e.g., Davis and Reynolds, 1996). The active SAF trace is segmented with restraining and releasing bends as well as stepovers (Wallace, 1990). The geometry of fault planes directly affects the surrounding stress and deformation fields, and this in turn induces specific structural and geomorphic features in and on the adjacent crustal blocks (Sylvester, 1988).

Folding

Folds accompany faults in accommodating deformation of the shallow crust. Geometric relationships in the folds are also important to quantify because they are direct signals regarding crustal behavior and maximum and minimum stress orientations (Figure 2). These relationships provide insights regarding the strength of the SAF.

Cross-sectional geometry: Flower Structure

Where strike-slip and fault normal shortening are combined, the effect is termed transpression. A network of outward verging, inward-dipping faults that slip obliquely uplift certain wedge-shaped blocks with respect to others (Park, 1997). The faults merge

together at depth, thus creating a flower-shaped profile such as those shown in Figure 3. Upward branching, convex-upward faults adjacent to a major strike-slip fault have been noted by a plethora of workers (Willis 1938, Wallace 1949, Sylvester and Smith 1976; Sylvester, 1988) and reproduced in analog models (Emmons, 1969; McClay and Bonora, 2001). It is an expected and thoroughly referenced model within zones of transpression where SAF-normal stress is relieved along reverse faults. Sylvester (1988) hypothesizes that thrusting is from mechanical delamination of the uplifted hanging wall block and shortening uplifts these flakelike bodies out of the deformation zone. Wallace (1949) proposed a similar theory regarding fault gouge getting squeezed upwards between rigid basement blocks.

My detailed mapping and cross sectional analysis (Plates 1 and 2) illustrates a representation of the shallow subsurface, and a flower structure model does not fit well with those observations.

Fault zone Evolution

Relative ages of the geologic units and the faults that offset them were documented through geologic mapping. The position of the SAF does not stay constant through time, as evidenced by the capture of continental crust onto the Pacific plate. Exotic bodies of volcanic rocks and gabbro in central California have been cut and translated by SAF tectonism (Ross, 1970; Mathews 1976). Some of these bodies are seemingly the wrong side of the fault (i.e., Gold Hill gabbro), and a complex migration of active fault strands has occurred in the Neogene as illustrated by the “Parkfield Shuffle”

(Sims, 1993). The geologic history of the area provides insight regarding fault zone evolution and migration of active SAF tectonism.

Tectonic geomorphology and sedimentation in strike-slip fault zones: Rift valley to rift arch

Much of the SAF zone throughout California exhibits a “rift-valley” surface expression (Lawson, 1908). This is a narrow elongated depression encompassing the active trace and associated structures. The valley is not a result of active rifting, but is usually a direct result of fault geometry, namely a releasing bend or stepover (Wallace, 1990). Also, elongate blocks and slivers with long axis parallel to the principal displacement zone (PDZ) can subside, warp, or tilt between parallel or echelon fault strands to form depressions (Sylvester, 1988). Furthermore, highly sheared and fractured rocks within the fault zone are more susceptible to erosion and are more likely to be transported out of the fault zone (Wallace 1990).

However, also in Lawson’s historic 1908 work, Gilbert and Fairbanks noted the opposite type of topographic expression: a ridge (Figure 4). Dickinson (1966) describes Middle Mountain as a “rift-arch” located at the northwestern end of Cholame Valley. Because topography is intimately tied to the structure within zones of active tectonics, this area provides an excellent opportunity to study these relationships where they are well manifest.

Sylvester (1979) notes that blocks within a fault zone typically rise and fall analogous to a porpoise swimming in water. The vertical movement of these blocks thus creates sediment sources and sinks over time. Middle Mountain is an elongate ridge that

rises about 900 feet above the surrounding valley floor. With its positive topography, it is presently a source of sediment to the lower Cholame Valley. However, terrestrial Pliocene deposits of the Paso Robles on the southwest side and Pliocene Varian Ranch sediments on the northeast side of the SAF imply that Middle Mountain reversed its topographic character since Paso Robles time.

Uplift

Middle Mountain's uplift pattern is likely controlled by the structural geology of the fault zone, or more specifically, the discontinuities of the faults within the zone. Restraining bend in fault strike, restraining stepover, variations of SAF dip at depth, or a combination of these various fault alignments can produce uplift. Past studies of young uplift features such as the Dragonsback in the Carrizo segment (Arrowsmith, 1995) and Whaleback within the Cholame segment (Stone, 2000) use fault discontinuities to explain the observed uplift. Arrowsmith (1995) uses a southwestward dipping bend in the SAF at depth to explain elongated uplift that is mostly constrained to the southwestern block, while Stone models a left step in the SAF lifting the Whaleback dome along the Cholame segment.

The SAF zone in the Salton trough (Mecca Hills, California) mapped by Sylvester and Smith (1976) exhibits uplift in a different manner. Two major convex-upward strike-slip faults bound a narrow zone that has been subjected to intense deformation from continual SAF tectonism. The shortened zone between the two faults, containing intensely folded sediments and pervasively sheared basement, apparently flowed upward due to the high horizontal compressive stresses.

Wallace (1949) mapped a SAF zone in southern California and he proposed a similar model. He noted uplifted ridges of fault gouge under terrace deposits near the center of the fault zone between adjacent coherent/rigid basement blocks. These features, named “center-trough ridges,” behaved plastically and were squeezed upwards due to compressional forces nearly perpendicular to the SAF.

Middle Mountain in the Parkfield segment is a larger and more complicated structure, but the same ideas of varying fault discontinuities and possible flow of fault zone materials help explain the proposed uplift hypotheses and structural relationships. This provides an important opportunity to understand active tectonic uplift, erosion, and related fault zone sedimentation.

Parkfield, CA is a special place

Parkfield segment is a transition zone (NW creeping, SE locked)

The SAF is separated into several segments dependent on different along-strike geometric and strain release characteristics (Figure 5). The Parkfield segment in Central California is a special place and has been a focus of earth science research for the past three decades due to the segment’s systematic rupture behavior (Bakun and Lindh, 1985; Bakun et al, 2005). The most recent September 2004 rupture along with numerous other historic earthquakes (1857, 1881, 1901, 1922, 1934, and 1966) provide scientists a valuable dataset in earthquake research. Much of the fault’s behavior in this region is due to the Parkfield segment’s variable character of strain release. The northern part of the segment is constantly creeping at ≥ 2.5 cm/yr (Titus et al, 2005) and largely aseismic,

while the southern portion of the segment is locked and releases stress through periodic magnitude 6 earthquakes (Bakun and Lindh, 1985; Bakun et al, 2005).

The Middle Mountain field area encompasses both locked and creeping fault behavior. The 1966 and 2004 earthquake ruptures are concentrated in the southeastern half of the field area (Brown et al, 1967, Rymer et al, in press). The northwestern part of the area slips through aseismic creep and repeating microearthquakes (Langbein et al, 1990, Hickman et al, 2004).

Parkfield Experiment

Similar seismograms and rupture locations from the 1966 and 1933 earthquakes, as well as moderate earthquake events in 1881, 1901, and 1922, led to the infamous assumption that the fault, at least in this local, was predictable. Bakun and Lindh (1985) surmised that the fault would rupture before 1993, and the Parkfield Experiment was born. It was a large research project aimed at capturing the next earthquake with a dense array of geophysical and geodetic instrumentation and furthering the understanding of earthquake physics and rupture behavior. In 2004, a moderate M 6 earthquake occurred. While the timing, epicenter location, and rupture propagation did not adhere to the Parkfield Experiment model, observations from the event provided detailed data regarding earthquake dynamics.

San Andreas Fault Observatory at Depth and related research

The NSF funded Earthscope project named SAFOD (San Andreas Fault Observatory at Depth; <http://www.earthscope.org/safod>) began in 2002 and is an ongoing multistage endeavor. The goal of SAFOD aims to ascertain intrinsic fault characteristics

and behaviors at seismogenic depths. The SAFOD site was located in the northwestern quarter of Middle Mountain because recurring microearthquakes provided an excellent subsurface target, and the area was already well instrumented from the Parkfield Experiment (Hickman et al, 2004). Some also felt that the geology of the surrounding area was simple and well understood. Bakun and Lindh (1985) state: “The Parkfield section of the San Andreas fault is a relatively simple part of the North American-Pacific plate boundary, with no major active intersecting faults nearby.” This was a dramatic misconception regarding the geologic structure of a fault zone. My mapping illustrates the complexity of the fault zone geology, and my observations can help correlate and link surface rock units and structures to SAFOD wellbore data.

Both the Parkfield Experiment and SAFOD projects have intensively studied the SAF in an attempt to further understand fault behavior. However, these studies were geophysically focused and the geology was not emphasized. Previous geologic interpretation of the area was based on small-scale (1:62,500 and 1:24,000) mapping. These scales were not comparable to the dense seismic and geodetic arrays in the Parkfield vicinity and the even finer wellbore analysis of SAFOD. The geophysical and geologic data could not be compared and contrasted fruitfully. My map illustrates the geology at a comparable degree of detail to the geophysical surveys, and it enables scientists to compare and contrast important similarities, differences, and possible trends regarding the local geology and geophysics.

SAF strength

Zoback et. al. (1987) suggest that the SAF does not behave in a typical Andersonian Byerlee framework. They cited in-situ stress indicators, a low heat flow anomaly, and nearby reverse faults and folds striking parallel to the SAF in central California to indicate maximum horizontal compressive stress orientations (S_{Hmax}) nearly perpendicular to the SAF strike (Figure 6).

Scholz (2000) argues that the SAF behaves within an Anderson-Byerlee framework. Stress measurements near the SAF show typical stress profiles for a strike-slip fault terrain and folds near the SAF are typical en echelon folds found throughout strike slip terrains with $\psi \sim 30-60^\circ$ (ψ is the angle between the strike of the secondary structure and the SAF) (Figure 6).

Although this scientific question is not the focus of the study, my field data illustrates crustal deformation near the fault zone. Relevant stress orientations within the adjacent crust can be deduced from fold axial planes and fault strikes, and the results are mixed.

Strike-slip terrains are important petroleum provinces

Transpressional uplifts, or pop-ups, are typically doubly plunging anticlinal structures that are created along a restraining bend or stepover (Sylvester, 1988). This geometry is favorable for the economic accumulation of petroleum. Sand box experiments of pop-ups created from restraining stepovers of strike-slip faults serve as analog models for industry geologists (McClay and Bonora, 2001). My mapping and detailed cross sectional analysis also represents a 3-dimensional model for a real-life,

heterogeneous, and highly complex pop-up structure. My model can serve as an analog to industry geologists to predict possible productive structures (folds) and compartmentalization structures (faults) within a pop-up oilfield. Furthermore, fault zones that bound basins formed in the Neogene may contain localized economic petroleum plays (Harding, 1976).

Research Statement

Detailed mapping and subsurface interpretation of shallow structure provides an unprecedented look at the rocks and structures of the SAF in an important place.

Agenda

This paper will now present an overview of relevant central California Geology, followed by an overview of my research methods and subsequent results entailing geologic unit descriptions and structural discoveries. A progressive SE to NW cross section discussion illustrates how crustal deformation changes through time and along SAF strike. Lastly, I present a discussion of strike-slip fault zone structure, fault zone sedimentation, fault density evaluations, fault zone strength and migration, tectonic uplift, and geologic history of the field area.

Overview of relevant central California geology

Although California has been a continental margin for most of its complex geologic history (Dickinson, 1981), our background will begin in the Mesozoic, when an Andean-type margin was in place on the western side of California. The large Farallon plate subducted underneath the North American continental lithosphere near the present day Sierra Nevada foothills. An exotic island arc clogged this trench in the late Mesozoic

and subduction processes migrated oceanward near the present day Coast Ranges (Dickinson, 1981). Subduction of the Farallon plate beneath the North American plate continued throughout the Jurassic, Cretaceous, and early Tertiary (Figure 7). The Franciscan complex, the Sierra Nevada batholith, and the Great Valley sequence were all formed during this time and are important geologic provinces within central California. The Franciscan assemblage is regarded as a textbook example of a *mélange*. It is a heterogeneous mixture of deformed rocks including sandstone, greywacke, chert, greenstone, and blueschist metamorphic facies. The Franciscan was probably scraped off in an accretionary wedge near the ancient trench (Page, 1981). The Sierra Nevada province is regarded as an extensive batholith that formed from arc magmatism due to the continual subduction of the ancient Farallon plate (Dickinson, 1981). The Great Valley sequence served as a large forearc basin in which clastic sediments from the Klamath/Sierra Nevada arc massif were deposited into (Dickinson, 1981).

The continental margin of California changed drastically about 29 Ma, when the oceanic spreading center separating the Farallon and Pacific plates was subducted under the trench and a triple junction between the North American, Pacific, and remnant Farallon plates initiated. Continued subduction of the oceanic spreading center split the triple junction into two separate entities, the Mendocino to the north and the Rivera to the south. Further oceanic ridge subduction migrated the Mendocino triple junction (transform-transform-trench) to the northwest and the Rivera triple junction (ridge-trench-transform) to the southeast. The structure linking these two triple junctions and

separating the Pacific plate from the North American plate is the San Andreas transform system (Figure 8) (Atwater, 1970).

The triple junctions have not been stable, however, as simply seen by the capturing of continental crust onto the Pacific plate (Dickinson and Snyder, 1979). The passage of the triple junctions and inception of SAF tectonism greatly influenced the nearby lithosphere. Absences of subducted oceanic crust (slab windows) were associated with both triple junctions. Dickinson and Snyder (1979) correlate northward movement of the Mendocino triple junction to deactivation of the inland magmatic arc and progressive northward extension inducing subsidence of Neogene sedimentary basins and initiating volcanic processes in the overriding plate (Figure 9). Heat generated from the young, thin oceanic crust and from upwelling asthenosphere may have weakened the overlying continental crust (Blake et al, 1978).

Tectonism along the SAF formed extensive marine basins in the mid-late Miocene in the present day Coast Ranges of central California (Blake et al, 1978; Harding, 1976, Dickinson and Snyder, 1979; Page et al, 1998). The sediments deposited into these basins are regional formations within my field area. The Monterey is interpreted to have been deposited in starved basins which collected a large amount of diatom ooze from upwelling ocean currents during climate change in the Miocene (Bramlette, 1946; Pisciotto and Garrison, 1981). The Etchegion was deposited in protected bay or estuarine environments with numerous sand shoals and tidal channels (Loomis, 1989). It was derived from both Coast Range terrains and volcanics from the Quien Sabe Volcanics (Steve Graham, personal communication).

The SAF trace was largely offshore during the Miocene (Dickinson, 1981). Oceanic spreading of the east Pacific rise separating the Baja California peninsula from mainland Mexico began near the Miocene-Pliocene boundary, and this migration was also associated with movement of the dominant strand of the SAF system inland to its present position in central California (Dickinson and Synder, 1979). This strand is usually regarded as the SAF proper and is much younger than the SAF transform system that began in the Oligocene and separates the two triples junctions.

The Salinian block in central California consists mostly of Cretaceous granite and tonalite plutons as well as some metasediments of unknown age (Page et al, 1998). Potassic intrusives in the Salinian block are similar to Sierran and Peninsular plutons and they are probably linked to the same magmatic belt (Page, 1981). The Salinian block was most likely originally connected to the western fringe of the Mojave block in the southern Sierra Nevada geological province. This allochthonous block has been transported northwest about 600 km to its present location in central California by right-lateral tectonism from the SAF (Dickinson, 1981; Page 1981). The Salinian block is approximately 9-10 km thick and probably overlies the schist of the Sierra de Salinas (correlative to the Pelona schist of southern California and western Arizona) (Page et al, 1998). The Franciscan complex now flanks both sides of the Salinian block in central California with the SAF serving as the NE boundary and the Sur-Nacimiento fault the SW boundary (Page, 1981).

Major tectonic shortening and uplift of the California Coast Ranges began around 3.5 Ma. Tectonism during the Plio-Pleistocene boundary permanently raised the central

California area above sea level and changed the setting from marine to non-marine (Page et al, 1998). This is indicated by many of the Plio-Pleistocene sedimentary units which have basal shallow marine or estuarine facies with overlying fluvial sediments. Another tectonic pulse occurred about 0.4 Ma which uplifted individual mountain ranges within the Coast Ranges and has continued to the present day (Page et al, 1998).

The present relative plate velocity between the Pacific and North American plates are approximately 4.8 cm/yr (DeMets and others, 1987). Present SAF slip rate calculations in central California vary. Geodetic analysis ranges from 2.5 cm/yr (Titus et al, 2005) to 3.3-3.7 cm/yr (Thatcher, 1990). Paleoseismic studies indicate the SAF is slipping 3.4 cm/yr (Sieh and Jahns, 1984). The difference between total plate motion and SAF slip is probably accommodated by numerous other faults in a wide zone extending from the continental margin to the Basin and Range geologic province (Wallace, 1990; Thatcher, 1990).

Review of previous geologic mapping in the Parkfield area

Bill Dickinson (1966), Tom Dibblee (1971), and John Sims (1990) previously conducted geologic mapping in the area. Dickinson published a simplified sketch version of his field mapping in his 1966 paper. The Middle Mountain field area was denoted as Quaternary Deposits with some sub parallel and echelon faults. Dibblee published a regional 1:62,500 map of the Parkfield region that is the most useful and cited work. His vast knowledge of Californian stratigraphy proved most beneficial for my studies, and he identified much of the structure in this area as well. John Sims of the USGS later published a 1:24,000 geologic map of the Parkfield quadrangle in 1990. He provided

three notable contributions: (1) He made the contact between the Tm and Te on the northeast block a reverse fault, (2) He mapped Dickinson's local Varian Ranch unit in certain locales that Dibblee mapped as granite and was the first to propose large slide block components within the unit, (3) He subdivided several terraces within the Quaternary alluvium unit.

These maps tended to lump structural features and geologic units together. For example, densely spaced faults were often merged into one large fault and resolution of fault zone complexity was not possible.

CHAPTER 2

METHODS

Overview

During the spring and summer of 2004 and summer of 2005, I (with some help from Ramon Arrowsmith) undertook an extensive field campaign to answer some of the research questions posed in the introduction. Large scale (1:6,000) old-fashioned geologic mapping was conducted on 20' contour topographic maps and aerial photographs with 100 meter grid spacing in a UTM NAD83 coordinate system. A handheld GPS unit was used to verify map locations, and accuracy of 4-8 meters was usually obtained. 89 person-mapping-days were invested, and a conservative estimate of 12 miles a day of walking yields a cumulative mileage of 1068 miles invested into the mapped contacts.

Rock Descriptions and Analysis

Previous geological units named by Dibblee and Sims were used whenever applicable. However, in certain instances they were revised, while some new ones were added when necessary. Unit descriptions will be addressed later in the results section, but a systematic outward (outcrop) to inward (hand lens) description method was employed.

Tectonic Geomorphology

Tectonic geomorphic features such as pressure ridges, topographic saddles, defeated channels, and sag ponds were observed in the field area. These observations helped locate and characterize the faults present in the field area, and they proved to be

most beneficial in an area with poor rock exposure. However, these geomorphic features were limited to my field notes as this was not the primary objective of my work.

Mapping

Geologic details visible in the field area were replicated on the field maps, and a special effort was made to capture and delineate all fault geometries present in the area. Figure 10 is a basic map showing the geographic position of the southeast-pointing arrowhead-shaped field area with respect to Parkfield and SAFOD. Rock relationships and characteristics actually seen in the field were replicated on my notes and field maps. The geology was *not* worked out on aerial photographs in stereo view or fitted to a preexisting geophysical model. 295 field pictures and 36 hand samples were taken for documentation. 23 granite/granodiorite samples were acquired throughout the fault zone for apatite fission track analysis. Absolute age dates and exhumation histories of these granitic bodies ultimately will be added to my study to help constrain the geologic history of the area, in particular vertical movements of the granitic bodies.

GIS Compilation

Once the field work was completed, the field maps were scanned and georeferenced into a UTM NAD 83 Zn 10 coordinate system using GIS/ArcMap software. Next a personal geodatabase containing a personal dataset was created in a GIS mxd (Arcmap digital map) file. Several feature class files (points, polylines, and polygons) within the personal dataset were produced. For example, polyline feature class files were created for fault and depositional contacts and point feature class files were made for strike and dip measurements.

Fault and depositional contacts were then digitally traced out from the georeferenced scanned field maps, and thereafter the digital polylines were in the correct positions in the respective coordinate system. Several different types of faults (normal, reverse, SAF trace) require different symbols in order to delineate their slip motion. Traditional geologic map symbology (e.g., Compton, 1985) for both fault and depositional contacts was assigned through value fields within each feature class. For example, all faults were contained within the fault feature class file, but the symbology of each digital fault was characterized through fault type and certainty value fields within the fault feature class (Figure 11). I personally typed every value field within the feature class attribute tables to characterize all of the mapped polylines.

Formation polygons were subsequently constructed and bound by the contact polylines. Again several different formations are contained within one polygon feature class, but value fields (formation symbol) within the attribute table characterized each polygon (Figure 11). Different unit colors were then assigned to each value field, and the formation polygons were then made 80% transparent in order to uncover the underlying topography shown by the contours.

Locations such as strike and dip measurements were first created in an Excel file that contained the respective easting, northing, bearing, and inclination obtained during field work. Next a CSV file was created within Excel, and that file was then imported into a point feature class within the personal geodatabase. Traditional strike and dip symbols were assigned to the point feature class. Each point was then rotated by the respective strike degree, and dip measurements were assigned as labels.

GIS software is useful in managing the large data sets obtained during field work. For example, 1008 location points and 467 strike and dip attitudes are data sets within the digital compilation. Attitude certainties were characterized to show areas of question or doubt. All attitudes and foliations that made it to the final map format were characterized as OK to excellent while in the field. Contact certainties as well as contact types are displayed on the map through traditional geologic symbology (e.g. Compton, 1985).

Cross Sections and Visualization

One short SAF-parallel and eleven SAF-normal cross sections were created (Sections A-A'/SAFOD through L-L' in Plate 2). Few fault planes were measurable with a compass, so fault and depositional plane orientations were determined based on contact behavior/interaction with topography. Structural attitudes of faults were computed as “3 point problems” and solved by trigonometric calculations or fitting a plane to two vectors in stereonet. Axial planes of folds were calculated by fitting a plane to the intersection of bedding planes and the bisector of the bedding poles. Limbs of the folds were drawn as kinked style. Simple along trend projections from nearby structures helped constrain some subsurface attitudes.

Apparent dips for every fault plane, depositional contact plane, fold axial plane, and bedding plane were calculated and projected onto each respective cross section. The cross sections accurately represent mapped relationships and quantitative analysis. These are *not* arbitrary interpretations. Rock type symbology was used to illustrate relative dips and stratigraphic relationships for the respective units (i.e. tilting; pinching out of facies).

Bedding patterns on the cross sections were rotated to relative dips in order to accurately display bedding planes.

It is important to note that bedding, fault, and axial planes are likely not planar or continuous in the field area. Active deformation in the area warps and bends originally rectilinear planes into highly sinuous features. Some mapped contacts show a highly variable dip along strike and the cross sections cannot represent that variability accurately. However, inferring the bending of contacts at depth is completely ambiguous. Therefore the calculated planes from the surface typically were extrapolated to the bottom of the section and contact ambiguity is displayed through dashed and queried symbology.

Sense of slip along faults is inferred to be right lateral. However, ambiguity prevents designation of fault movement symbology outside of the SAF trace. Therefore the sense of slip along most faults has been left undesignated on the cross sections.

Stratigraphic thicknesses were difficult to obtain within the Middle Mountain fault zone because of the abundance of faults, so Dibblee's regional 1971 map was referenced. Units lying laterally outward from the fault zone were more coherent and continuous, so stratigraphic thicknesses were calculated using basic trigonometric calculations (Table 1). Subsurface data from oil and gas well logs, SAFOD data, and past geophysical surveys helped provide subsurface constraints for the cross-section interpretation, and all relevant assumptions are listed on Table 1. Generalized stratigraphic columns and relationship figures were created to show superposition, thickness, and depositional relationships of the mapped units (Plate 3).

CHAPTER 3

RESULTS

Overview

The SAF has juxtaposed geologic units by 315 kilometers in the past 23.5 Ma (Ross, 1970; Matthews, 1976; Sims 1993), and therefore a stark contrast of rock types and related structures are expected on opposite sides of the fault. Although some exceptions to this rule have been discovered (Paso Robles and Salinian granite on the NE side-see below), it is beneficial to separate the two terrains for this discussion.

Figure 10 is a simplified geologic map and illustrates the general trends and structural relationships for the field area (see also Plate 1).

The northeastern side is comprised of Miocene to Pliocene marine sedimentary units and Plio-Pleistocene terrestrial sedimentary units. Dominant structures include several high angle faults striking sub-parallel to the main SAF trace that bound marble, granites, and Tertiary sedimentary units. Fault density increases near the active SAF trace. The Gold Hill fault is a reverse fault of varying southwest dip that surfaces along the eastern margin of Middle Mountain and places the Miocene Monterey shale over Pliocene Etchigoin sandstone. Alternating synclines and anticlines with axes trending parallel to the strike of the Gold Hill fault are present within the hanging and foot walls.

A 450 meter thick package of the Plio-Pleistocene Paso Robles Formation dominates the southwestern terrain and is deformed by en echelon folds and secondary faults. Some of the faults strike nearly normal to the SAF, offset Tertiary and Quaternary units, and tend to be northwest-side up. Several SAF-parallel striking faults slice Tertiary

and Quaternary sedimentary units and granitic bodies. A fault on the southwestern side of Cholame Creek juxtaposes Tertiary rhyolitic rocks (Pinnacle-Neenach equivalent) (e.g., Mathews, 1972) against Salinian granite.

NE Terrain

Rocks on the Northeast side of the San Andreas Fault

gr--Granite/Granodiorite

Cliff former, with occasional slopes. Usually a granodiorite indicated by a lack of significant potassium feldspar. White to medium gray. Often medium to coarse crystalline, 40-60% (40% avg) quartz, 20-50% plagioclase (40% avg), 10-30% biotite (20% avg) , with traces of potassium feldspar and hornblende. Weathers in blocky columns to loose grainy surface designated as Qgs (see below). Usually extremely sheared, weathered, weak, and friable with a grusy weathering style. Biotite usually individual planar crystals (not booklets), and some are weathered to a medium brown color on the outermost fringes of the crystal. Some carbonate replacement of plagioclase crystals and some biotite crystal alignment parallel to fault planes. Aplite dikes and small 2-5cm calcite veins present in part.

bs--Biotite Schist

Cliff former. Low grade schist composed primarily of biotite (60%), feldspar (20%, mostly plagioclase), and quartz (20%). Biotite crystals are medium to coarse crystalline; quartz and plagioclase crystals are finely crystalline. Definite alignment of biotite with schistosity. Outcrops are usually small (5-10m) and fault-bounded.

m--Marble

Moderate slope former except in fault-bounded tectonic slivers where it is a cliff former. Mostly white to cream, very calcareous, usually sugary texture; but grainy texture in part. Crystals are about 2 mm in diameter. No visible bedding and often highly sheared. Unit includes some thin gray limey shales. Marble is usually hard, while the limey shales are weakly lithified. Almost always associated with thick brushy vegetation on hillslopes. Some marble is tinted blue with alternating dark gray and white foliations/banding about 1-3 cm wide. 10-50 meters thick.

Tm--Monterey Shale

Moderate slope former. Orange, cream, to light brown porcelaneous siliceous shale. Outcrops usually highly fractured with no preferred orientations. Usually massive, although decimeter-scale planar bedding is present in part. Weathers into hard, tabular, and angular pebble-sized chips that sit within a light to medium brown silt matrix. Weathers black in places due to iron oxide staining, though usually light orange or white due to surface bleaching (Bramlette, 1946). Often highly folded in the NE block. McClure Shale Member (Dibblee, 1973; Dickinson, 1966) that is dominated by a thick upper siliceous facies of diatomaceous rocks as well as secondary diagenetic rocks such as chert and porcelanite (Pisciotta and Garrison, 1981). Basal and middle transitional members are not found in the field area (Dibblee, 1973). 500-1200 meters thick.

Te—Etchegoin Formation

Steep slope former. Predominantly arkosic marine sandstone. Light to medium gray on fresh surface, weathers orange/yellow to medium brown. Very fine to medium grained, sub-angular to sub-rounded, moderately-well sorted. Varying cement compositions of clay and calcite create weak to moderate lithification respectively. Some andesitic volcanic grains create a salt and peppery texture, and some facies contain an extremely high amount (~60%) of light blue coarse andesite grains (Dibblee's blue member, 1973). Usually massive, but some lenticular bedding present. Some small (1mm-5cm) clay interbeds are isolated and laterally discontinuous. Some interbedded pebble stringers of rounded granite, basalt, and chert clasts. Some orange iron-oxide staining, calcite veins, and mollusk fossils. Abundant deformation bands 5-15 cm wide and vertical fractures near faults. Some sparse Tm lithics. Varies from a lithic rich (volcanics/KJf) fine to medium grained calcite cemented well-lithified sandstone to a medium grained gray nearly unconsolidated massive and porous homogeneous quartzofeldspathic sandstone with weak clay cement. Prevalent 0.15-1.5 meter long oval or shark finned hard carbonate concretions that roughly align with bedding planes. Approximately 720 meters thick.

Tec--Etchegoin Conglomerate

Slope former. Minor pebble/cobble conglomerate composed of well-rounded polished basaltic and andesitic clasts, angular granitic clasts, and some small Tm pebble chips in a medium grained gray sandstone matrix (Te sand). Highly resistant and hard

unit. Often highly sheared. Massive bedding. Provenance unknown, though KJf source or Quien Sabe Volcanics seems likely. 10-50 meters thick.

Tvr--Varian Ranch Formation

Local formation with two different facies: 1) Arkosic sandstone; 2) Sedimentary breccia. Combined thickness of approximately 520 meters.

Arkosic Sandstone Member

Steep slope former. Light-medium gray, angular to sub-angular, fine to very coarse grained terrestrial arkosic sandstone. Some interbedded siltstones and shales. Lithic rich in coarser beds, and varies from well sorted in the fine grained beds to poorly/moderately sorted in the coarser and lithic-rich beds. Usually clay cemented, although some calcite cement present in coarser beds. Abundant fine crystalline granodiorite pebble sized clasts create distinctive granitic pebble stringers. Some sparse Te and Tm clasts also. Massive in part. Bi-directional cross-bedding in stacked fluvial channel sands. Fining-upward (clast dominated at bottom, matrix dominated at top) sequence. Some 1-2 meter thick beds of green tinted shale suggest standing water environment, and shale beds thicken in the east. Abundant vertical fractures. Brushy vegetation. Tvr unconformably overlies Te. Few detrital biotite crystals suggest granitic source nearby. Internal angular unconformities suggest syntectonic sedimentation (Figure 22).

Breccia Member

Steep slope former. Brown to gray clast dominated unit. Matrix consists of silt and fine to coarse grained, sub-angular to sub-rounded, unconsolidated sandstone. All

matrixes are very-calcareous (either due to marble content or fault fluid interaction) with some red FeO staining. Clasts are mostly monolithic granitic/granodiorite in comp (about 95%), with sparse clasts of m, biot schist, KJf chert, volcanics (basaltic/gabbro), Te, and Tm. Clasts sub-rounded to angular, small pebble to large boulder (usually pebbles and cobbles) in size. Westward imbrication of tabular marble clasts indicates eastward-directed paleocurrent. Isolated large dark granitic and white marble slide blocks (10s to 100s of meter scale) totally encased within unit. Unit usually massive and highly sheared. Thick brushy vegetation. Unit weathers in part to abundant granitic grains (Qgs) and some marble clasts in a silty matrix.

Qf--Alluvial Fan

Gentle slope former. Medium brown to dark gray, matrix-dominated unit consisting of clay and silt with some fine sand. Usually non-calcareous but some isolated pockets of caliche are very calcareous. Usually massive and difficult to obtain attitudes. Hard clumps of cohesive clay in part.

Clasts are rounded to sub-rounded and range in size from grains to boulders, but predominantly medium pebble to small cobble. Franciscan (KJf) dominated provenance (chert and greenstone) with smaller fractions of granite/granodiorite, marble, basalt, Monterey (Tm), Etchegoin (Te), quartzite, and red-brown rhyolite. Pebble-sized chips are mostly sub-angular Tm chips or sub-rounded granite. Qf mostly granitic near granite slivers, indicating source dependence. Greenstone clasts serpentinized ip. Landslides common. Sparse-grassy vegetation. Thickness less than 85 meters.

QTfr--Fault Rocks

Usually cliff formers. Unit comprises extremely sheared and fractured rocks for which protolith is ambiguous. Fault rocks are either fault breccias or cataclasites. Rock strength varies from extremely well lithified (probably due to strain hardening) to weakly lithified (probably due to excessive shearing and cataclastic flow). Clasts often fractured in situ. Extremely calcareous-- probably due to carbonate replacement/diagenesis from fault fluid interaction.

Fault breccias have angular pebble to cobble-sized clasts of varying composition: granodiorite, granite, m, quartzite, biotite schist, serpentinite/volcanics, Te, Tm. Matrix can be well-lithified calcite cemented sand or weakly consolidated sand. Sometimes tar-cemented and very well lithified where fault interacts with Tm at depth.

Cataclasite often looks like granite on the outside but has internal sandy matrix. Cream to brown, fine to medium grained, very calcareous sandy matrix. Clayey and very weak/friable (almost fault gouge) in part. Can often crush with hand. Some green crystals look like old biotite-some possible epidote alteration on the outside. Some black and white small 2-10 cm wide hard resistant ledges—possibly due to strain hardening within a localized shear zone, but usually no definitive shear fabrics or planes are visible due to the chaotic nature of the unit.

Qsp--Sag Pond

Clay-filled shallow depression sometimes created from a right stepover along the SAF trace or sub-parallel fault. Small deposits tens of m² in area and under 10 meters thick.

Qls--Landslide

Geomorphic feature that shows recent downward transport of material. Visible scarp at the very uppermost reaches and hummocky topography throughout the main body and toe. Usually associated with nearby faulting and clay-rich formations such as the QTpc. Unit confined to the near sub-surface (under 10 meters thick).

Qgs--Granitic Soil

Gentle slope former. Brown to orange, medium to coarse grained sandy soil predominantly composed of unconsolidated quartz and feldspar grains. Some detrital biotite along with larger pebble-sized clasts of crystalline granite of varying felsic components. Probable underlying granitic source, although no granite outcrops are visible. Some marbe clasts in the Qgs unit over Tvr breccia deposits. Thickness probably under 10 meters—thin veneer cover.

Qt--Terrace

Matrix dominated, near horizontal unit consisting of dark black clay or silt w/sparse granitic grns. Usually devoid of larger clasts and present within level topography on drainages or hillslopes. Thickness under 10 meters.

Qa--Alluvium

Rock unit consisting of unconsolidated sand, silt, and gravel deposited as terraces in present valleys and canyon flood plains. 10-50 meters thick.

Structural Geology of the Fault Zone---NE Side

Sub parallel faults

Structural geology of the northeastern block includes numerous faults that strike nearly parallel to the SAF and are hereafter regarded as “sub parallel” faults. The density of these faults increases near the active SAF trace, as shown best in cross section I-I' and K-K' (Plates 1 & 2) and Figure 12. These faults are moderate to steeply dipping and most likely accommodate strike slip motion.

Sub parallel faults within 100-200 meters of the active SAF trace probably merge into the main SAF trace at depth. The age of these sub parallel faults are probably late Pliocene to Pliostocene due to the presence of fault-bounded Miocene Monterey and Pliocene Etchigoin sedimentary units. Some are quite active (Brown et al, 1967) and produce distinctive geomorphic features such as sag ponds, pressure ridges, and notched saddles usually associated with SAF trace deformation (Wallace, 1990). However, some have warped planes (Figure 13) implying they are likely dormant and have been folded by subsequent deformation (Dickinson, 1966; Bridwell 1975).

We are unable to determine offsets due to the lack of definitive marker beds within the exotic and sedimentary units, but regional relationships imply less than 10 km of horizontal movement. Dip-slip estimates can be obtained from the cross sections.

Gold Hill Fault

The Gold Hill Fault (GHF) is a reverse fault that extends along the eastern margin of Middle Mountain in the southern half of the field area (Figure 14). It was named after the gabbroic Gold Hill (Ross, 1970) further to the southeast (although it does not actually

bound that translated block) where it uplifts the lower-Miocene Temblor formation over the middle-Miocene Monterey (Sims, 1988). In the Middle Mountain vicinity, the Gold Hill fault emplaces the Miocene Monterey formation over the Pliocene Etchegoin formation. The GHF strikes sub-parallel to the SAF trace and dips vary considerably from 33-76° (average 53°) from F-F' through K-K' cross sections. Several thin fault breccias are visible along the GHF surface trace. It is currently unknown whether some strike slip motion has occurred along it or whether it is entirely dip slip.

Folding

The NE-SW shortening that created the GHF also folded the Tertiary units (Figure 15 and Section I-I'). These folds strike parallel to the SAF and GHF and exhibit nearly vertical axial planes. They probably formed contemporaneously with the GHF. These could be fault-propagated folds ahead of the Gold Hill Fault. They could also be en echelon folds that have been subsequently rotated to a SAF-parallel position. This would imply the same rotation of the GHF plane.

Miscellaneous Structures

The Gold Hill fault crosses Little Cholame Creek and extends outside of the field area near the F' in F-F' line. Many other reverse faults originate to the southwest of the Gold Hill Fault near the F-F' line and in turn accommodate much of the SAF-normal stresses. These faults become dense and complex with various splays and backthrusts (Cross Section F-F' in Plate 2). It is a minor fault zone within the SAF zone. Further to the northwest, a fault-bounded granite sliver is thrust up and over the Etchegoin

formation, illustrating an impressive example of tectonic uplift since the Pliocene (Section E-E' in Plate 2).

SW Terrain

Rocks on the Southwest side of the San Andreas Fault

gr--Granite/Granodiorite

Cliff former, with occasional slopes. Varies between granite and granodiorite. Usually light gray, although white to light orange in places. Crystal size varies from medium to very coarse crystalline, but usually coarse crystalline. 30-60% quartz (50% avg.), plagioclase 10-40% (25% avg.), 0-20% potassium feldspar (10% avg.), 10-20% bt (15 avg.). Biotite usually thin individual planar crystals, except the granitic sliver within Tusg contains granite with thick biotite booklets. Biotite crystals weathered brown in part. Some banding between biotite and plagioclase crystals. Often highly sheared, weathered, and extremely weak (can often crush with hand). Breaks preferentially along pre-existing fractures with iron oxide staining. Brecciated near faults. Calcareous in part due to carbonate replacement of plagioclase crystals. Weathers to a grainy soil (Qgs).

Tvc--Volcanic Rocks

Steep slope former. Hard maroon-gray rhyolitic flows and flow breccias. Flows contain fine scale 1/2 – 5 mm thick flow banding. Some rhyolitic autobreccia---angular clasts of rhyolite within a quartz/feldspar rich pink microcrystalline matrix. Some gray to pink microcrystalline rhyolite or quartz porphyry ---quartz phenocrysts in an aphanitic matrix. Weathers light gray into cobble size blocks within brown sandy quartz-rich

matrix. Abundant lichen growth and moderate brushy vegetation. Coorelative to Sims' Lang Canyon Volcanics. Thickness about 800 meters (Irwin, 1990).

Tm--Monterey Shale

Moderate slope former. Orange, cream, to light brown siliceous shale and porcelanite with some sparse small scale (10-20 m wide) fine grained laterally discontinuous sandstone lenses. Outcrops usually highly fractured with chaotic orientations. Usually massive, although decimeter-scale planar bedding is present in part. Weathers into hard, tabular, and angular pebble-sized chips that sit within a light to medium brown silt matrix. Weathers black in places due to iron oxide staining, though usually light orange or white due to surface bleaching (Bramlette, 1946). Very similar to Tm on northeastern side of SAF, so it most likely is the McClure Shale Member (Dibblee, 1973 and Dickinson, 1966). Lithologically similar Gould Shale Member pinches out to the southeast (Dibblee, 1973). 550-1000 meters thick.

Tn--Dibblee Conglomerate Unit

Gentle slope former. Matrix-supported conglomerate. Matrix is red-orange to brown, quartz and feldspar-rich silt, but some coarse grained sand also present. Clasts are usually well-rounded small cobbles, but small boulders also present. Clast composition is mostly granitic with some volcanic (Tvc) contribution. Sparse components of KJf chert, greywacke, quartzite, flint, and m clasts. Usually massive and weathers to a granitic soil (matrix) and promotes willowy/brushy vegetation. Highly sheared near faults. Tn unconformably overlies granite. Sims (1990) merged this unit into the basal part of the Santa Margarita Formation, but it is distinctive from the Santa

Margarita because of its rounded cobble clasts in a red silt matrix. Approximately 90 meters thick.

Tsm--Santa Margarita

Gentle slope former. White, medium to coarse-grained, sub-rounded to sub-angular, very well sorted, non-calcareous, very weakly consolidated marine arkosic sandstone. Massive with some 5-10 cm-wide deformation bands present. Extremely high porosity and permeability with few lithics. Distinctive unit due to its white color and extremely weak consolidation. Tsm conformably overlies Tn. 370 meters thick.

Tusg--Unnamed sand and gravel

Steep slope former, with occasional cliffs. Both sandstone and gravel (breccia) facies are within Tusg. Gravel is clast dominated with small cobble to small boulder, sub-angular to sub-rounded clasts in a white, fine to medium-grained arkosic sandstone matrix. Clast composition is predominantly granodiorite/granite/quartzite of multiple sources, but there are occasional limestone, andesite, quartz porphyry, greywacke, flint, and white slate clasts. Massive bedding.

Sandstone is a white to light brown, fine to coarse grained, clay cemented, well-lithified, lithic-rich sandstone. Predominantly feldspar and quartz grains. Lithics are usually granodiorite/granite pebbles that create some pebble stringers within the unit. Usually massive and non-calcareous, but calcareous in part. Highly porous and permeable and usually moderately consolidated.

Similar clasts and white sand matrix suggests the two members are just a facies change. Both are laterally discontinuous. Sandstone could be a sedimentary derivative

of the gravel. Brushy-grassy vegetation. Could be coorelative to Santa Margarita submarine fans found in southern Temblor Range (Ryder and Thomson, 1989) and it is correlative to Dibblee's Tsg unit (1971). Tusg unconformably overlies granite on Middle Mountain. 300 meters thick.

Tebp—Etchegoin-Big Pappa

Steep slope former, with some cliffs. Predominantly shallow marine sandstone (Loomis, 1989). Light gray where fresh, weathers medium brown. Fine to medium grained, sub angular to sub rounded, moderately sorted sandstone. Predominantly quartz, some feldspar, and sparse mafic volcanic grains. None to slightly calcareous. Dominantly orange clay cement, though some calcite cement present. Abundant small to medium pebble-sized Tm chips. Oval-shaped 0.25-0.75 meter long carbonate concretions present. Usually moderately consolidated, very porous and permeable. Interbedded conglomerate and shale intervals. Interbedded conglomerates are well-rounded, medium to large pebbles of granite and quartzite within a sandy matrix. Conglomerates are usually thin (1-10 m), laterally discontinuous, and planar to lenticular bedded. Shale beds usually localized ½ to 1 meter thick deposits that are laterally discontinuous. Approximately 730 meters thick.

QTpc--Paso Robles Clay Member

Gentle slope former. Dark brown to gray matrix-dominated unit. Matrix predominantly clay, but some silt present. Massive bedding, abundant surface cracks, little vegetation. Clay is hard due to its high cohesion. Extremely sparse clasts, but those found were usually small sub-rounded pebble size Tm chips or fine grained limestone

pebbles. Some rust-colored medium-grained sand lenses in QTpc. The basal member of Paso Robles is marine in other parts of central California (Galehouse, 1967; Page et al, 1998). QTpc might be shallow marine or estuarine environment. An angular unconformity is present within the QTpc. QTpc unconformably overlies Tusc.

QTp--Paso Robles Fluvial Member

Gentle to steep slope former. Brown to gray interbedded conglomerate, sandstone, and siltstone with some sparse mudstone. Conglomerate is clast dominated with sub to well rounded pebble to cobble sized clasts of varying composition: KJf (chert and greenstone/serpentinite), granite/granodiorite, Tvc (rhyolite), basalt/andesite, Tm, Te, m, biotite schist, greywacke, quartzite, and flint. Matrix varies markedly also between sand/silt/clay. Lenticular and planar interbedding of conglomerate and sand layers. Cross-bedding visible within conglomerate beds. Conglomerate laterally discontinuous and lenticular due to cut and fill action. Certain areas within QTp are dominantly granitic, KJf, or Tm derivatives. Related to different sources and probably different aged deposits within QTp.

Sand is mostly quartz with some feldspar grains, cream to light gray in color, medium to coarse grained, somewhat to very calcareous, weakly consolidated, very porous, very permeable, and usually contains rounded pebble sized clasts. Some planar interbedding (1/2-1 meter thick) of silt layers. Massive in part.

Light-dark gray clay matrix is non-calcareous with sparse clasts that are usually grains to small pebbles with various compositions of gr, Te, Tm, KJf chert/greenstone. Hard with abundant cracks. Usually massive.

In situ fracturing of clasts near SAF/other faults. Some deep red Fe oxide staining. Grassy-brushy vegetation cover. Multiple terrestrial braided channels within a river floodplain comprise the inferred paleoenvironment. QTp unconformably overlies Tm and Tebp. Combined thickness of QTp and QTpc is approximately 450 meters.

QTfr--Fault Rocks

Usually cliff formers. Unit characterizes extremely sheared and fractured rocks in which protolith is ambiguous. Fault rocks either fault breccias or cataclasites. Rock strength varies from extremely well lithified (due to strain hardening) to weakly lithified (due to excessive shearing). Clasts often fractured in situ. Everything is highly calcareous, probably due to carbonate replacement/diagenesis from fault fluid interaction.

Fault breccias have angular pebble to cobble-sized clasts of varying composition: granodiorite, granite, m, quartzite, biotite schist, serpentinite/volcanics, Te, Tm. Matrix can be well-lithified calcite cemented sand or weakly consolidated sand. Cataclasite often looks like granite on the outside but has internal sandy matrix. Cream to brown, fine to medium grained, very calcareous sandy matrix. See some green crystals that look like old biotite-some possible epidote alteration on the outside. Clayey and very weak/friable (almost fault gouge) in part. Can often crush with hand. Some sparse black and white small 2-10 cm wide hard resistant ledges, possibly due to strain hardening within a localized shear zone, but usually no definitive shear fabrics or planes are visible due to the chaotic nature of the unit.

Qsp--Sag Pond

Clay filled shallow depressions typically created from right stepover on SAF trace or sub-parallel fault. Small deposits tens of m² in area and under 10 meters thick.

Qls--Landslide

Geomorphic feature that shows recent downward transport of material. Visible scarp at the very uppermost reaches and hummocky topography throughout the main body and toe. Usually associated with nearby faulting and clay-rich formations such as the QTpc. Unit confined to the near sub-surface (under 10 meters thick).

Qgs--Granitic soil

Gentle slope former. Brown to orange, medium to coarse grained sandy soil predominantly composed of unconsolidated quartz and feldspar grains. Some detrital biotite flakes. Larger pebble sized clasts of crystalline granite of varying felsic components. Probable underlying granitic source, although no granite outcrops are visible. Some marbe clasts in the Qgs unit over Tvr deposits. Thickness probably under 10 meters—thin veneer cover.

Qt--Terrace

Matrix dominated, near horizontal unit consisting of dark black clay or silt w/sparse quartz grains. Usually devoid of larger clasts and present within level topography on drainages or hillslopes. Thickness under 10 meters.

Qa--Alluvium

Rock unit consisting of unconsolidated sand, silt, and gravel deposited as terraces in present valleys. 10-50 meters thick.

Structural Geology of the Fault Zone—SW Side

Sub parallel Faults

The southwestern terrain of the field area shows a markedly different geological configuration than the northeastern side. Sub-parallel faults are still present within the southwestern block, but they are not as prevalent compared to the NE block. This is due to the different rock types and different exposure qualities. The southwestern side contains a thicker Quaternary cover (QTp) and does not have as many deeply incised drainages that provide windows into the underlying geology near the trace. The SAF trace runs along the eastern flank of the axis of Middle Mountain, and the Paso Robles unit directly bordering the trace near the crest of the ridge has been subjected to a lesser degree of erosion. While there are most likely numerous sub-parallel faults near the trace on the SW side, the poor exposure limits my ability to document them.

En echelon folds

Several folds are present on the southwestern side. They are different from those found on the northeastern side because they strike obliquely to the SAF. Such en echelon folds are classical strike slip deformation features found in simple shear zones and illustrated in Figure 2.

The Middle Mountain syncline in the southwestern part of Middle Mountain is a gentle en echelon fold (Figure 16). This structure could be a manifestation of deformation in a simple shear zone, or it might have formed from offset along an underlying blind fault. While the first hypothesis is the simpler explanation, the second one cannot be easily discounted. A large fault that offsets Tusg against QTp (best shown

in cross sections G-G', H-H', and Figure 16) lines up particularly well with the active southwest fracture zone (Brown et al, 1967) shown in Plate 1. If the two are indeed connected, and if there was a vertical component to its slip motion, folding of the overlying QTp unit is plausible.

Transverse Faults

A peculiar finding within the southwestern terrain is the presence of faults that strike roughly perpendicular to the SAF trace, hereafter called transverse faults. These faults upthrow the northwestern block with respect to the southeastern block.

Fault plane stereonet vector calculations using the fault trace and topography yielded NE/SW strike and a NW dip, thus indicating that these are reverse faults. Reverse faults strike obliquely (040°) to the principal displacement zone (PDZ) in Figure 2 from Sylvester and Smith (1976). Although our transverse fault angles strike at a higher angle to PDZ (average 076°), reverse faulting in simple shear is compatible with our field observations.

The largest transverse fault is found in the northern part of the field area on the C-C' cross section line. Monterey (Tm), Etchegoin Big Pappa (Tebp), and Paso Robles (QTp) formations are present in the northwestern block, and QTp constitutes the southwestern block (Figure 17). Our mapping to the southeast suggests that the QTp unconformably overlies the Tug unit rather than Tm or Tebp. The absence of the regional Monterey and Etchegoin units suggests this fault marks a substantial boundary and is thus a significant factor in the geologic history of the area. A clear lineation extends from this fault plane at Middle Mountain to the western side of Cholame Creek.

There the rock units display markedly different relationships across the boundary of the inferred fault plane. To the southeast of the fault, the Tn and Tsm display an upright stratigraphic sequence of Tsm over Tn (Section D-D' in Plate 2). To the northwest of the fault, the units are apparently overturned with Tn being on top of Tsm (Section B-B' in Plate 2). Motion along the transverse fault may help to partition this deformation and explain the structural discontinuity.

Figure 18 is a picture of a transverse fault that offsets Quaternary alluvium against QTpc, thus indicating that this fault is active. Slip along these faults might help explain some geodetic anomalies measured on the southwestern side in which some control points were migrating to the southeast contrary to their expected NW-Pacific plate motion (John Langbein, personal communication; Murray and Langbein, in press). While these faults are considered mostly dip slip because of their inferred attitudes, it is possible that these are actually strike-slip faults. Clay cake models show antithetic strike-slip faults that are conjugate Riedel shears (R' shears) that form at a high angle (75°) to the main line of faulting or PDZ (Wilcox et al, 1973). However, some oblique slip must have occurred in order to juxtapose the units to their current mapped positions.

Teddy's Faults

A series of faults are present on the western side of Cholame Creek (Figure 19). These faults were named Teddy's faults after Teddy Gilbert, a friendly local rancher who allowed us access onto his land. These faults maintain a SAF-parallel strike but vary in dip considerably and offset Tertiary volcanics (Tvc), Salinian granite (gr), and Tertiary sediments (Tn, Tsm). The fault juxtaposing volcanic rocks from granite suggests

considerable displacement. The significance of these faults will be addressed further in the discussion section under fault zone evolution.

Cross Section Progression

The following section presents descriptions regarding relevant stratigraphic and structural interpretations within each cross section. One SAF-parallel cross section (L-L') was completed to illustrate an important structure and will be addressed first in the order. The other eleven SAF-normal cross sections are spaced 0.75-1 km apart and are perpendicular to the active SAF trace. The southeastern end of Middle Mountain is geomorphically younger and less deformed than the northwestern portion. Therefore a progression of youngest to oldest from the southeast to northwest will be followed, thus relating deformation features to timing of the uplift. This creates an inverted alphabetical sequence, but it links the geologic history and timing of deformation in a cognitively sensible manner. Furthermore, each cross sectional discussion will progress from southwest to northeast for clarity. Refer to Plate 1 for the geologic map, Plate 2 for all cross sections, and Table 1 for assumptions regarding geologic interpretation.

L-L'

Cross section L-L' illustrates a sub parallel fault (relative dip 22° SE) juxtaposing Monterey shale (Tm) and Etchegoin Big Pappa sandstone (Tebp). The teeth symbols mark the direction the plane dips with respect to the field of view (this fault projects away from the plane of view). A reverse fault dipping 27° NW emplaces Tm and Tebp over the Paso Robles (QTp) unit. Small bodies of Tebp and QTp are bounded by splay and

backthrust faults emanating from the reverse fault near the surface. Another sub parallel fault projects into the field of view and cuts QTpc and QTp (20° SE relative dip).

K-K'

Cross section K-K' shows a relatively simple fault zone. The southwestern block is dominated by the Paso Robles formation (QTp) unconformably overlying the Tvc and Tusg units. Middle Mountain syncline is the broad en-echelon fold (axial plane dips 83°NE) within the Paso Robles (QTp) formation. The inferred fault that separates the Tvc and Tusg units might also account for the folding in the QTp. Numerous sub-parallel faults offset Paso Robles blocks near the SAF trace, creating several small wedge shaped blocks near the trace. The SAF is actually two separate segments on this cross section line, with the southwestern one dipping 48°NE and merging into the other dipping 85°NE. A granodiorite sliver, a Tm sliver, and a Te block dominate the northeastern terrain. The Gold Hill fault is present in the far northeastern corner of the section where it uplifts Tm over Te. A Quaternary alluvial fan unit (Qf) unconformably overlies the gr and Tm units.

J-J'

Cross section J-J' is another fairly simple fault zone. The QTp unit and Middle Mountain syncline (axial plane still 83°NE), overlying an inferred (blind?) fault separating Tvc from Tusg, again dominates the southwest side. The SAF dips 73°NE. A dramatic increase in folding occurs on the northeast side. The Tertiary sedimentary units (Tm and Te) are highly deformed from folds with near vertical axial planes that strike

parallel to the Gold Hill fault (GHF). GHF exhibits its steepest dip in the field area (76° SW). Qf unconformably overlies the granodiorite and Tertiary sedimentary units.

I-I'

Cross section I-I' shows the first complex configuration of crustal blocks within the fault zone that will continue throughout the area. The Tn unit consisting of a red silty conglomerate unconformably overlies the granitic body in the far southwest. The fault offsetting gr against Tvc is nearly vertical here. The inferred fault separating Tvc and Tusg is still present. The QTp now contains an en-echelon anticline (axial plane dips 79° NE) striking parallel to the Middle Mountain syncline (axial plane dips 86° NE). Numerous sub-parallel faults (most dipping moderate or steeply to the northeast) slice the crust near the present SAF trace, evoking a deck of cards model. The SAF itself dips 82° NE. The northeast terrain is dominated by the GHF that emplaces Monterey (Tm) over Etchegoin (Te) along a 72° SW dipping fault plane. The SAF-normal shortening that drove formation of the GHF probably also accounts for the associated GHF-parallel folding in both the hanging and footwalls of the fault. A steep syncline holds a small bowl-shaped body of Te in the hanging wall. The anticline near the GHF might be a fault-propagated fold with the axial plane merging into the GHF at depth. Folding in the footwall of the Etchegoin unit is still present with a near vertical (85° SW) axial plane.

H-H'

Cross section H-H' shows a fault and depositional contact between the Tn and gr in the far southwestern terrain. The fault juxtaposing gr against Tvc is now dipping 62° NE. QTp and QTpc unconformably overlying both the Tvc and Tusg units, which are

now separated by a reverse fault (29°NE) that propagates to the surface. This fault likely steepens at depth, which creates extension and a normal fault in the hanging wall. The QTp/Tusg contact, initially horizontal, is now dipping 69°NE in the small fault block. This indicates about 69° of clockwise rotation. Preferential slip along the reverse fault is the most likely explanation, though extensive strike-slip motion could also rotate the block over time. Stratigraphic relationships within the Paso Robles unit are well illustrated in this cross section. Most of the basal part of the Paso Robles is a clay-rich unit (QTpc), essentially devoid of clasts. Interfingered and largely overlying the QTpc unit is the fluviatile QTp. A fault-bounded wedge of QTp is adjacent to the SAF, which dips 66°NE . The Tm unit is still folded with a small syncline in the hanging wall of the GHF. The GHF shallows considerably between I-I' and H-H' and now dips 40°SW . A large marble body with a near horizontal basal contact overlies Tm.

G-G'

Cross section G-G' illustrates more faulting within the granitic block in the southwestern terrain. The fault offsetting granite (gr) against rhyolitic volcanics (Tvc) dips 54°NE . A SW dipping reverse fault on the SW side emplaces Tusg over QTp. QTpc unconformably overlies Tusg. The SAF dips 73°NE . A pie shaped wedge of QTp is present on the NE side of the SAF. A thin tabular fault-bounded marble sliver is cut by the SAF at shallow depth. An inferred fault separates Te against Tm in the hanging wall of the GHF. The GHF probably steepens near the surface, thus promoting a backthrust in the hanging wall. GHF dips 33°SW and emplaces Miocene Monterey (Tm) over Pliocene Etchegoin (Te). Tvr unconformably overlies both Te and Tm, Qf

unconformably overlies Tvr. A thin veneer of Qgs overlies Tvr, and a small marble block overlies the Qgs unit.

F-F'

Cross section F-F' shows a continuous upright sequence of gr, Tn, and Tsm dipping 45° to the northeast. The fault-bounded wedge of Tvc and QTp is progressively getting smaller towards the northwest. A fault-bounded granite sliver that resembles a ship's keel is encased within younger Tusg sediments. The two bounding faults are inferred to merge into a single vertical fault at a shallow depth. Severe en echelon folding within QTp bedding is probably associated with the southwestern dipping fault offsetting Tusg against QTp in the southwestern terrain. The SAF dips 72° to the NE. The QTp wedge and marble sliver are still present near the SAF trace in the northeastern block. A tabular Tm body is bounded by the GHF and a newly formed reverse fault. This fault steepens near the surface, creating several backthrusts in the hangingwall. These backthrusts warp the Tvr bedding and cut and fold the Etchegoin where they surface.

E-E'

Cross section E-E' shows an inferred fault offsetting two granite bodies on the southwest. The upright NE dipping sequence of gr, Tn, Tsm, and Tusg dominates the southwestern terrain instead of the volcanic (Tvc) basement wedge found further to the southeast. Another upright sequence of gr, Tusg, QTpc is present to the northeast. A SW-dipping fault offsets QTpc and Tusg against QTp. En echelon folds within the QTp contain axial planes dipping 87°SW and 52°NE. The SAF dips 60° SW--one of only 2

places with a southwestern dip. Two fault-bounded blocks showing Qf unconformably overlying Tvr are present in the NE terrain. An exotic sliver of granodiorite is juxtaposed between Tertiary sedimentary units by reverse faulting. This granitic body is an extensive coherent mass bound by continuous inward dipping faults and thus is unlikely a large slide block. Tm is likely still over Te from the GHF that is now outside of the field area/cross section line.

D-D'

Cross section D-D' displays tilted crustal blocks with ordered stratigraphy. The strata in the far southwestern block of gr, Tn, and Tsm dip 17° SW. Another NE-dipping sequence of gr, Tn, Tsm, and Tusg is inferred below Qa. Two other blocks consisting of gr, Tusg, QTp, and QTpc round out the southwestern terrain. All the faults (4) on the southwest side of the SAF dip to the southwest. The SAF reverts back to a NE dip (65°). The faults on the northeastern side also tend to dip away from the SAF and cut sedimentary units. The uplifted granitic body dominates the far NE end of the section. The numerous outward dipping faults contradict a flower structure model (see below).

C-C'

Cross section C-C' contains a large transverse fault that separates two blocks on the southwestern side. The transverse fault is symbolized with the black teeth marks (triangles) and projects in and out of the field of view and strikes nearly parallel to the C-C' line. The previous upright section of gr, Tn, Tsm, and Tusg is now overturned. An overturned sequence of Tsm over Tn is required due to the following map and stratigraphic relationships: 1) Tsm conformably overlies Tn further to the south; 2) Tn was

mapped northeast of Tsm near B-B'; 3) Both units dip 48° to the northeast. The complex transverse fault emplaces Tm/Tebp/QTp/QTpc over QTp near the center of the section. The hanging wall of the transverse fault is cut by numerous steeply dipping sub-parallel faults. The footwall contains largely undeformed QTp. The SAF dips 60° NE, and a steep (72° SW) reverse fault emplaces Te over Tvr in the northeastern block.

B-B'

Cross section B-B' shows an upright sequence of gr, Tn, Tsm at the far southwestern corner of the section. A fault bounded overturned syncline exists on the western side of Cholame Creek, mainly derived from the stratigraphic relationships of Tn and Tsm and their mapped positions (refer to C-C' for more discussion). A thin fault-bounded sliver of Monterey shale is pinched out at depth due to the merging of faults. An overturned block with Tebp (older) over QTp (younger) is present to the northeast of the Tm sliver. This relationship is most likely due to rotation induced from preferential slip along the fault that uplifts the Tm sliver. The southwestern terrain shows rich stratigraphic relationships, mainly the interfingering nature of the QTp and QTpc and those units unconformably overlying the Tebp unit. The SAF dips 79° NE. The fault offsetting Te and Tvr now dips 68° to the northeast.

A-A'/SAFOD

Cross section A-A' incorporates the SAFOD location and wellbore, and wellbore picks within this section will be conducted in feet to correlate with logging measurements and basic drilling protocol. The overturned syncline on the western side of Cholame Creek is still present due to map and stratigraphic relationships around C-C' and B-B'. A

fault bounding the west side of this synclinal structure dips roughly 54° at the surface but likely shallows out at depth and cuts the bottommost part of the overturned syncline. An increase in cataclasite was found at roughly 3400' measured depth (MD) in the SAFOD wellbore (Draper, personal communication), and I have inferred the two faults merge. The next fault to the northeast (approximately $\frac{1}{4}$ of the way over from the A line in the section) juxtaposes Tusg against Tsm. Although the two units are perhaps stratigraphically related, the opposing dips measured in the field prompt inference of Tusg as an allochthonous fault-bounded block. The Tusg/Tsm fault is clearly visible in the field and dips 48° NE. A geologic change from Etchegoin Big Pappa sandstone to granite was measured at 2000' in the SAFOD wellbore mudlog. A continuation of this fault plane matches up nicely with the geologic change in the wellbore.

The mapped relationships between the Tebp and QTp illustrate an undulating plane rather than a rectilinear one, and this is indicative of an unconformity. I have inferred a shallow unconformity contact between the two units at approximately 400' measured depth in the SAFOD wellbore due to the increase in sandstone composition and the nearby mapped Tebp.

A steeply dipping fault (88° SW) offsets different blocks of Tebp. This fault may be the Buzzard Canyon Fault noted by some USGS scientists (Rymer, personal communication), but no definitive mapped fault position is currently available in a publication so the correlation is premature. Another southwestern dipping fault (59°) offsets Tebp against QTp. The two faults have to merge at a relatively shallow depth (1100'). I have inferred the steeper one to cut the shallower one due to different extents

of shearing visible at the surface. Also, a small 4 meter wide fault-bounded lozenge of Tm (not shown in the cross section) is present within the steep 88°SW dipping fault zone, suggesting a larger amount of offset along that fault. A small syncline with an axial plane of 87°SW is present within a small bowl-shaped QTp body.

A 53°SW dipping fault places QTp against Tebp. The SAF dips 84° SW at the surface and offsets different facies of the Etchegoin formation. The fault separating Tvr and Te now dips 79°SW, showing the gradual warping between A-A' and C-C' and heterogeneous along-strike fault plane orientations within the fault zone. The Tvr unit contains numerous near horizontal granite and marble slide blocks.

SAFOD data indicates a striking geologic change from granite to arkosic sandstone at 6310' MD in the wellbore (Hickman et al, 2005). I have inferred this change to merge with the 88°SW and 53°SW faults mapped at the surface. I interpreted the lithologic changes at 6480', 7370', and 8350' from the SAFOD mudlog to be a downsection progression from Tebp to Tusg to Tsm to Tm. I also inferred a fault contact at 8830' to separate the Tm from another Tsm body. Finally, I've made the formation calls myself from the mudlog.

A clay-rich shear zone consisting of illite and smectite was cored within the Tsm unit at 10,062'(3067m) (Solum et al, 2005; Hickman et al, 2005).

A geologic change from arkosic sandstone to an interbedded siltstone and shale belonging to the Great Valley sequence (Kgv) occurs at 10,360' (Evans et al, 2005). Active casing deformation occurring at 10,876' (Zoback and Hickman, 2005), a low velocity zone and serpentinite peak at 10,942' (Solum et al, 2005), a moderate M=0

earthquake in May 2005 at 11,204' (Ellsworth et al, 2005), a marked change in bedding at 11,581' (Hickman et al, 2005), and a large drilling break at 12,746' (Hickman et al, 2005) are factors that delineate separate fault planes within the Kgv unit.

The Kgv is interpreted to be Cretaceous due to distinctive microfossils found in the drill cuttings indicative of the Great Valley sequence (Hickman, personal communication). The Great Valley sequence overlies the Franciscan complex (Dibblee, 1973), but the Franciscan is exposed at the surface in the far northeastern end of the cross section (Dibblee, 1971). I infer that the fault separating Tvr and KJf at the surface splays and bounds the Kgv unit, implying a fault-bounded lozenge of Kgv with several internal faults. Other Tertiary units below the Etchegoin are inferred, but adhere to regional stratigraphic relationships (thicknesses and age, Dibblee, 1973).

The cross section was drawn in January-February 2006. While some details of unit descriptions, other mudlog calls, and reported transitions may change, the essential character of the fault zone structure as depicted in A-A'/SAFOD will not.

This cross section illustrates a steeply inclined shear zone approximately 610m (2000') thick composed of numerous faults with similar orientations. This suggests the image of a tilted deck of cards model in which the thin crustal blocks are analogous to cards that move laterally with respect to each other in non-rigid deformation (Davis and Reynolds, 1996).

CHAPTER 4

DISCUSSION

Fault Density

Fault density in this area is uncertain due to the extensive Quaternary units partially or wholly covering faults. Some structures were undoubtedly missed because they are obscured at the surface.

Figure 20 shows the field area broken up into four different sections, beginning in the southeastern part (Section 1) and moving progressively toward the far northwestern end (Section 4). This progression correlates to timing of deformation—southeastern end being younger than the northwestern end. Section 1 contains cross sections J-J' and K-K'; section 2 incorporates G-G', H-H', and I-I'; section 3 contains D-D', E-E', and F-F'; and section 4 incorporates A-A', B-B', and C-C'. The bar graphs show lateral fault distribution from the SAF in 500 meter bins, but excluding the SAF itself.

Figure 20.1 (Section 1) shows: (1) The lack of numerous faults, and (2) The relative closeness of the faults to the SAF trace.

Figure 20.2 (Section 2) shows: (1) A marked increase in the number of faults present, (2) The relative closeness of the faults to the SAF, and (3) The beginning of the lateral migration of these faults outward, particularly to the SW into the Teddy's Faults locale.

Figure 20.3 (Section 3) illustrates: (1) A decrease in the number of faults within 500 meters of the SAF on both sides, (2) A jump in the number of faults to the NE in the 1000-1500 bin, and (3) A generalized distribution of faults in the SW portion.

Figure 20.4 (Section 4) shows: (1) An even further decrease in the number of faults directly adjacent to the SAF (500 meters on each side). (2) An increase in the density of faults in the SW side, as well as a spike in the 1000-1500 bin. .

These data illustrate the evolution of fault zone width through the fault zone. The younger area shows a localized 1 km wide area that contains most of the faults, whereas the older northwestern section shows a generalized distribution of faults laterally outward in a wide 3 km zone. The fault zone becomes progressively wider with time most likely due to progressive shearing or deeper exhumation.

Flower Structure Model

My extensive cross sectional analysis allows me to ask a simple yet important question: Does the flower structure model (Figure 3) work in this locale? While uncertainty develops in the cross-sections below 300 feet (that uncertainty is reflected in the cross-section symbology), the fault attitudes at the surface were accurately calculated and their orientations represent a structural model throughout the study area. The northeast side actually does show a slight propensity for flower structure characteristics with inward dipping reverse faults. The southwest side, however, does not show a preferred dip direction. I find a complex series of faulted and translated blocks rather than a neat flower structure depiction (Plate 2).

Another important feature of the flower structure model (Figure 3) is a vertical master strike slip fault in which all the other reverse faults merge into at depth, usually regarded as the SAF trace. However, my eleven SAF attitude calculations yield a much richer result. The SAF is not vertical. It yields a northeastern dip for 9 of the

calculations, and a southwestward dip at two cross section locations (Figure 21). My 84 degree southwestward dip on the SAF at A-A' is verified by the SAFOD wellbore data that calculated an 85 degree southwestern dip (Hickman et al, 2005). This strong correlation between surface and subsurface fault planes lends credibility to my fault plane calculations.

Because the SAF has been migrating to the northeast since the late Miocene (Dickinson, 1981), some might argue that the southwestern-dipping faults on the southwestern side might have been created in a past flower structure setting when the terrain in question was actually on the northeastern side of the active SAF. Such a scenario is illustrated in Figure 22, where the blue faults would exemplify the faults in question. However, several of these faults offset the QTP that was deposited on the southwestern side of the SAF in the Plio-Pliocene (Galehouse, 1967). Therefore the timing of motion along these southwest-dipping faults is constrained to be after deposition of the QTP and post emplacement of the present SAF trace location. These faults likely originated with their current geometries near their current positions, thus further discounting a flower structure model at this locale.

Subhorizontal Detachments

Because zones of transpression are associated with shear and PDZ-normal shortening, geologists have had a propensity to use flower structure models to explain the structure. Many assume all the deformation has to merge into the SAF at depth because it is the only thing that can accommodate strain. This is not the only possible scenario. Page et al (1998) thoroughly discussed the geological evolution of the Coast Ranges in

southern and central California. They noted P-wave velocity discontinuities along subhorizontal boundaries probably due to a detachment zone with ductile shear. They proposed a middle crust with ductile rheology that has been horizontally shortened and vertically thickened due to compression normal to the SAF (Figure 23).

A horizontal detachment zone in the lower crust has been postulated to explain paleomagnetic rotation of blocks in the Transverse Ranges as well as deep seismic flat reflectors in the Mojave Desert and Transverse Ranges (Sylvester, 1988). Hearn and Clayton (1986) used tomography of P-waves and velocity variations at a depth of approximately 10 kilometers to suggest detachment zones within the crust in southern California. Sylvester (1988) notes that major strike-slip faults are not seismically imaged below these horizontal detachments, and postulates that the faults may be cut by the detachments. Sub horizontal reflectors within the Salinian block at 6 to 14 km depths near SAFOD have been recently imaged by seismic surveys (Ryberg et al, 2005).

A ductile zone within the middle crust decoupled from the rigid lower crust (Page et al, 1998) allows strain from folds and faults in the upper crust to merge into this zone rather than the SAF. This result would thus explain the activity of the structures adjacent to, but not clearly associated with the SAF.

Transverse Fault development

Figure 2 from Sylvester and Smith (1976) shows a diagram of secondary structures within a strike-slip simple shear zone, most notably reverse and normal faults striking obliquely (040°) to the principal shear zone. I mapped three faults that strike nearly perpendicular to the SAF on the southwest side. Fault plane calculations and field

relationships indicate that these are NE/SW striking, NW dipping reverse faults. Major strike slip faults contain reverse faults that extend outward short distances (Sylvester and Smith, 1976).

The mapped faults strike at a higher angle (076°) to the PDZ than those in a typical simple shear zone. However, laboratory models cannot capture the complexity and heterogeneity of nature. Stress variations creating a higher strike angle could account for their nearly SAF-normal orientation.

The southwestern dip of the SAF plane in E-E' may obstruct northwestward movement of the Pacific plate by acting as a "speed bump". This in turn increases compression within the southwestern block possibly promoting the formation of these reverse faults. The large transverse fault (Figure 17) presently lies 1.7 km northwest of the main restraining SAF dip but was directly adjacent to the E-E' restraining dip approximately 51,000 years ago (assuming 3.5 cm/yr Pacific plate velocity). If the restraining SAF dip was still present at that time, it would likely induce compression nearby in the southwestern block and form the observed reverse faults.

Geodetic anomalies measured on the southwestern side in which some control points were migrating to the southeast contrary to their expected NW-Pacific plate motion (John Langbein, personal communication; Murray and Langbein, in press) can also be explained by these faults. If the GPS positions are located in hanging wall of these reverse faults and active slip is occurring (as documented in Figure 18), then the northwestern block could temporarily translate to the southeast against Pacific plate motion.

Transverse fault interaction with the SAF is still ambiguous. The transverse faults probably do not merge into the SAF because they are not inward (NE) dipping. I do not conclude that a flower structure explains Middle Mountain deformation. Instead, these are secondary structures formed in a simple shear zone (similar to en echelon folds) due to strike-slip stresses in the upper crust. A subhorizontal decoupled layer/zone in a ductile middle crust (Page et al, 1998) would allow these transverse faults to merge into it rather than bending severely around into the SAF.

Recent data from the SAFOD wellbore indicates that the least principal stress (σ_3) is vertical (Zoback and Hickman, 2005). This data is indicative of reverse faulting more than strike-slip faulting with respect to Andersonian mechanics. Perhaps these transverse faults are a manifestation of complicated stress fields within the fault zone that switch between strike-slip and reverse fault settings.

Fault Zone Evolution

Varying Ages

The complexity of Middle Mountain makes it difficult to work out the evolution of this fault zone. Rock exposures in the area are usually poor to terrible due to the young ages (except for the granites) of the rock units, weak clay and silt matrixes holding the grains and clasts together, and pervasive shearing throughout the area. The ages of the faults vary, and this in turn is manifest in their surface expression. Young faults tend to be straight and rectilinear while old ones are sinuous (Figure 13) due to subsequent deformation along newer faults and folds (Dickinson, 1966). Also,

earthquakes along strike-slip faults induce bending moments on the fault plane that may create a sinuous strike over time (Bridwell, 1975).

Young faults exhibit striking tectonic geomorphic features, while old ones do not. Relative ages of the faults are simply known by the units that they cut. These observations helped me note that many of the faults located on Middle Mountain, except for a few notable sub parallel faults on the northeast side of the trace, tended to be relatively straight, exhibit young geomorphic features, and cut late-Tertiary and Quaternary units. The faults located on the west side of Cholame Creek lack considerable geomorphic signatures, do not display continuous planar geometries, and juxtapose Tertiary and Cretaceous (gr) rock units. Therefore, the faults to the west of Cholame Creek are probably older and less active than those located within Middle Mountain.

A number of factors suggest that the northwestern part of Middle Mountain is older than the southeastern end. Mid-late Tertiary units are present in the northwest, while Quaternary units dominate the southeastern end. This indicates erosion has been at work longer in the northwest and overlying Quaternary units have been transported away. Also, the apex of Middle Mountain lies in the northwestern section, suggesting more time in which uplifting forces have been at work. More faults are exposed at the northwest section, and the geomorphology indicates younger features in the southeastern end of the uplift.

Remnant SAF

The outward migration of the Mendocino and Rivera triple junctions has extended the length of the San Andreas since the Oligocene (Atwater, 1970). Dickinson and Snyder (1979) correlated northward movement of the Mendocino triple junction to extension and volcanic processes in the overriding plate. Several volcanic fields initiated by this extension are found in central California, and the Pinnacles, Neenach, and Lang Canyon volcanic complexes are directly relevant to this study.

Petrologically similar flow-banded rhyolite, andesite, dacite, and lapilli tuff assemblages overlying granitic basement are present within the Pinnacle and Neenach volcanic fields (Matthews, 1976; Sims, 1993). The volcanic rocks in our field area, denoted Tvc, were named the Lang Canyon volcanics by Sims (1990) and are mostly rhyolitic flows and autobreccias. The striking similarities of these three bodies suggest they were once a contiguous mass. Subsequent SAF tectonism translated the Lang Canyon and Pinnacles volcanic bodies, 207 km and 315 km respectively, to the northwest from the Neenach volcanics (Turner et al, 1970; Sims, 1990). Offset of the Pinnacles and Neenach units, both dated at 23.5 Ma, yield a minimum long-term slip rate of 1.3-1.4 cm/yr in central California (Matthews 1976).

The fault offsetting the Tvc against the granite on the western side of Cholame Creek likely accommodated several tens and probably nearly one hundred kilometers of movement between the Pacific and North American plates. Another concealed fault to the east of the mapped Tvc unit (possibly the SW fracture zone—Brown et al, 1967; Plate

1) likely accommodated 10s to 100s km of offset in the past 23.5 Ma. Both were likely active plate bounding faults in the past.

If the gr/Tvc contact is indeed a remnant SAF trace, it is now most likely dormant due to the severe warping of the fault plane. The active SAF trace presently lies approximately 2.9 kilometers to the northeast, illustrating an overall northeastward progression of the active trace through the field area. Details of the northeastward migration velocity are ambiguous because of the questionable timing of Tvc emplacement varying from 17 to 1 Ma, though this allocthonous block was likely emplaced 2-7 Ma. This yields a generalized range of 0.4-1.45 km/Ma northeastward migration rate. Matthews (1976) noted a similar relationship to the northwest in the Pinnacles volcanic field where the Miocene SAF trace (the Cholone Creek fault) that translated the volcanic body now lies 6.5 km southwest of the present day active SAF trace.

Fault Zone Sedimentation

The Varian Ranch formation, named by Bill Dickinson after the local Varian family, is a localized terrestrial sedimentary unit on the northeast side of the SAF that consists of arkosic sandstone and breccia. Its varying characteristics within a small area along with several angular unconformities (Figure 24) suggest syntectonic sedimentation during its deposition. The poorly sorted nature of this unit reveals a nearby source, and imbrication of tabular marble pebble clasts indicates a west to east paleocurrent. Furthermore, the marble and granitic clasts are not correlative to the Franciscan rock

bodies of the northeastern side but rather are probably derived from the Salinian block on the southwestern side (Page, 1981; Page et al, 1998).

An interesting geological feature found within the Varian Ranch are the small to large (basal area: 25-115,000 m²) isolated blocks of marble and granite that overly Tertiary units mostly in the G-G' to H-H' vicinity (Plate 1). These exotic bodies exhibit nearly horizontal basal contacts and likely have a southwestern provenance similar to smaller imbricated clasts within the sandstone facies. Previous work hypothesized that these were klippen from L-shaped faults in which the fault plane shallowed out considerably near the surface (Dickinson, 1966). Sylvester and Smith (1976) mapped an analogous structure named the Painted Canyon Fault near the Salton Trough fault zone. This outward verging fault bifurcates and shallows considerably near the surface. Sims (1990) proposed an alternative scenario stating these granite and marble bodies were actually large slide blocks. Both hypotheses are illustrated in Figure 25.

The detailed observations support the slide block hypothesis. Most of the basal contacts dip to the east at a very low angle (1-5°). The L-shaped fault would have to bend its orientation from nearly vertical at depth to horizontal at the surface without splaying in the shallow subsurface. Such a fault is unlikely to originate or maintain this configuration for a significant amount of geologic time. Also, our mapping shows small to large bodies of marble and granite lying on the surface in a chaotic configuration rather than along a definitive plane. The chaotic layout correlates well with the large slide block scenario. Abundant earthquakes along this stretch of the SAF would provide ample ground shaking to create fractures that isolate blocks from the parent country rock. If the

southwestern terrain were topographically higher, the blocks would naturally move downslope due to gravitational forces. These blocks are entombed within the Varian Ranch formation that had to be topographically low due to its ability to capture 520 meters of terrestrial sediments during the late Pliocene. Ryder and Thomson (1989) cite similar debris avalanche dynamics to explain the transport of large boulders and blocks several kilometers from their source into the Santa Margarita formation in the southern Temblor Range. The marble and granite sources have been translated to the northwest by SAF movement since Varian Ranch time.

Fault Rocks

Secondary alteration of rocks is present throughout the field area. Microstructural analysis was beyond the scope of this field study, as almost every rock exposure in the area had visible shearing ranging from moderate to severe. In some places the rock was unrecognizable as any of the surrounding units, and a QTfr (Quaternary/Tertiary fault rock) designation was applied. Most/all of the mapped QTfr in the region were either fault breccias or cataclasites—fine to medium grained, well-cemented, lithic-rich rocks that resembled well lithified sandstones on fresh surfaces. Some precipitation of gypsum and other evaporites were found along fault planes, most likely derived from fault fluids.

Deformation mechanisms are confined to microfracturing, cataclasis, and frictional sliding. The abundant microfractures and linkages of these fractures, as well as high differential stresses, allow these units to flow even at shallow depths (Davis and Reynolds, 1996). Sylvester and Smith (1976) mapped a fault zone near the Salton

Trough area and noted basement so pervasively sheared that deformation occurred through cataclastic flow by piecemeal slip on the brittle fractures and shear planes.

Tectonic uplift, fluvial processes, landsliding

Uplift

A fierce battle is forever ongoing in active geological terrains. The constructive forces of tectonism wrestle, scratch, and spit against the destructive forces of erosion. Uplifts of individual ranges in the Coast Range province are a result of compressive stress normal to the SAF, and the transverse shortening above a decoupled zone mentioned previously (Page et al, 1998).

The apex of Middle Mountain lies 800 feet (243 meters) above the adjacent alluvial-filled Cholame Creek and 10.8 kilometers northwest of the southeasternmost nose of Middle Mountain (inferred initiation of uplift) (Figure 21). Middle Mountain is a large and complicated structure likely uplifted from varying fault discontinuities and possible flow of fault zone materials.

The most important issue determining uplift or subsidence is the bending geometry of the fault surface with respect to the slip vector (Sylvester, 1988). Indeed, the fault trace bends from a 319.5° azimuth in the southeastern end of the field area to a 315° azimuth at the northwestern end, a change of 4.5° over a distance of 13.4 km. Bakun and Lindh (1985) noted this characteristic in their Parkfield Earthquake prediction.

Dip discontinuities (Figure 21) also affect the geometry of the fault surface with respect to the slip vector. A 59° southwestward dip at E-E' obstructs the SAF slip vector which probably compresses the SW block. This stress is likely accommodated by the

large transverse/reverse fault nearby. Another hypothesis involves this southwestern dipping SAF acting as a knuckle to the overriding southwestern block, thus creating uplift (e.g., Arrowsmith, 1995). The apex of Middle Mountain lies in between the southwestern dipping SAF and the transverse fault, and overall uplift is probably a complex combination of restraining bend in strike, restraining bend in dip, and the transverse fault. Pervasive shearing of all the units throughout the zone allowed them to flow cataclastically.

Fluvial Processes

Older Tertiary units become more prevalent to the northwest on both sides of the SAF due to longer exposure to erosional forces that scraped off the thick Quaternary units. Erosional forces are not quickly degrading the topography of the rift-arch.

Fluvial processes at Middle Mountain are diminished in strength because the streams are ephemeral in the semi-arid climate. They make axis-normal incisions that provide windows through the Quaternary units.

Landsliding

Landslides are most susceptible in weak, clay-rich units. A majority lie within or adjacent to the Paso Robles clay member. This intrinsically weak unit is often fault-bounded along one contact, and periodic shaking from moderate earthquakes would tend to induce landsliding. However, some of the local ranchers attest that some landslides have occurred within the past few decades mainly due to overgrazing of grasslands by cattle (Gilbert, personal communication). Lower natural vegetation cover would make

the soil less cohesive and therefore more susceptible to destabilize and shear in a landslide event.

Slivering Ideas

Dickinson (1966) first noted the probability of exotic fault bounded slivers existing in this locale. My quantitative cross-sectional work shows the granites on the NE side are bounded by near vertical faults and these tabular bodies probably extend down to at least a 1 km depth. The granitic fault-bounded sliver on the SW side encapsulated within Tusg resembles a ship's keel (Cross Section F-F' in Plate 1), and both bounding faults merge into a single fault at shallow depth. The granitic body in this case seems to be surfing along the crust lending new credence and an even finer scale to Dickinson's "raft tectonics" theory (1966).

Other sub parallel faults bound both granite/granidiorite and marble bodies. These rocks are correlative with of the Salinian block on the southwest side of the SAF (Dibblee 1973; Page 1981). However, some granite and marble fault-bounded blocks are located on the northeast side of the SAF, raising the question of how these units were emplaced. They cannot be explained by a slide block hypothesis due to the continuous alignment of the bodies along definitive northwest-southeast fabrics. The most likely scenario involves the granite and marble originally being on the southwestern side of the fault, but later extensive bending of the fault plane and subsequent conception of a new straight fault to the southwest of the bent fault (analogous to Bridwell's model) could explain the mapped geometric anomaly. A similar example is illustrated by Sims (1993) to explain the presence of the Gold Hill gabbro within the northeastern terrain.

Spatial and Temporal Discontinuity of the SAF Rupture Trace

Figure 26 shows rupture mapping for both the 1966 and September 2004 Parkfield earthquakes. The 1966 rupture mapping, performed by Brown, et al (1967) and compiled by Lienkaemper and Brown (1985), is denoted by the en echelon red ticks. The September 2004 earthquake rupture was mapped by Arrowsmith and Toke and is labeled with the blue lines. I mapped both faults during the 2004 field campaign prior to the 2004 earthquake. The SAF trace juxtaposes Paso Robles (QTp) against an alluvial fan (Qf) unit in the southern area, while in the northern section it offsets different volumes of QTp. The sub-parallel fault to the southwest offsets QTp against its clay member (QTpc).

These observations suggest that the active trace varies in location from rupture to rupture. The 2004 trace is straighter and more consistent with the regional SAF orientation. The more irregular 1966 trace may be less common due to its peculiar dogleg geometry and the 2004 trace's stronger geomorphic features. This behavior may explain the transfer of rocks from the southwest to the northeast side and vice versa that I have noted elsewhere on Middle Mountain. Note also that the 1966 event started only 900 meters to the NW of this area and ruptured to the SE while the 2004 event initiated 10s of km to the SE of this area and propagated to the NW (Bakun et al, 2005). Perhaps variations in propagation direction influenced the position of the ground cracking.

Bridwell (1975) remarkably modeled a similar occurrence with earthquake simulations. An originally rectilinear strike-slip fault trace bends into a curved geometry during the earthquake process from bending moments between an epicenter and the fault

tip. Repeated earthquakes along that fault plane, as seen in on the Parkfield segment (Bakun and Lindh, 1985), creates and even more prominent bend in fault strike. Eventually, the bending moment becomes large enough to lock the fault, and a new straight rectilinear fault is formed that cuts the older structure. The combined mapping efforts of Brown et al, Thayer, Arrowsmith, and Toke (Figure 26) show Bridwell's model occurring in real time!

Recent data from the SAFOD wellbore suggests that active deformation from fault creep is a different plane from the SAF plane identified through geological analysis (Zoback and Hickman, 2005). Clay-rich shear zones, geologic changes, low velocity zones, serpentine peaks, casing deformation, changes in bedding, and large drilling breaks indicate the probability of several fault planes in the SAFOD wellbore (Hickman et al, 2005; A-A'/SAFOD cross section in Plate 2). Nadeau et al (2004) reprocessed decades of microearthquake data near the SAFOD site using advanced analysis techniques, and they postulated two actively creeping sub-parallel fault strands approximately 300 m apart at 2-3 km depth. Langbein, et al (1990) used extensive geodetic analysis to propose that Middle Mountain contains multiple active traces that accommodate slip.

The assumption that the SAF trace is a single active fault plane is thus questionable, and a more likely model incorporates multiple planes. However, this hypothesis might only be valid where at least one trace makes a significant bend in its geometry thus creating an inefficient means of relieving stress accumulation. If a fault plane is clearly rectilinear and stress orientations are constant, the straight fault would

theoretically be able to accommodate deformation by itself as seen elsewhere in California. It is also clearly time dependent and varies over timescales of Ma to years or months.

Fault Zone Strength

A debate regarding strength of the SAF currently exists (Zoback et al, 1987; Scholz, 2000). This is not the primary research goal of our project, but we can discuss surrounding crustal deformation and stress orientations.

The northeastern side of Middle Mountain contains the Gold Hill fault (GHF), which strikes sub parallel to the SAF and emplaces Miocene Monterey shale over Pliocene Etchegoin sandstone. Folds within both the hanging and footwalls, with their axes trending parallel to the SAF as well, seem intricately linked to the GHF. The GHF and associated folds indicate that the angle (ψ) between $S_{H_{max}}$ (σ_1) and SAF strike is nearly 90° in the northeastern block.

The southwestern terrain displays classic en echelon faults and folds within the thick Paso Robles formation. These features, striking obliquely to the SAF [thrusts ($\psi \sim 37^\circ$); folds ($\psi \sim 26^\circ$)], indicate σ_1 ($S_{H_{max}}$) has a more traditional orientation ($\psi \sim 30^\circ$) in the southwestern terrain. This deformation is compatible with a simple shear zone parallel to the main SAF and Andersonian-Byerlee mechanics (Wilcox et al, 1973).

En-echelon folds and thrust faults form in early simple shear deformation, are perpendicular to the axis of shortening (σ_1 or $S_{H_{max}}$), and theoretically strike at a 45° angle to the principal displacement zone (Sylvester, 1988). Folds with SAF-parallel strikes could have originally formed as en echelon folds striking obliquely to the SAF,

but have been subsequently rotated clockwise to a SAF-parallel strike (Scholtz, 2000). However, Hickman and Zoback (2004) note a clockwise rotation of ψ from 025° (1-1.15m) to 070° (2.0-2.2 km) depth in the SAFOD pilot hole. Wellbore breakouts in the inclined portion of SAFOD show ψ rotating and increasing with depth, suggesting suggest low shear stresses on the SAF at depth (Zoback and Hickman, 2005). The southwestern side of Middle Mountain may reflect deformation related to shallow stress orientations and the northeastern structures were deformed by deeper stress orientations that have been subsequently uplifted to the surface. Although this is consistent with the apparent level of exhumation (southwest side is shallower than the northeast side), the SAF-parallel structures (i.e., Gold Hill fault and folds) are not inferred to be excessively deep or old.

Perhaps these different structures may not represent the strength of the SAF but are best explained as manifestations of strain partitioning of the basement units. The southwestern side contains more Salinian basement that is stronger than the Franciscan complex. The stronger material properties of the Salinian basement may induce similar surface deformations, while the weak Franciscan properties would promote weak structures indicative of the basement and not the SAF itself.

General Regional Geology

The simplified structural interpretation for the SAF in central California of the Salinian block juxtaposed next to the Franciscan complex is not valid within the fault zone itself. Our data suggest that steeply dipping regional Tertiary sedimentary units constitute the fault zone. Substantial vertical movements of crustal blocks within the

fault zone likely occurred, with sediments filling in the topographic lows near the active faults. SAFOD data indicates sedimentary units at substantial depth (>10,000 ft) on both sides of the SAF (Evans, 2005) as shown in Section A-A'/SAFOD (Plate 1).

The southwestern terrain includes several fault-bounded slivers of Salinian granite, but in general these granite bodies are rather limited in extent. Perhaps the allochthonous Salinian block was not transported as one cohesive rigid block, but (at least at the SAF edge) in pulses that were ripped off by SAF tectonism. Easily transported sediments derived from Salinia likely filled in the depressions and constitute much of the fault zone.

In the SAFOD wellbore, the eastern side of the fault is probably Great Valley sequence rather than Franciscan (Hickman, personal communication). Yet Franciscan constitutes the northeast side at the surface (Dibblee, 1971), thus suggesting some structural complexity. Thrusting of the Franciscan over the Great Valley, or a fault-bounded lozenge of Great Valley within a large Franciscan body are possibilities. I prefer the sliver theory (A-A'/SAFOD cross section in Plate 2) because several similar features were found within my field area and my mapping provides documentation of a slivering mechanism that would explain emplacement of the exotic blocks encountered by SAFOD. Furthermore, it is unlikely that prior mapping by Dibblee would have missed a large reverse fault.

Therefore, both sides of the fault do not obey the conventional often-cited Franciscan against Salinia model within the fault zone. Further outward laterally, the

generalization of Salinian granite composing the southwest side and Franciscan composing the northeast side is reasonable.

Petroleum Potential

SAF tectonism essentially created Neogene basins and later molded them into favorable petroleum provinces. The formation of these basins (as much as 6 km thick in the Caliente Basin) in southern and central California developed from extensional strain in a broad zone of right-lateral shear (Blake et al, 1978). A more westerly relative shear direction (azimuth) between the Pacific and North American plates about 10 Ma and continued right-lateral slip along the SAF system created localized extension that developed these basins (Blake et al, 1978; Harding 1976; Dickinson and Snyder, 1979). Thick deposits of the organic rich Monterey shale accumulated during the Miocene (Bramlette, 1946; Pisciotto and Garrison, 1981) and would later serve as important source rocks for petroleum generation.

Folding of these basins began in the mid-Miocene and growth of preexisting structures and inception of new folds and reverse faults increased substantially during the Pliocene and Pleistocene epochs due to SAF movement (Harding, 1976) and SAF-normal compression (Blake et al, 1978). These structures grew contemporaneously with continual deposition of sediments, thus creating complex anticlinal and fault petroleum traps (Blake et al, 1978). Some of the most prolific oilfields in North America (the supergiants Midway Sunset and Elk Hills) are located nearby in the San Joaquin Valley (Dibblee, 1973; California Geological Survey) and are a manifestation of folding in simple shear by wrench faulting (Harding, 1976; Sylvester, 1988).

Harding (1976) notes a progressively outward expansion of basin deformation through the Neogene. Some subsurface folds grew during deposition of early reservoirs, but others became inactive while deformation moved basinward. Structural traps from these deactivated structures may be hidden below younger sediments near the basin margin (Harding, 1976). Fault zones bounding Neogene basins (including the SAF zone) might provide localized economic petroleum fields in complex structural traps and detailed structural analysis from surface mapping and subsurface exploration could discover them.

Pop-up structures created from transpressional deformation can contain favorable geometries for the economic accumulation of petroleum. Pop-ups from restraining stepovers of strike-slip faults have created oilfields in the Laramie basin of Wyoming (Stone, 1995) and the Los Angeles basin (Wright, 1991). McClay and Bonora (2001) and produced extensive 3-D sand box models of pop-up structures from varying stepover fault geometries that serve as an analog for pop-up oilfields. My mapping and detailed cross sectional analysis also represents a 3-dimensional model that can serve as an analog for pop-up structures formed from a restraining bend. The structural representation of Middle Mountain can serve as an analog to industry geologists to predict possible productive structures (folds) and compartmentalization structures (faults) within a pop-up oilfield. Furthermore, the heterogeneity of rock units and structures in transpressional uplifts are nearly impossible to replicate in a sand/clay model but are accurately revealed by detailed structural analysis.

Geologic History

The geologic history of the region begins in the mid-Miocene with the deposition of thick sequences of diatomaceous Monterey shale in deep basins near the continental shelf that contained embayments to the nearby ocean (Bramlette, 1946; Pisciotto and Garrison, 1981). These basins were most likely continually lowered by wrench faulting associated with ancient SAF-related tectonic motions that created room for a large accumulation of Monterey shale (Bramlette, 1946; Harding 1976; Blake et al, 1978; Dickinson and Snyder, 1979).

During the late Miocene, regional uplift or sea level regression induced widespread erosion of some Monterey shale members, most markedly in the southwestern terrain. Small amounts of terrestrial conglomerate composing the Tn unit were deposited unconformably over Salinian granite in the southwestern block. Sea level transgression followed soon after, and the Santa Margarita sandstone was deposited over the Tn unit by eastward prograding submarine fans and fan deltas from granitic sources to the west (Ryder and Thompson, 1989).

During this time (late Miocene) the active SAF was located on the western side of Cholame Creek. The SAF moved Salinian granite to the northwest with respect to the Lang Canyon volcanics, though intervening blocks of Tertiary sediments were probably present. This fault likely accommodated at least 100 km of offset. The active trace began migrating (either slowly or in one/multiple jumps) to the northeast around this time.

The region reinitiated subsidence of its marine basins in the late-Miocene and early Pliocene. The Etchegoin was then deposited during the Pliocene in protected bay or estuarine environment with numerous sand shoals and tidal channels (Loomis, 1989).

Uplift of the Santa Lucia and La Panza ranges in the early Pliocene began Paso Robles deposition into a marine basin near the present-day southern San Joaquin Valley (Galehouse, 1967). Major uplift in west central California began about 3.5 Ma (Page et al, 1998) that uplifted part of central California above sea level, thus ending Etchegoin deposition on the northeast side. Also, the Paso Robles unit gradually changed into a terrestrial floodplain environment with fluvial sediments overlying the shallow marine facies (Page et al, 1998).

The SAF trace completed its northeastward migration (2.9 km) and probably was in its current geographic position by the mid-Pliocene. In the Middle Mountain vicinity a granite/marble highland dominated the southwestern terrain in a non-marine setting during the late-Pliocene. A large elongated depression above the Etchegoin constituted the northeastern side, and this depression captured a significant amount of granitic detritus with large slide blocks derived from the southwestern highland, all of which composes the Varian Ranch formation.

Uplift of the Temblor Range around the Plio-Pleistocene boundary ended most Paso Robles deposition on the southwestern side of the SAF (Galehouse, 1967). During the Pleistocene, uplift of Middle Mountain began due to a 4.5° restraining bend in SAF strike and a restraining southwestern dip on the main SAF. Movement along secondary faults within the fault zone and cataclastic flow of units helped further uplift, and Middle

Mountain became the present day ridge rising directly out of the Cholame Valley. The SAF and secondary faults of Middle Mountain have continuously accommodated lateral (and some reverse) slip induced by Pacific and North American plate motion and localized stress fields.

Conclusions

Active fault zones along major plate boundaries are more complex than previously conceived. Past structural research has generalized them due to their inherent complexity, and recent geological studies have emphasized tectonic geomorphology and earthquake geology (paleoseismology) concentrated on the active SAF. My findings suggest that secondary faults, not usually observed in regional mapping and often disregarded within paleoseismic studies, are important structures that play an integral role in crustal deformation.

Intense geophysical and wellbore studies of the area provide a unique opportunity to compare and contrast our field observations to subsurface data. Coupling geologic and geophysical disciplines provide a comprehensive view of fault zone behavior.

The discovery that my detailed geologic mapping matched up reasonably well with subsurface observations from the SAFOD wellbore indicates the possible usefulness the endeavor. Future earthquake research should incorporate detailed geologic mapping to characterize the geometric relationships of fault zones. This will in turn provide insight into important geologic terrains that have been largely overlooked and oversimplified.

Table 1

<i>Cross Section</i>	<i>Assumption</i>
All except A-A'/SAFOD	SAF becomes vertical after 1000 feet.
All	Fault and depositional planes are definite (calculated) for the top 300 feet, and queried/uncertain for the lower 750 feet.
All	Unconformity attitudes are the same as that of the overlying strata.
All	Qa thickness approximately 100 feet thick.
All	Qls and Qgs are thin (under 50 feet) veneers.
All	Qf 280 feet thick.
All	Tn 300 feet thick.
All	Tusg 1000 feet thick.
All	Tsm 1200 feet thick. Regional stratigraphic relationship calculated from Dibblee, 1971.
All	QTp and QTpc are 1450 feet thick (combined). Regional stratigraphic relationship calculated from Dibblee, 1971.
All	Tvr is 1700 feet thick.
All	Tm on NE side is 1700 feet thick. Regional stratigraphic relationship calculated from Dibblee, 1971.
All	Tm on SW side is 1850 feet thick. Regional stratigraphic relationship calculated from Dibblee, 1971.
All	Te is 2350 feet thick. Regional stratigraphic relationship calculated from Dibblee, 1971.
All	Tebp is 2400 feet thick. Regional stratigraphic relationship calculated from Dibblee, 1971.
A-A'/SAFOD, B-B', C-C'	Overtured sequence of gr, Tn, Tsm in syncline (see text).
A-A'/SAFOD, B-B'	Presence of Tusg below Tsm.
A-A'/SAFOD	Presence of QTp below Tusg.
A-A'/SAFOD	Inferred fault bounding NE side of Tusg, covered by Qa.
A-A'/SAFOD	Tebp/gr contact is a faulted contact.
A-A'/SAFOD	Gr and m bodies within Tvr are essentially horizontal and tabular.
B-B'	Gr underneath Qa.
B-B'	Small fault-bounded wedge of Tusg underneath Qa.
B-B'	Overtured sequence of Tebp and QTp in fault-bounded wedge.
B-B'	QTpc and QTp interfinger each other stratigraphically.
B-B'	Tusg underlies QTp and QTpc.
C-C'	Inferred vertical fault under Qa separating gr from QTp.
C-C'	Tm bedding in wedge is the same as the bounding faults.
C-C'	Tebp dipping 45 degrees southwest.
C-C'	Sub parallel faults cut by transverse fault.
D-D'	Continuous upright sequence of gr, Tn, Tsm, and Tusg under Qa.
D-D'	Inferred fault offsetting Tusg against gr under Qa.

<i>Cross Section</i>	<i>Assumption</i>
E-E'	Tsm overlies Tn underneath Qa, same NE dips.
E-E'	Tusg overlies Tsm underneath Qa. Tusg probably correlative to Dibblee's Tsg unit (1971).
E-E'	Inferred fault offsetting Tusg against gr underneath Qa.
E-E'	Inferred vertical fault projected from mapping to the northwest that offsets different Qf volumes.
F-F'	Tsm overlies Tn and dips 45 degrees NE.
F-F'	Inferred fault separating Tsm from Tvc and QTp
F-F'	Faults bounding gr "keel" merge into a vertical fault.
F-F'	QTP wedge just east of the SAF has horizontal dip.
F-F'	Reverse fault plane steepens near the ground surface, inducing several backthrusts that merge into it and fold the Tvr in the hanging wall.
F-F' thru K-K'	QTP unconformably overlies Tvc.
G-G'	Outward (SW) dipping fault cuts inward (NE) dipping fault in southwestern block. Emplaces QTpc, Tusg, and gr over QTP.
G-G'	Inferred fault from nearby mapping offsetting Tvr and Te against Tm. Merges into the GHF at depth.
G-G'	Backthrust offsetting Te against Tm due to increase in GHF dip near the ground surface.
G-G'	Marble near SAF is a fault bounded tabular body.
G-G' and H-H'	Marble overlying Qgs (G-G') and Tm (H-H') is a slide block.
H-H'	Tn/gr contact is a fault in the far SW part of cross section.
H-H'	Small normal fault created from bend in reverse fault inducing extension in the hanging wall. Clockwise rotation of wedge composed of Tusg and QTP in southwestern terrain.
H-H'	QTP/QTpc contact is a facies transition.
I-I', J-J', K-K'	Inferred fault separates Tvc and Tusg.
I-I'	Tusg thicker than 1000 feet here—no granite.
I-I'	Sub parallel fault just west of SAF becomes vertical after 1000 ft.
I-I'	Anticline in hanging wall of GHF cut by GHF.
K-K'	Sub parallel faults offsetting QTP and QTpc merge into the SAF at a shallow depth.
K-K'	SAF is two separate strands, one dipping 48 degrees NE and the other 85 degrees NE. 85 degree plane dominant and cuts the 48 degree plane near the ground surface.
K-K'	GHF is dipping approximately 65 degrees SW.
L-L'	The NW dipping reverse fault cuts the sub parallel fault in the hanging wall.
L-L'	The backthrust fault is cut by the main reverse fault.
L-L'	The two reverse faults merge and the resulting plane is the bisector of those two.

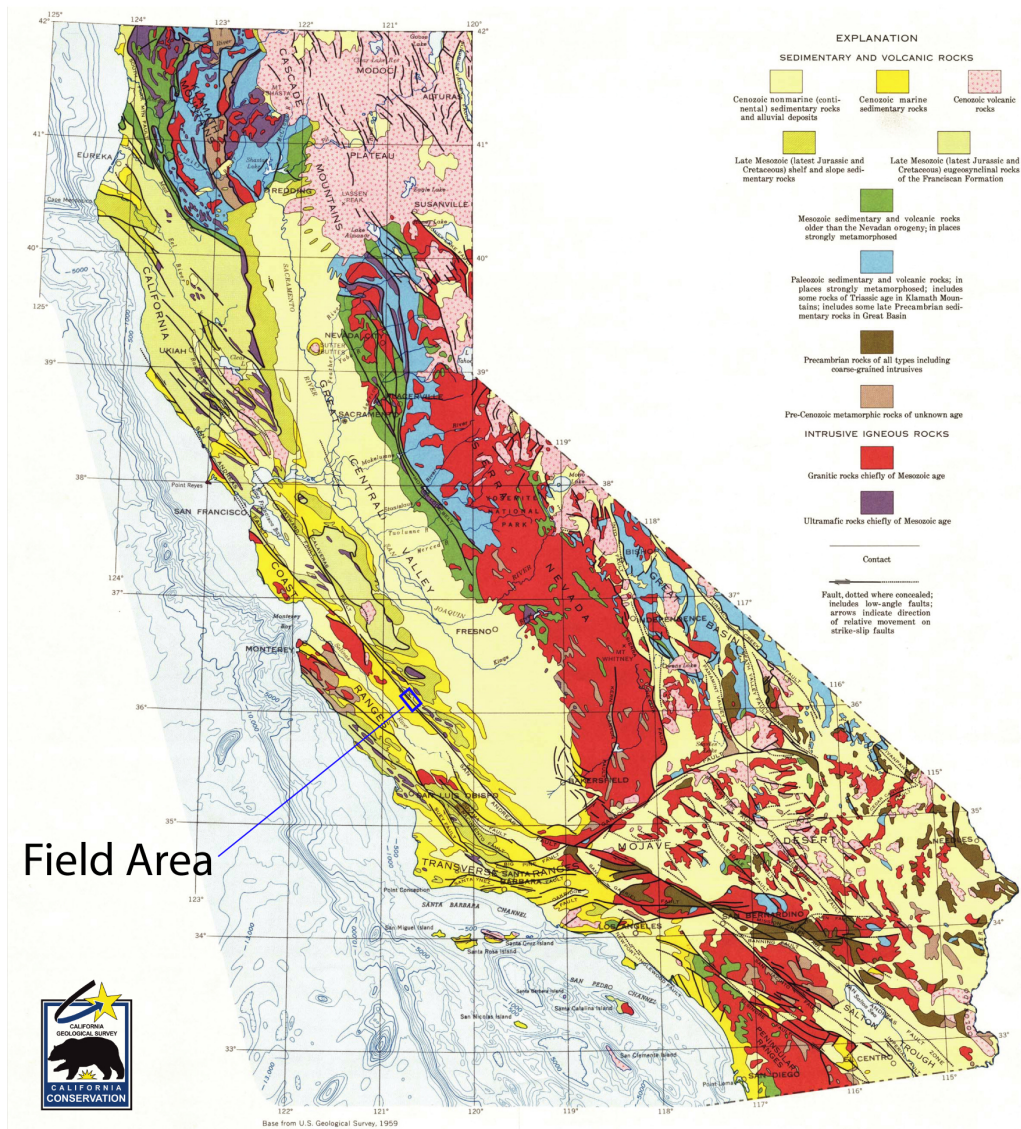


Figure 1. Figure showing regional California geology and the location of the study area near Parkfield, CA. The regional geologic units are shown in the upper right and the field area is denoted by a blue rectangle. The field area consists of the SAF separating Mesozoic Franciscan rocks to the northeast and Cenozoic marine sedimentary rocks to the southwest. Map from the California Geological Survey.

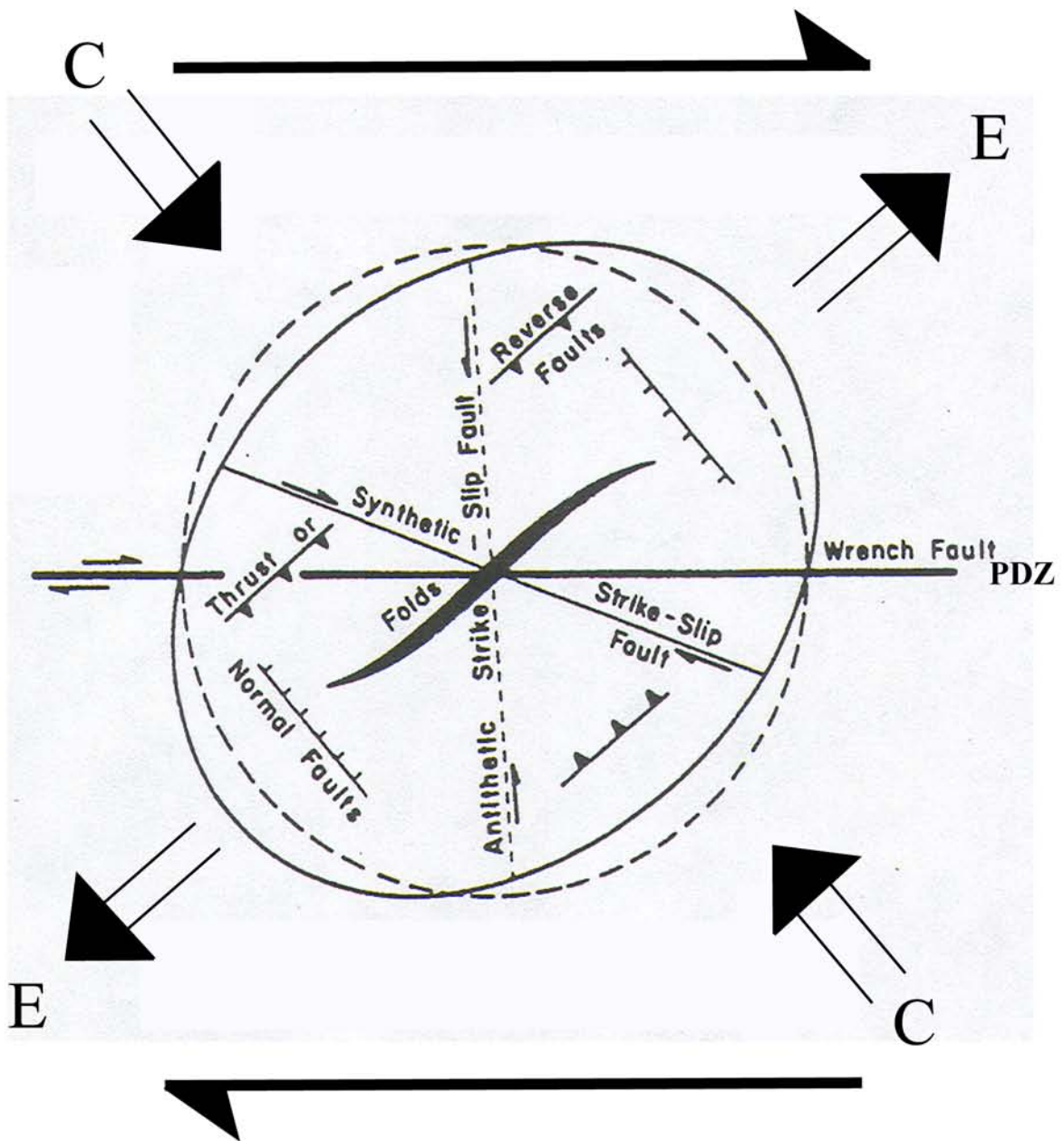


Figure 2. Deformation structures created by continual right-lateral strike-slip (wrench) faulting in simple shear. The long skinny arrows indicate relative motion along the main (center) strike-slip fault, the thick shorter arrows indicate directions of maximum contraction (C) and maximum extension (E), and PDZ is the principal displacement zone parallel to the main wrench fault. Reverse faults and en echelon folds form perpendicular to the direction of maximum contraction, and the normal faults form perpendicular to the direction of maximum extension. Once the structures form they may rotate as passive members within the zone of simple shear. Modified from Sylvester and Smith (1976).

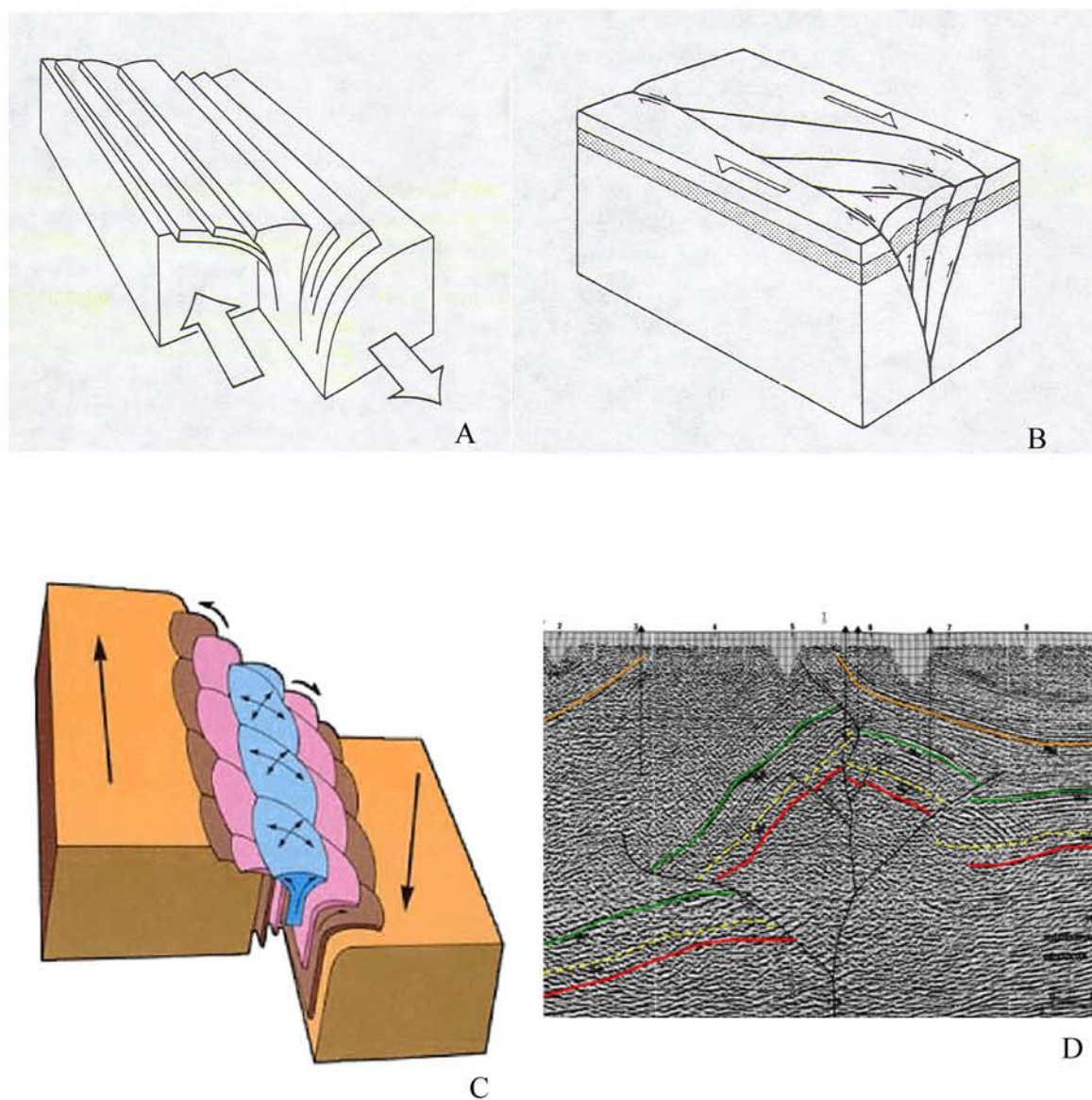


Figure 3. Examples of flower structure models. Several inward-dipping, convex-upward reverse faults merge into a master strike-slip fault at depth. Crustal blocks bound by the reverse faults move vertically upward relative to the blocks lying laterally outward. Examples A, B, and C modified from Sylvester, 1988. Example D from http://www.3d-geo.com/extension/extensional_structural.asp#strikeslipfaulting. Flower structures can accumulate petroleum through structural traps and have been imaged with reflection seismology.

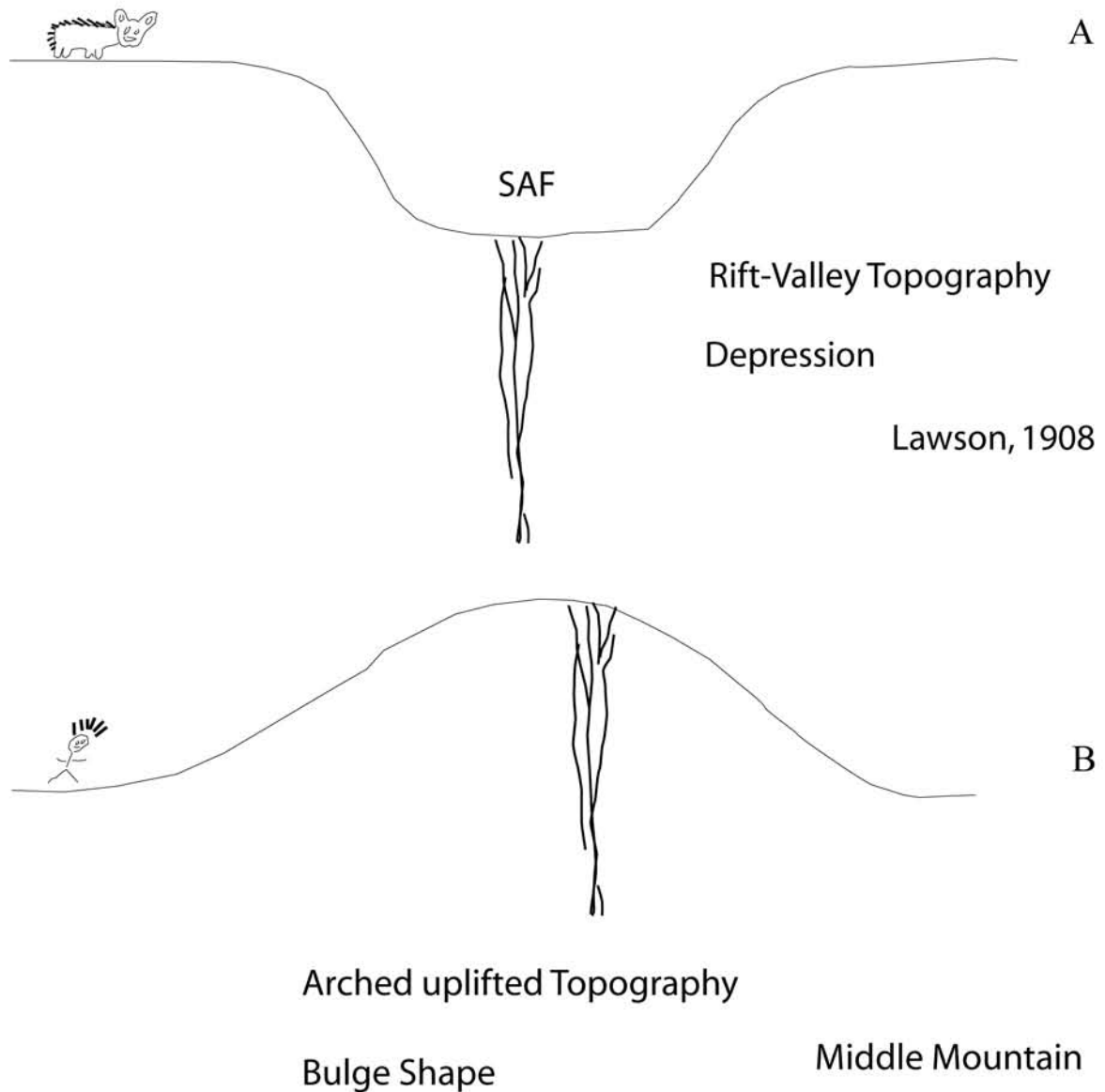


Figure 4. Conceptual diagram showing the different topographic surface morphologies seen along SAF fault zones. Example A shows a typical "rift-valley" profile, while example B illustrates the ridge topography observed at Middle Mountain. Thick accumulations of Pliocene sediments on the northeastern side and Plio-Pleistocene sediments on the southwestern side suggest that Middle Mountain was initially a depression (example A). Active SAF tectonism has inverted the profile to the present-day positive ridge (example B).

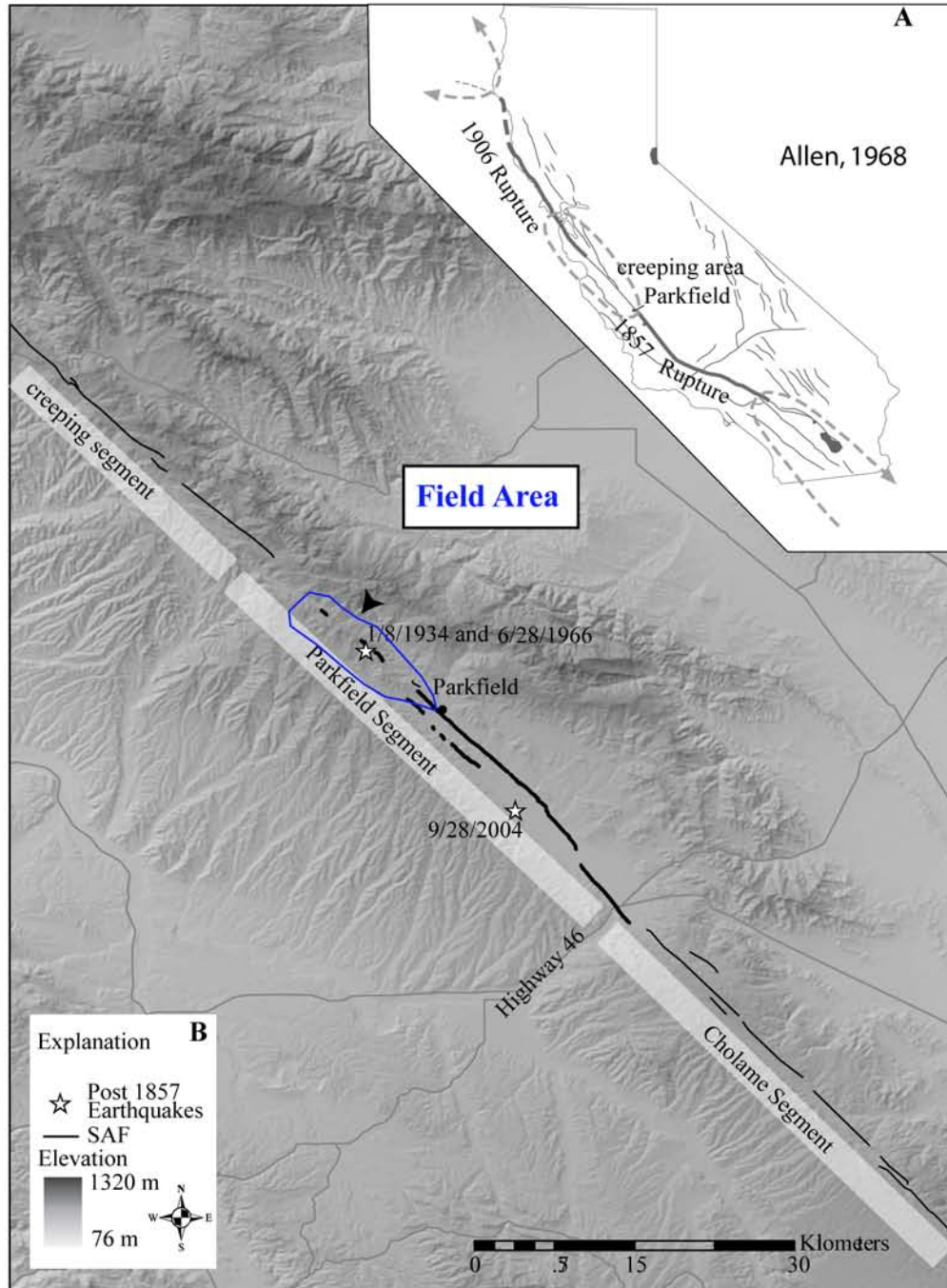


Figure 5. Figure showing three distinct segments of the SAF trace in central California: Creeping, Parkfield, and Cholame segments. The creeping section slips aseismically, while the Cholame segment is currently locked and releases stress through large earthquakes. The Parkfield segment marks the transition between the two slip behaviors and releases stress through fault creep and periodic moderate earthquakes. The last 3 historic earthquakes are denoted by the stars. A) from Toke and Arrowsmith (2005) and B) modified from Allen (1968).

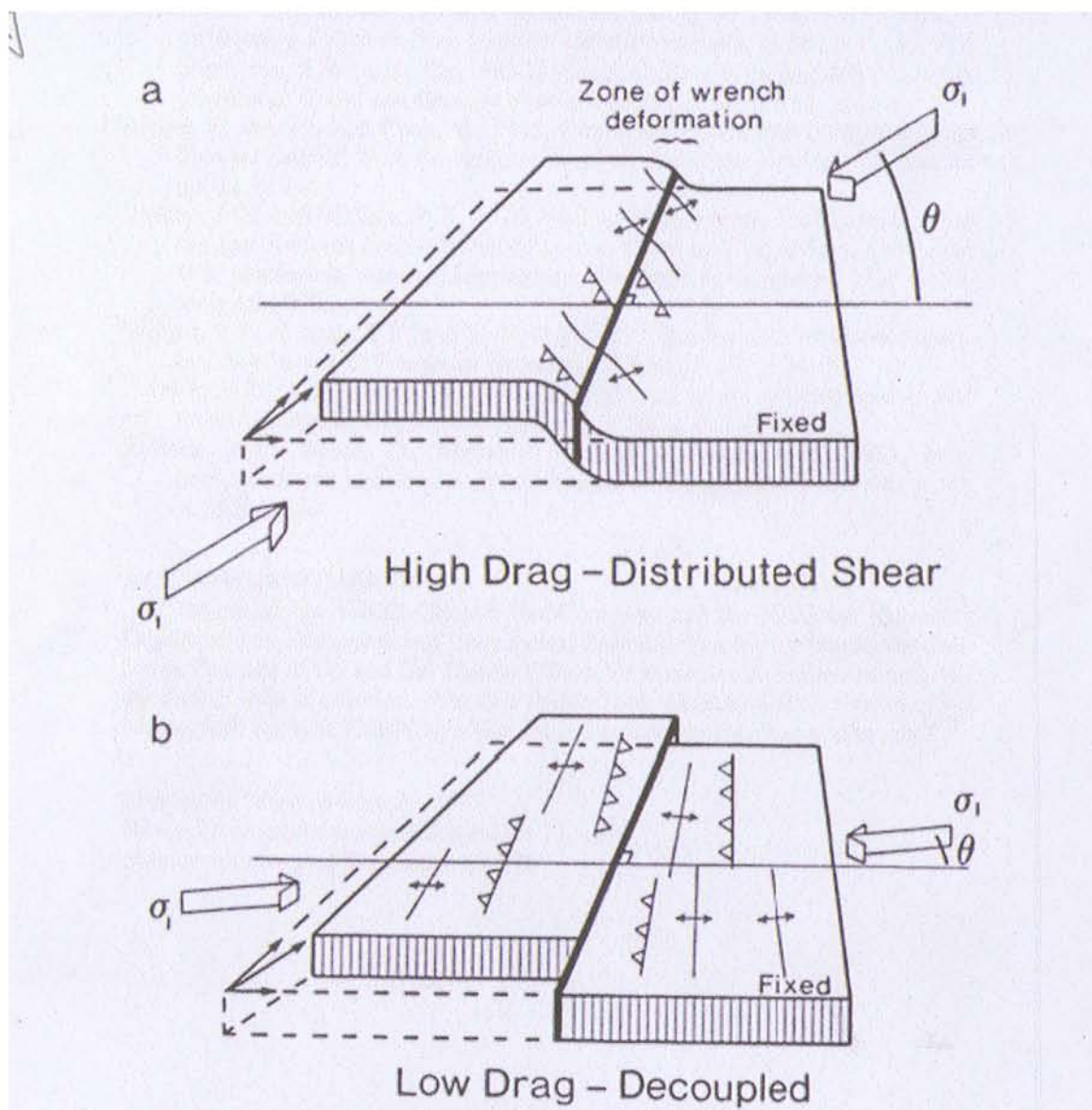


Figure 6. Illustration of different types of deformation related to the strength of the main SAF. Maximum stress orientations are shown by the arrows and are at different orientations for the different models. Strikes of both reverse faults and folds are shown to be perpendicular to the maximum stress orientation. In model a, the main SAF behaves within Anderson-Byerlee high strength framework with normal drag and associated structures. Model b shows a decoupled main SAF with low drag. Middle Mountain deformation can be explained by both models, with the southwest side adhering to the high drag model and the northeast side correlating with the low drag model. Modified from Mount & Suppe, 1987.

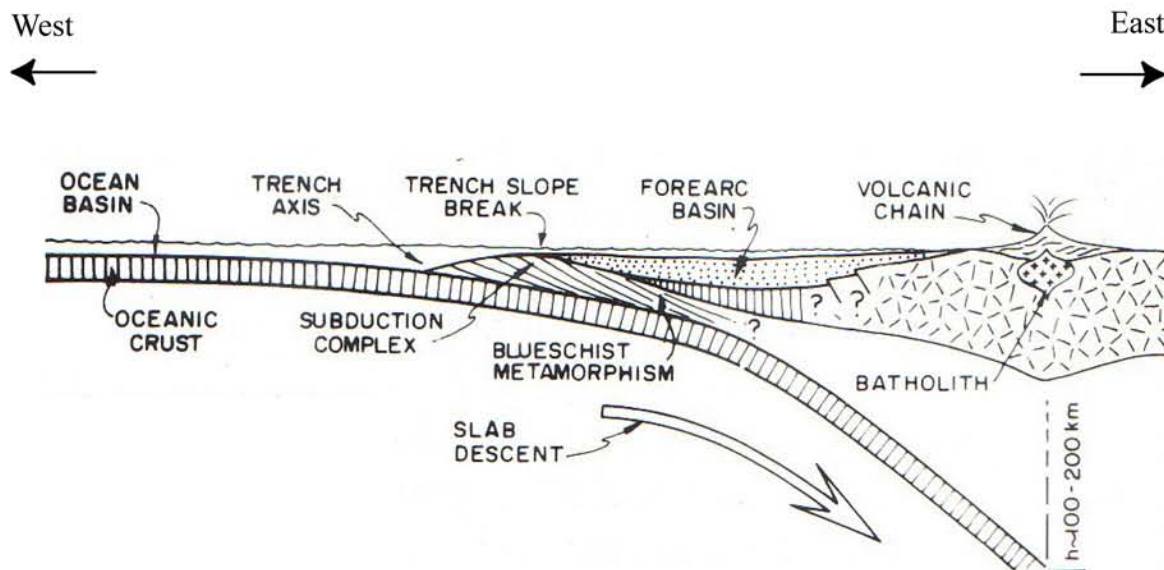


Figure 7. Andean-type subduction associated with underthrusting of thin oceanic crust is subducted below thick continental crust on the California continental margin during most of the Mesozoic. This model explains several of the regional geologic units that dominate central California today. The Franciscan complex was scraped off in an accretionary wedge near the trench axis. A large batholith formed from arc magmatism created the Sierra Nevada geologic province. A large forearc basin captured significant amounts of clastic sediments from the Sierra Nevada and Klamath mountains and comprises the Great Valley sequence. Modified from Dickinson, 1981.

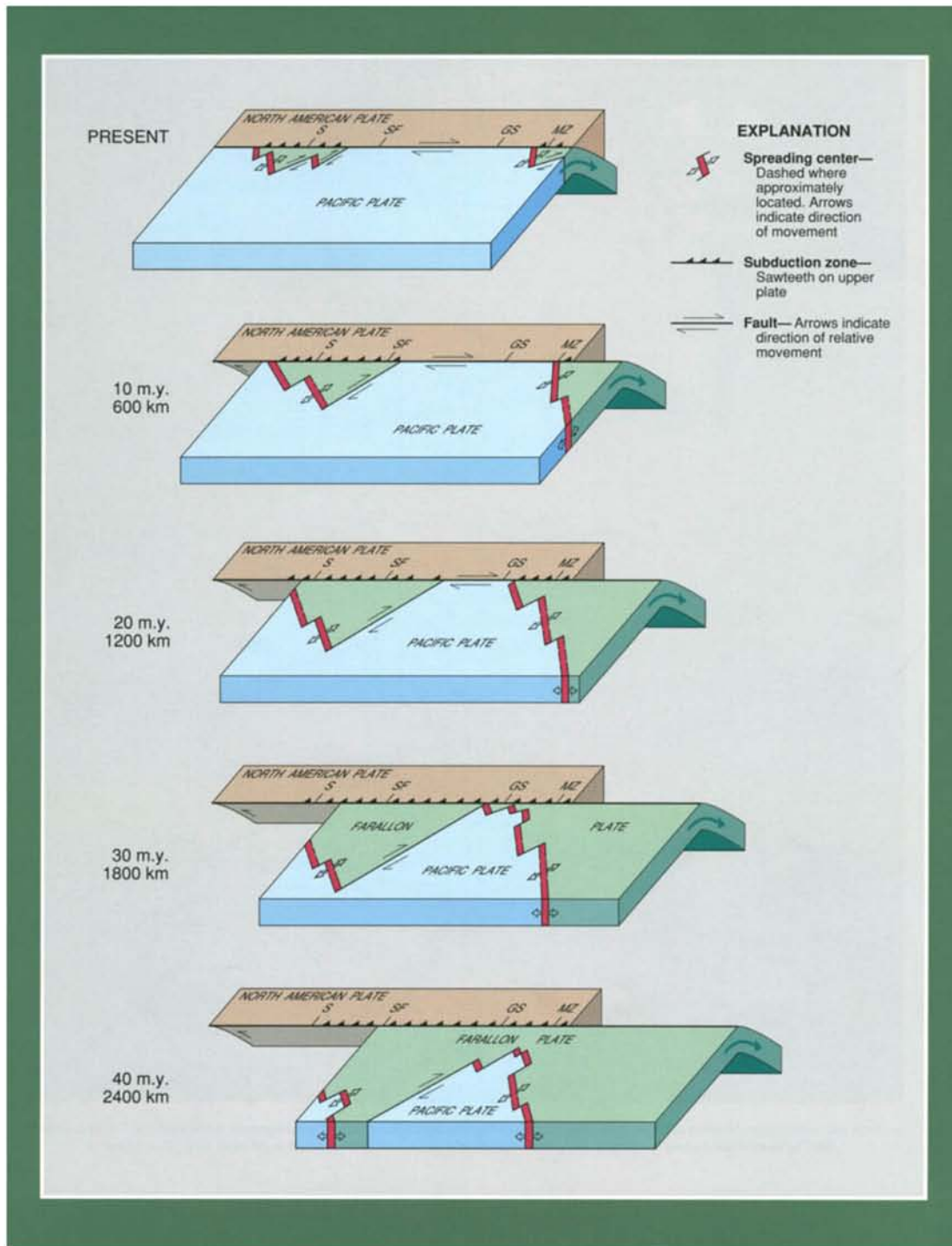


Figure 8. The evolution of the SAF transform system during the mid-Tertiary to present day. The subduction of a mid-ocean spreading center at 29 Ma initiates the transform system and continued subduction of Farallon plate remnants increases the length of the SAF system over time. From Wallace, 1990; modified from Atwater, 1970.

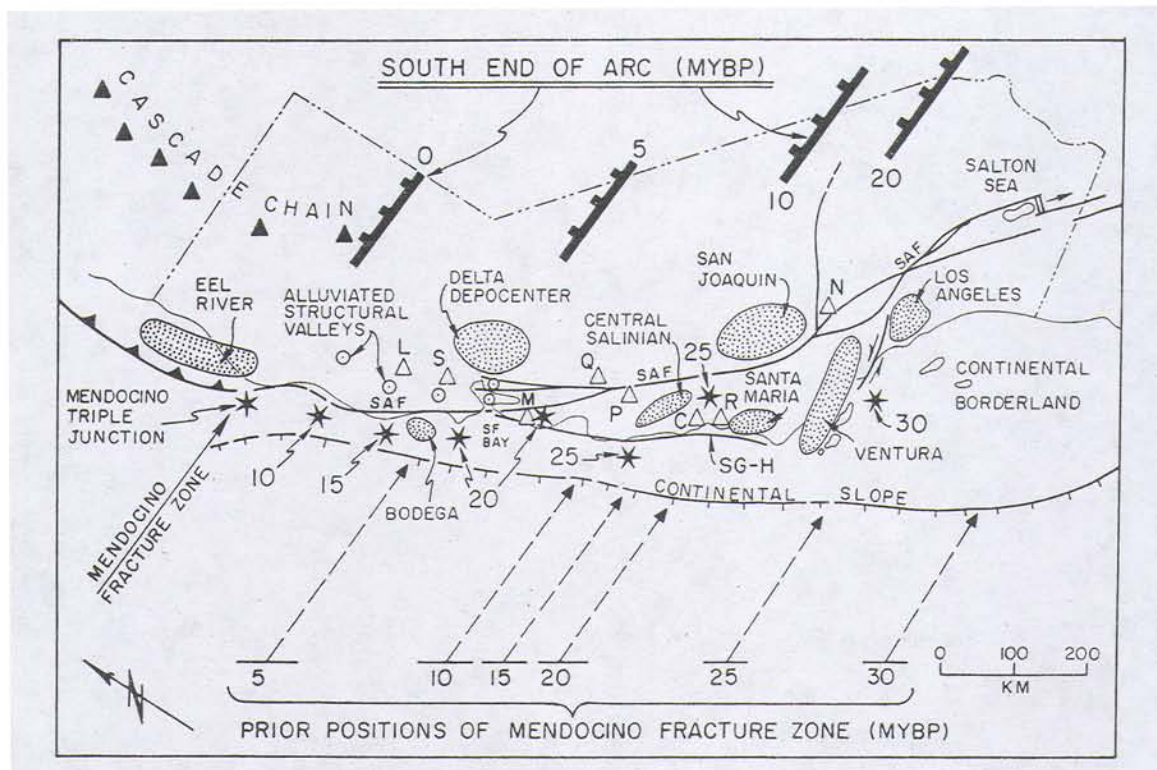


Figure 9. Generalized figure of the western coast of California showing the geologic setting during the Neogene. A northwestward migration of the triple junction is accompanied by formation of the basins and volcanic fields (both likely driven by local/regional extension) and termination of arc magmatism further inland. Stars show northwestward migration of the Mendocino Triple Junction, thick bold lines with cross hatches show the southern boundary of active arc magmatism in the foreland, open triangles are major Cenozoic volcanic fields, and the stippled regions show major Cenozoic sedimentary basins. From Dickinson and Snyder, 1979.

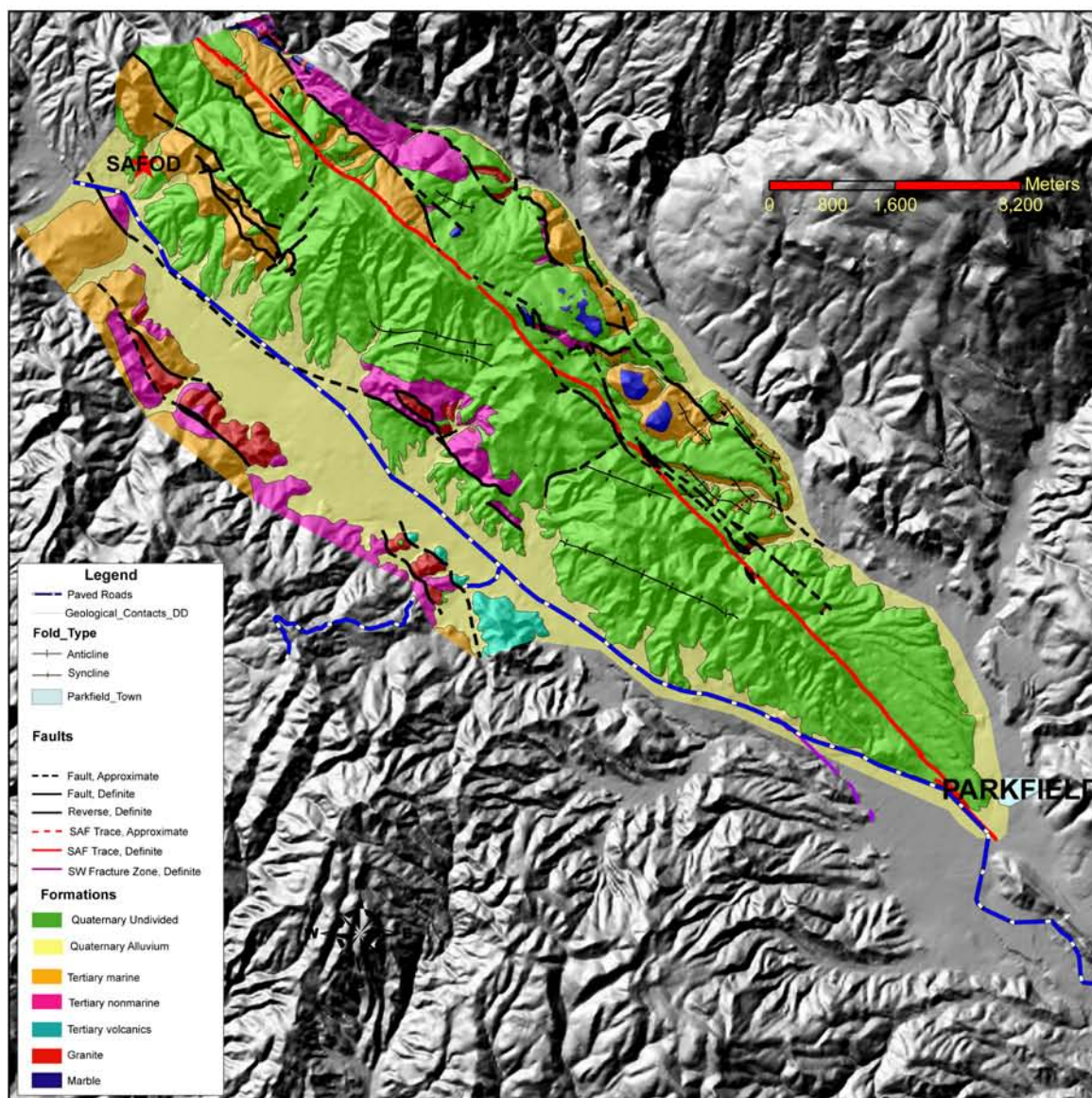


Figure 10. Simplified geologic map of the field area. The arrowhead-shaped mapping area is situated between Parkfield to the southeast and SAFOD to the northwest. It is dominated by Quaternary sediments in the southern half, while Tertiary sediments (both marine and non-marine) tend to dominate the northern half. Exotic blocks of granite, rhyolitic volcanics, and marble are present on both sides of the SAF shown in red, green, and blue respectively. Other major secondary faults and folds are also shown.

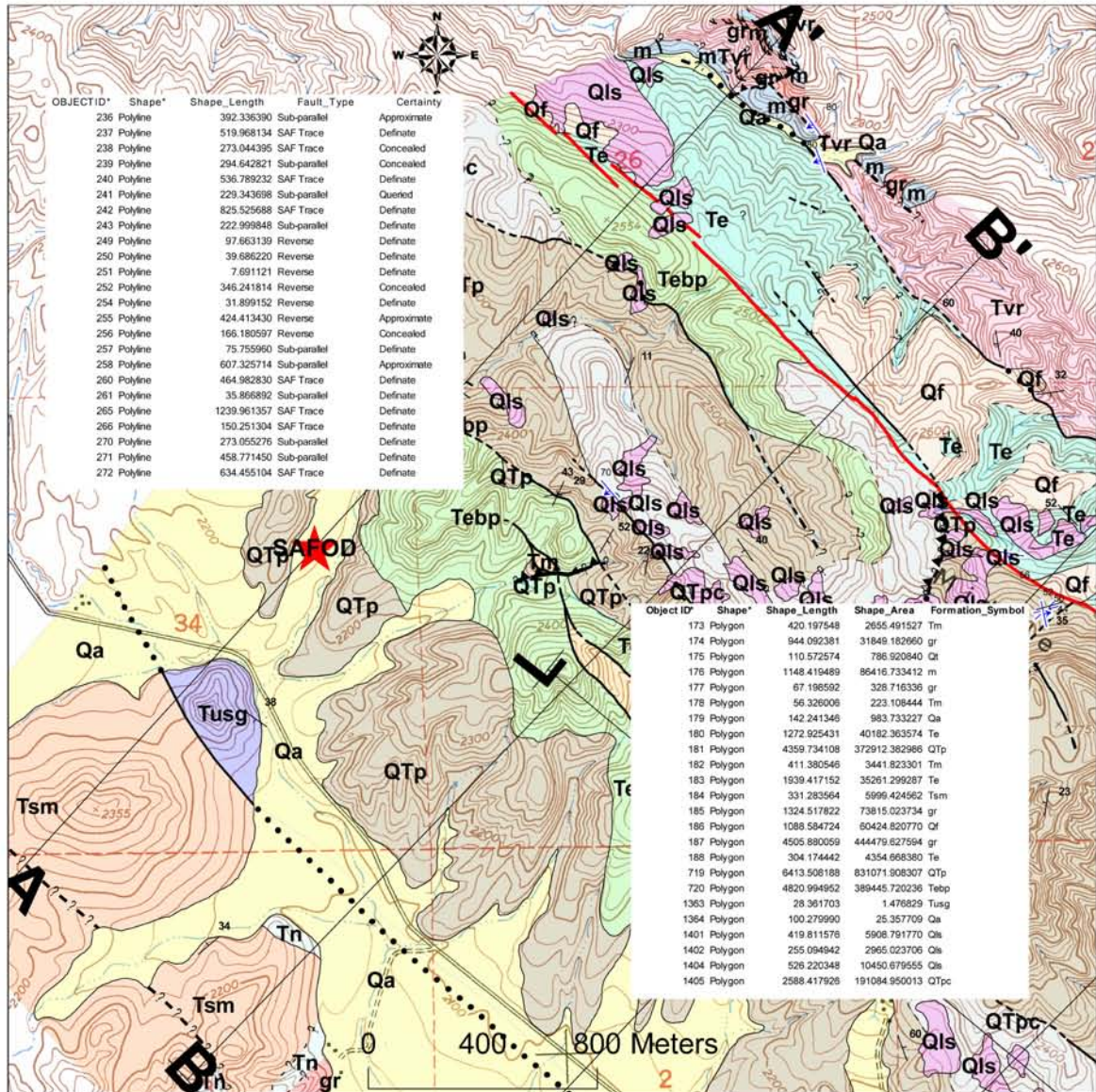


Figure 11. Figure showing attribute tables of feature class files within ArcMap/GIS software. The fault feature class attribute table is shown in the upper left, while the formation feature class is the table to the lower right. Both are superimposed over a zoomed in portion of the geologic map near SAFOD. Fault type and certainty are descriptive value fields within the fault feature class, while the formation symbol is the lone descriptive value field for the formation feature class.

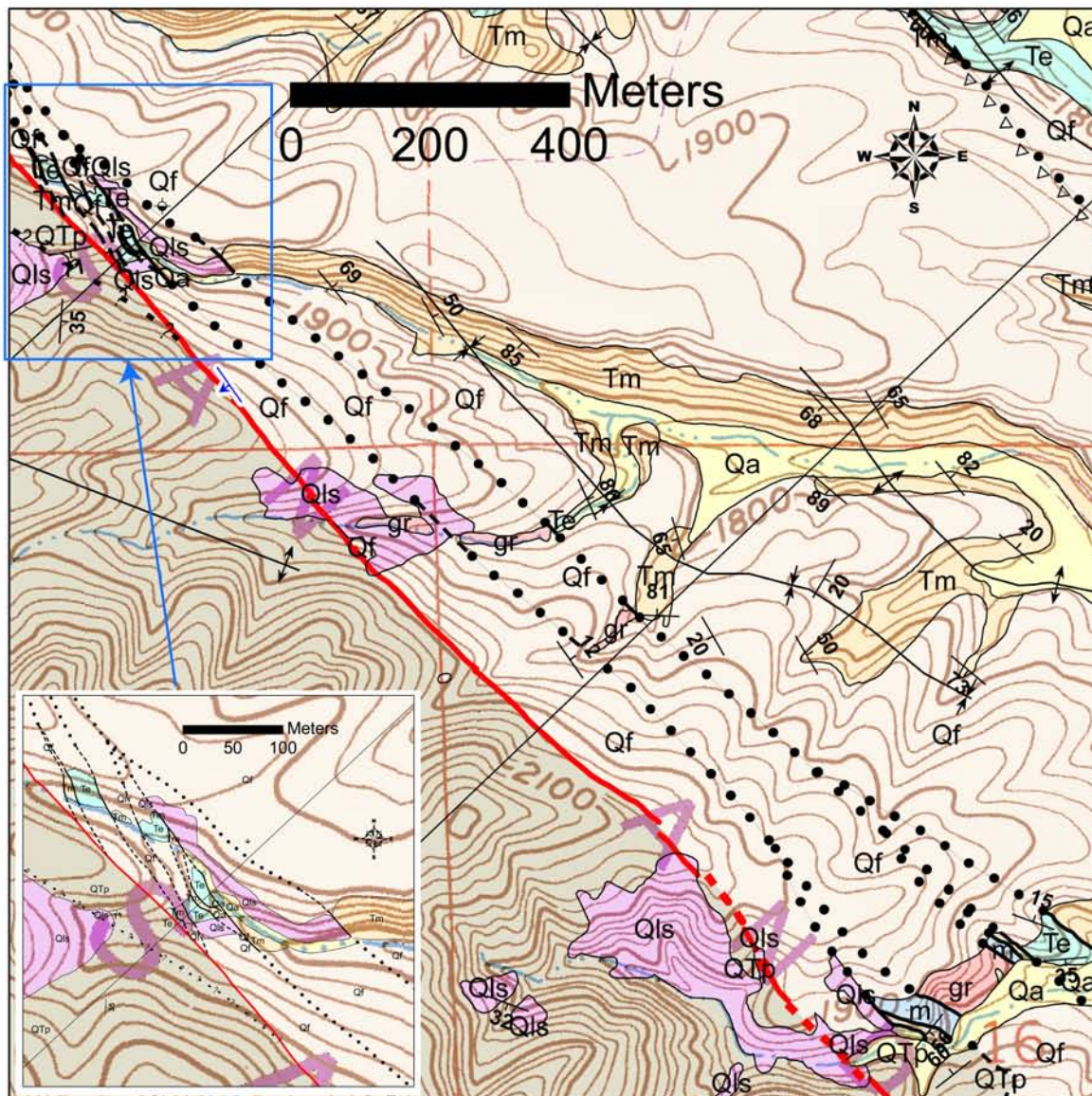


Figure 12. Two zoomed-in portions of the geologic map illustrating several faults striking sub parallel to the SAF. The larger map shows continuation of several faults bounding granite (gr), marble (m), Monterey (Tm), Etchegoin (Te), and Paso Robles (QTP). The faults are partially covered by the Qf unit, and have been denoted as concealed where juxtaposition of units were not visible. The inset map illustrates several densely spaced sub parallel faults cutting Monterey (Tm) and Etchegoin (Te) units. Some of the fault planes are visibly warped in this large scale view. See Figure 13.



Figure 13. Photograph showing a severely warped fault plane. View to the west. Miocene Monterey shale is the orange unit to the left, while the Pliocene Etchegoin sandstone is the white unit to the right. This fault has likely been inactive and warped by surrounding deformation or a through-going shear zone. Location is from the zoomed-in portion of Figure 12 showing faulted Tm/Te blocks.

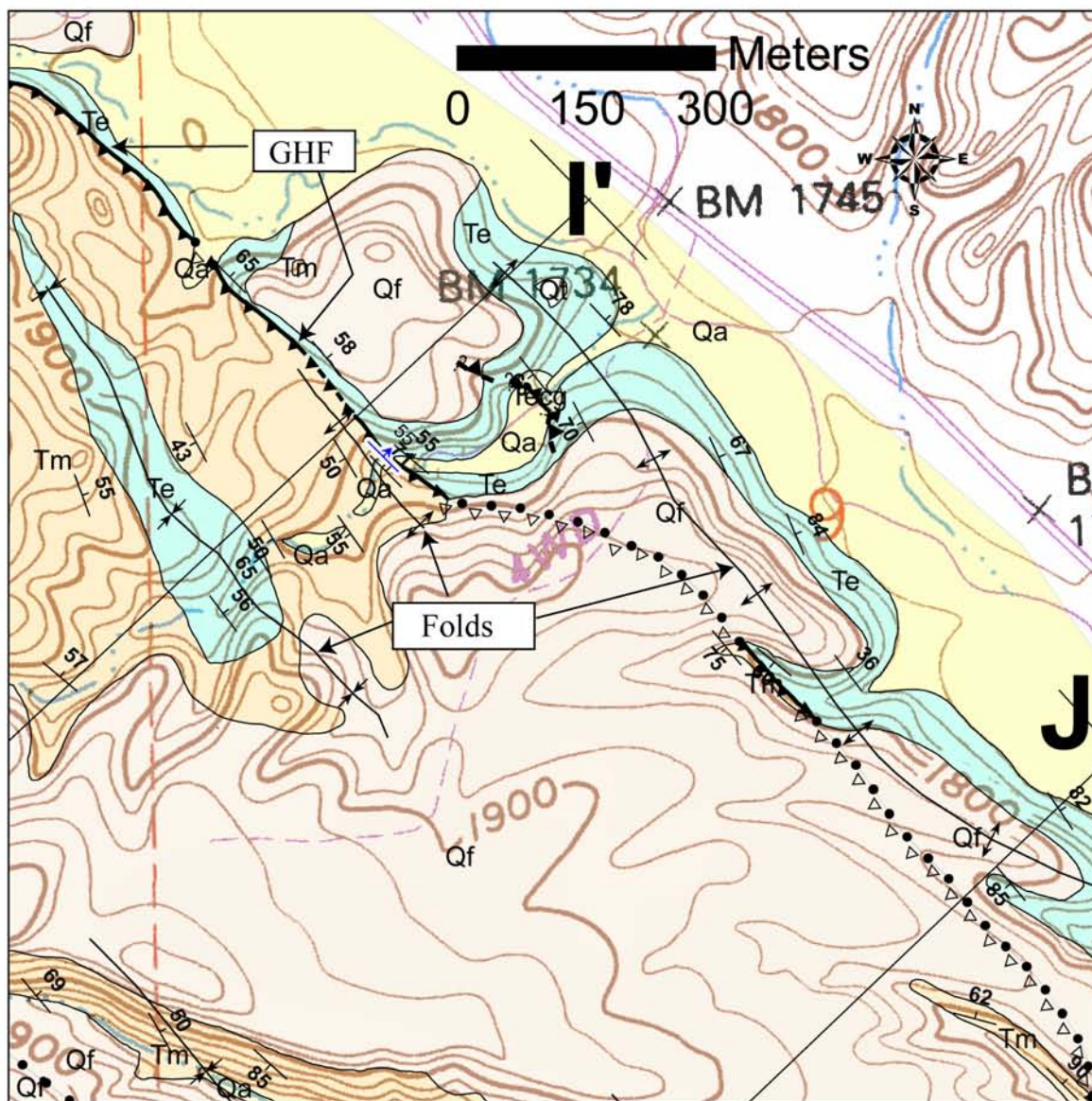


Figure 15. Figure showing a zoomed in portion of the eastern margin of Middle Mountain. Three folds strike parallel to sub parallel to the Gold Hill Fault (GHF). The folds likely formed from the same shortening event that created the GHF and are found in both the hanging and footwalls of the GHF. See I-I' and J-J' for cross section interpretation.

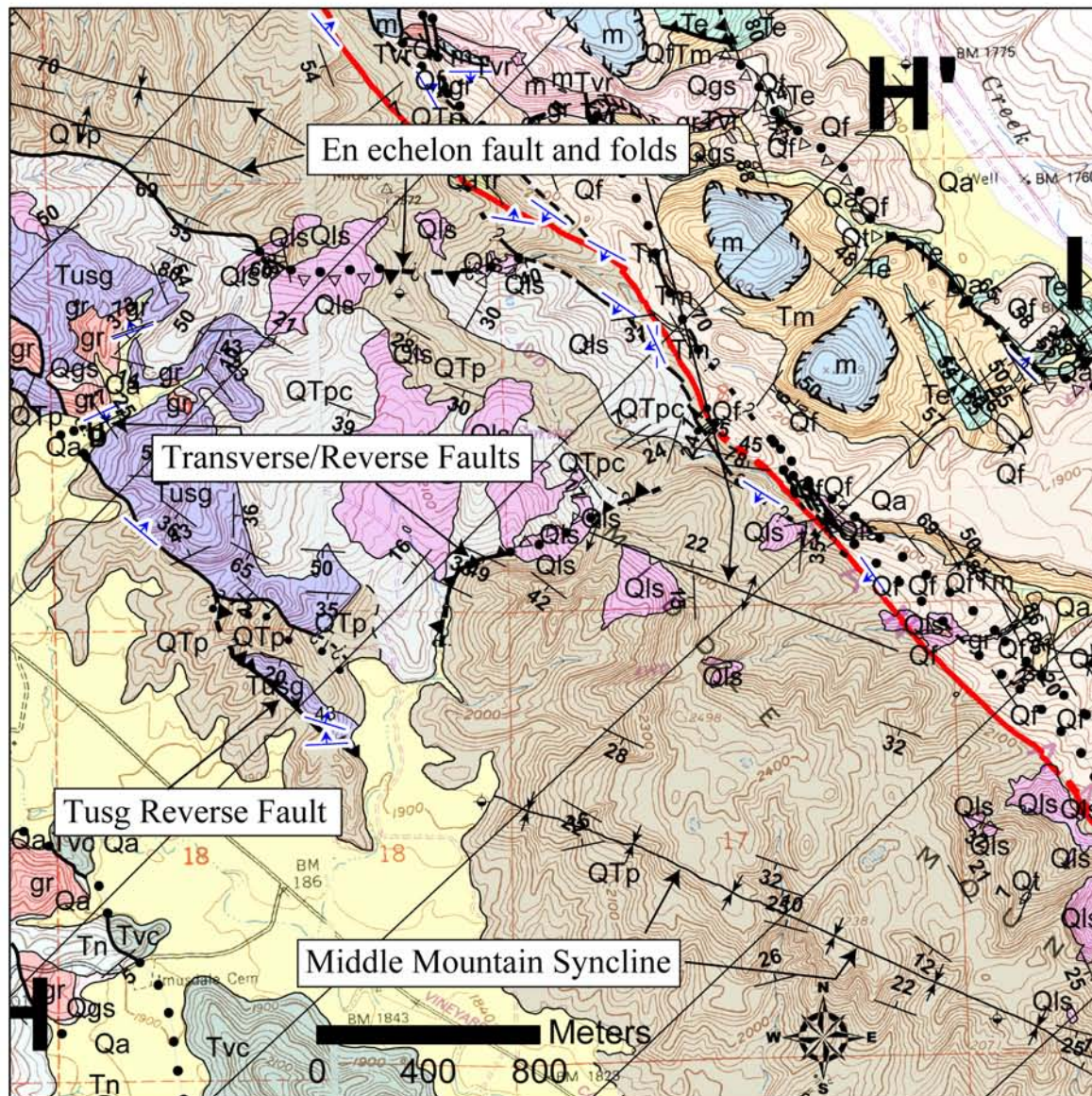


Figure 16. Figure illustrating several structures in the southwestern terrain. The Middle Mountain syncline and three other unnamed folds are interpreted as classic en echelon structures typically found within strike slip fault zones behaving in simple shear. The Tusg reverse fault might be an extension of the active Southwest Fracture Zone (e.g., Brown et al, 1967). Two transverse faults are present within the figure and are likely reverse faults with northwest side up.

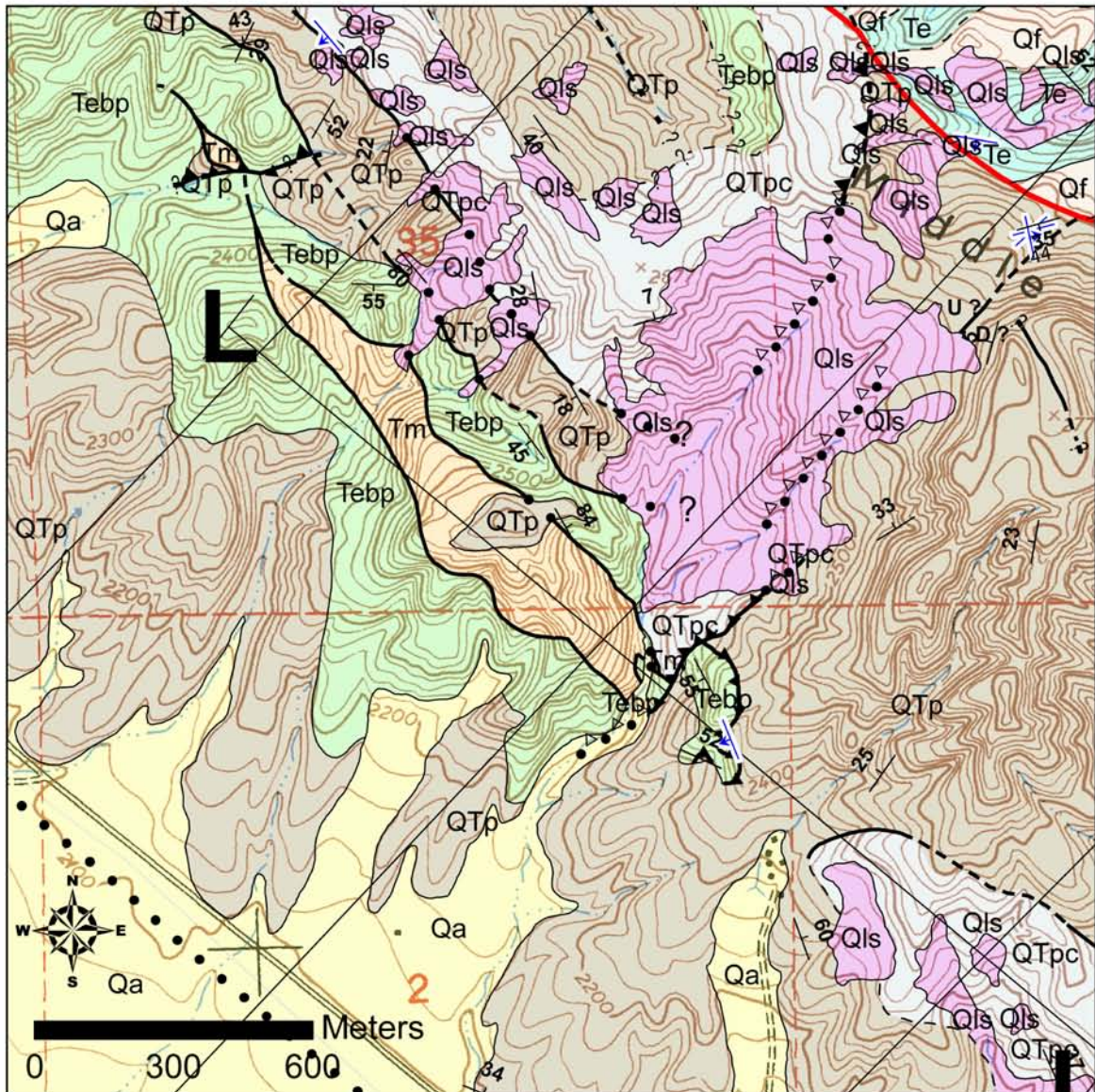


Figure 17. Large reverse fault striking nearly perpendicular to the SAF (shown in red). The fault is likely a high angle reverse fault with Tertiary sedimentary units (Tebp and Tm) being emplaced over the Plio-Pleistocene Paso Robles (QTP). This fault is likely en echelon in geometry, with two small splay faults emanating from the main reverse fault. One separates a Tebp body on the southeast side of the transverse fault, and another is in a distinctive geomorphic saddle denoted by the U? and D? symbology.



Figure 18. Picture looking northwest of an active transverse fault. The right yellow unit is Quaternary alluvium, and the dark brown unit is Paso Robles clay (QTpc). The young alluvium is severely sheared and drag folded. This fault strikes 065° , a 070° difference from the active SAF strike (135°). The cowboy hat and clipboard serve as a scale.

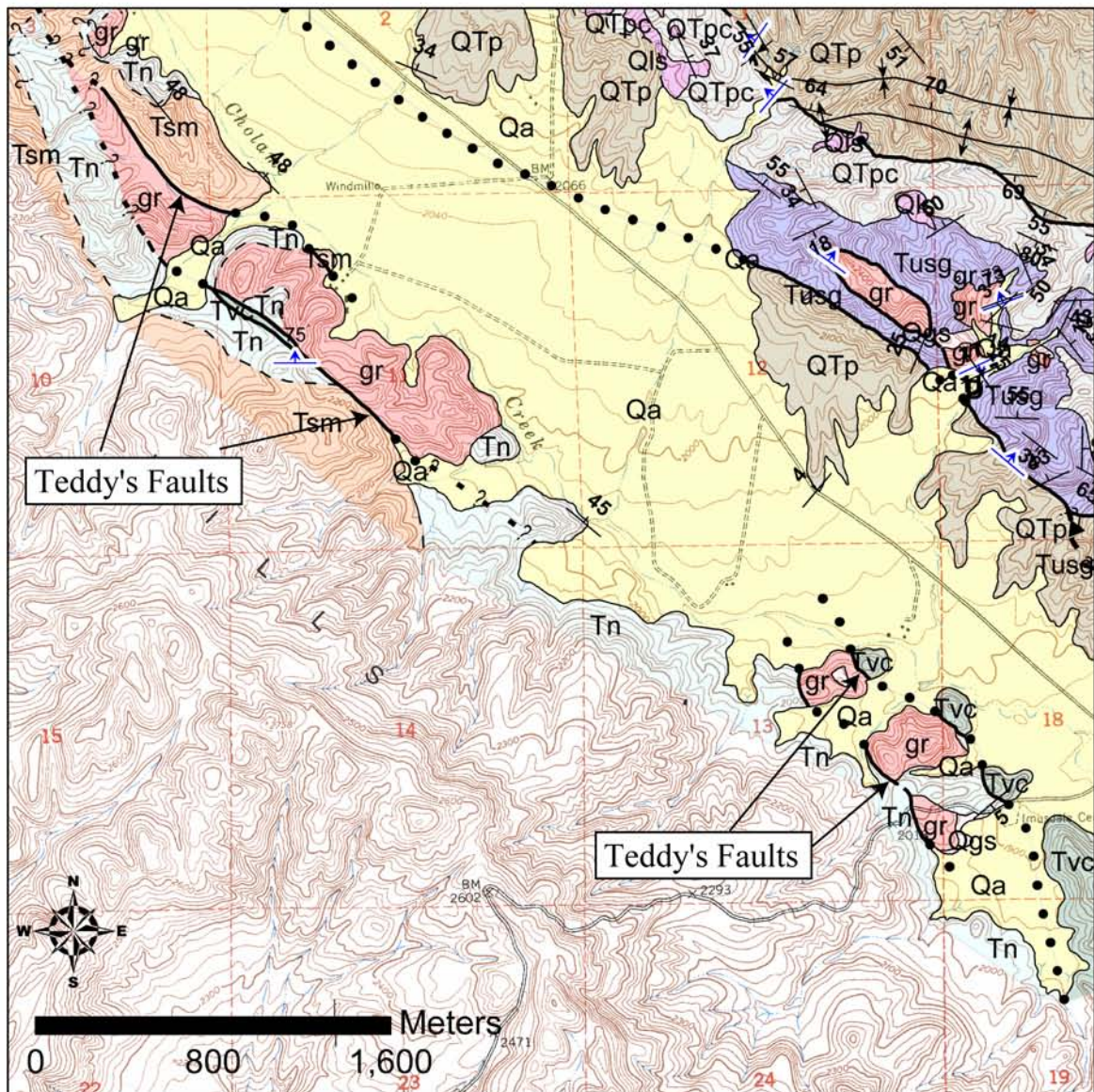
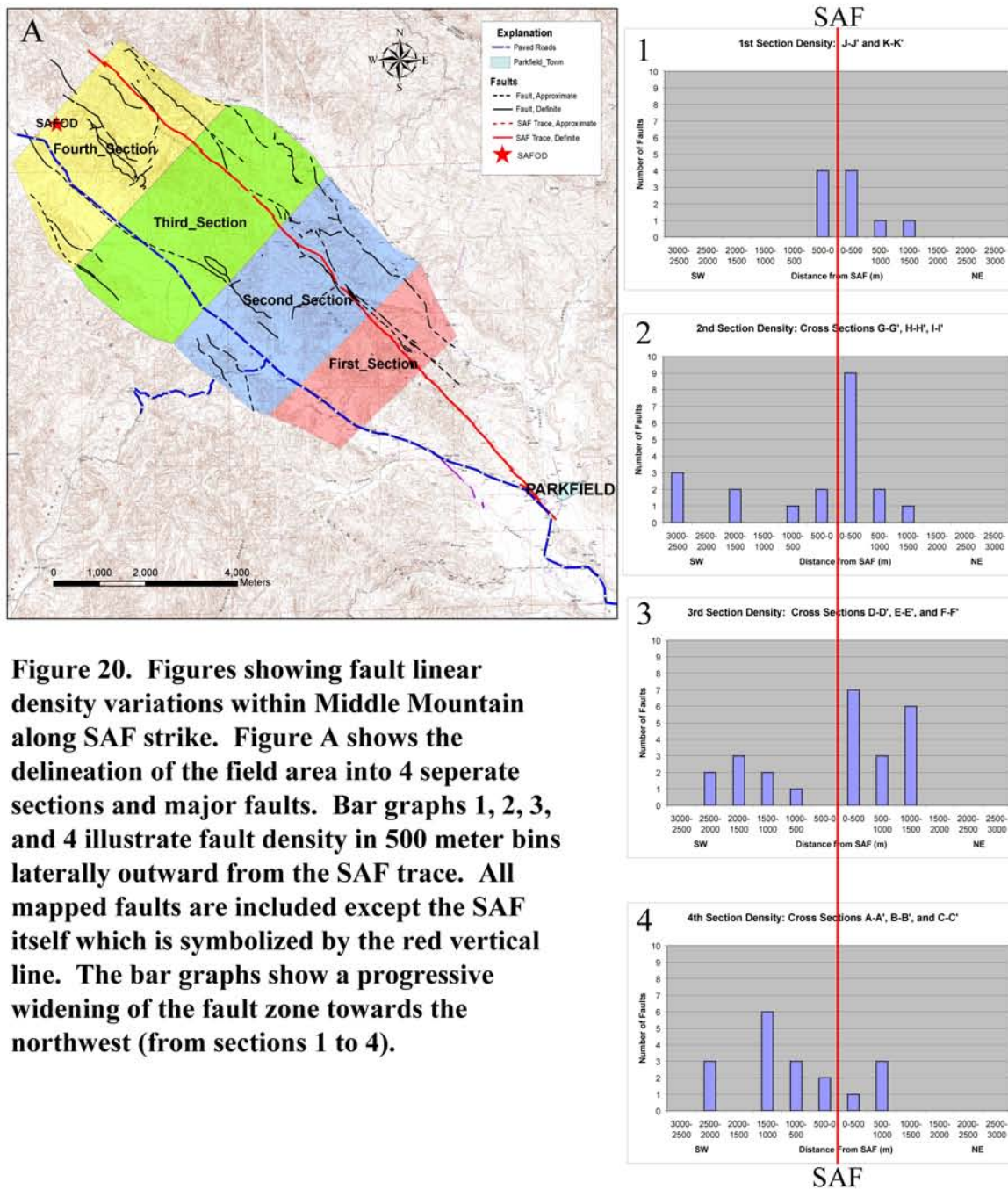


Figure 19. Figure annotating Teddy's faults on the southwestern side of Cholame Creek. These faults cut granite (gr), rhyolitic volcanics (Tvc), and Tertiary sedimentary units (Tn and Tsm). Some are strongly warped.



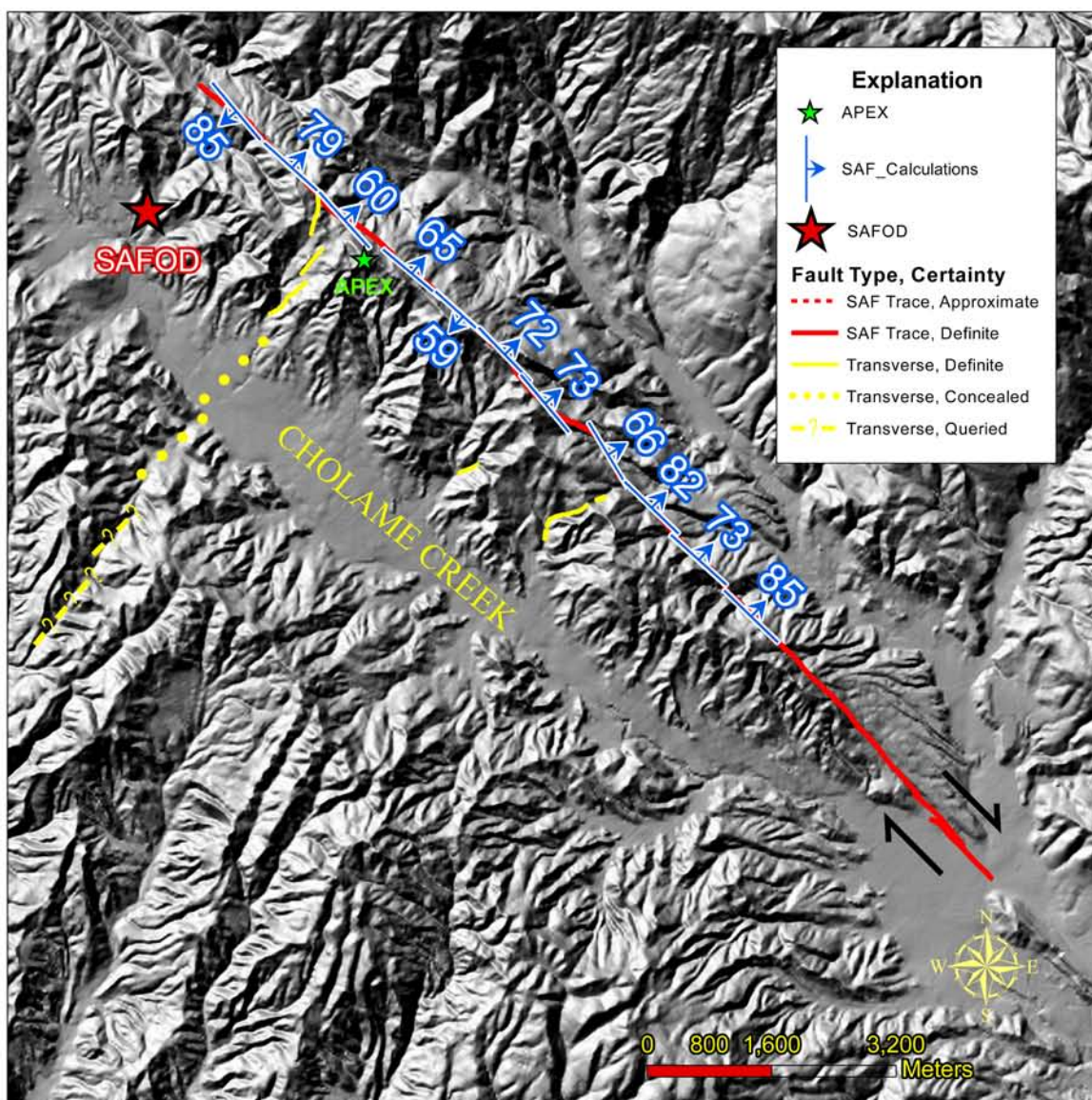


Figure 21. Digital Elevation Model of Middle Mountain with the mapped SAF trace and transverse faults. The location of the APEX and large transverse fault are just northwest of the first southwestern dip (59°) of the SAF at E-E'. The 59° SW dip would theoretically behave as a restraining bend (vertical orientation) and induce compression in the SW block. The APEX and large transverse fault are likely manifestations of the shortening induced from slip along this SAF discontinuity. Secondly, similar lineations on the southwestern side of Cholame Creek seem to match up with the mapped transverse fault on Middle Mountain, suggesting that these structures may be quite large and important. See map explanation for description of features. SAF attitude calculations (from each cross section) are represented by the blue fault symbols (labels are dips).

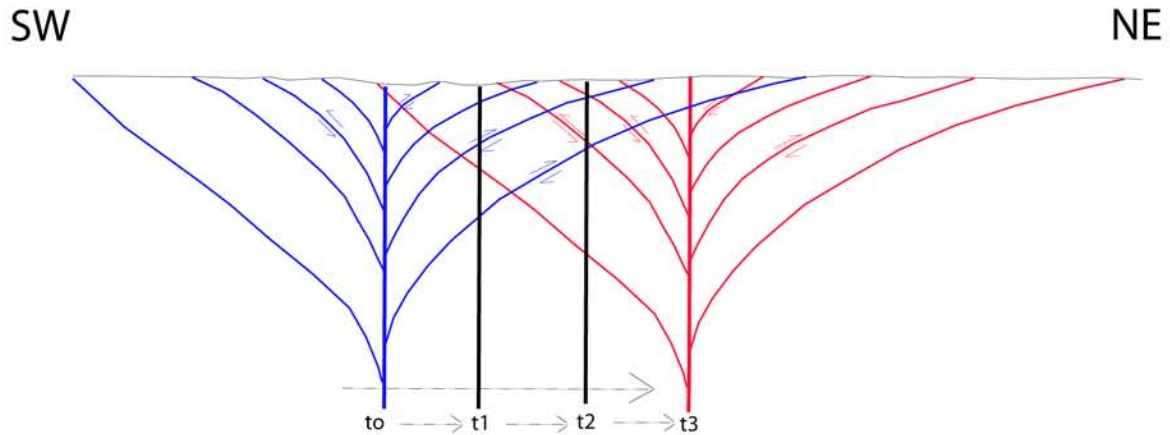


Figure 22. Figure showing a migrating flower structure. The initial (time= t_0) flower structure is noted in blue and the final (time= t_3) flower structure is red. The SAF has been migrating to the NE since the Miocene (Dickinson, 1981), and if a flower structure dominated the crustal deformation throughout the Neogene a scenario like this might be expected. Young faults (red) would be superimposed over older faults (blue) in this scenario and could explain some of the southwestern dipping faults found on southwestern side (SW dipping blue faults). However, relative dating of these southwest dipping faults suggests they likely originated with the current geometries near their current positions.

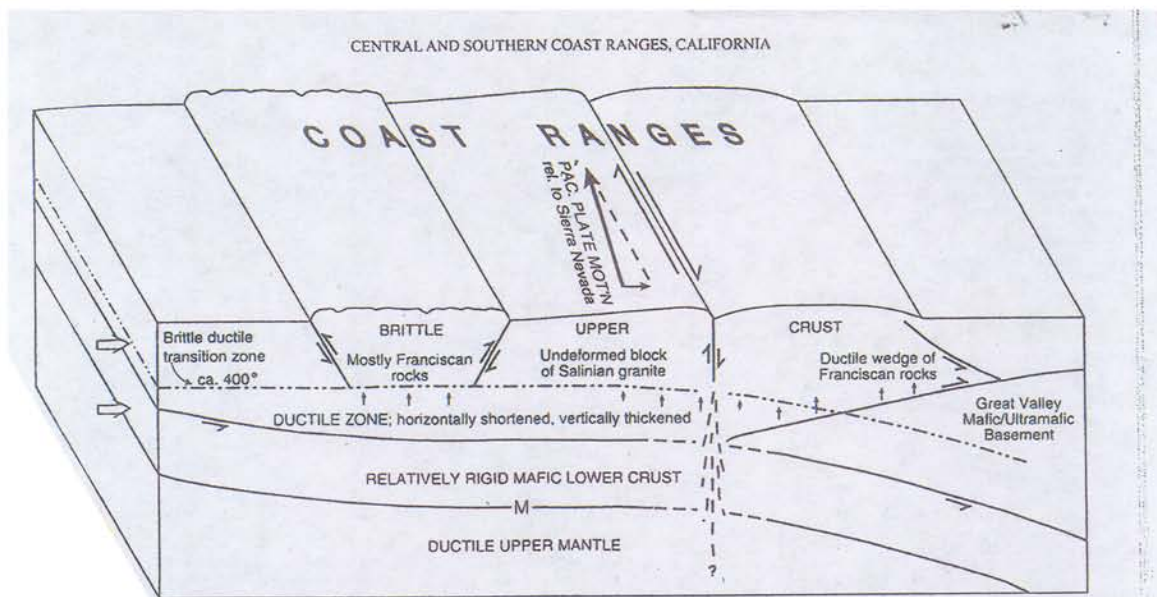
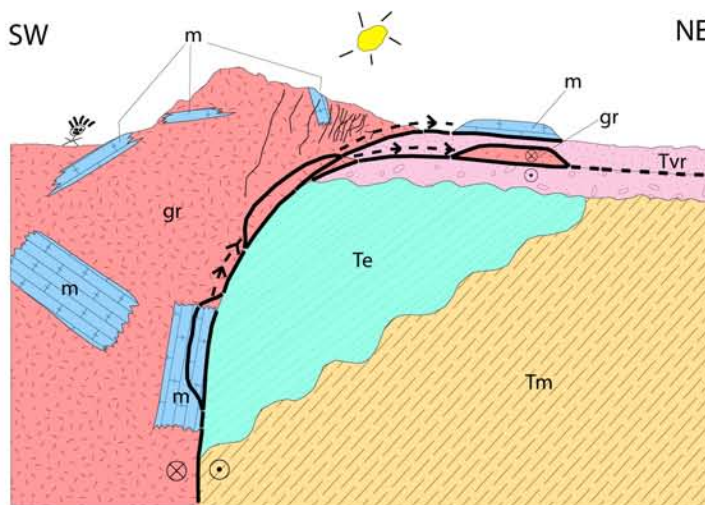


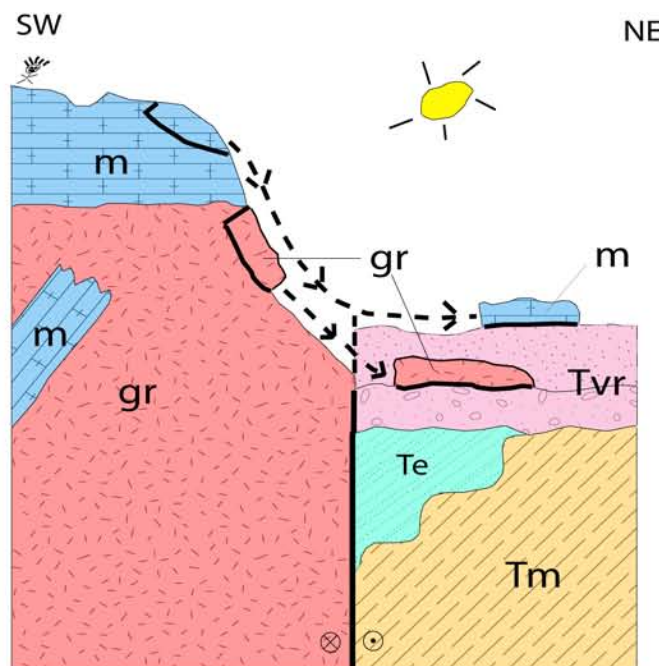
Figure 23. Figure showing different rheological behaviors of the crust in the California Coast Ranges (Page et al, 1998). Upper crust behaves in a brittle manner, the middle crust behaves ductily, and the lower crust deforms with a brittle rheology. The horizontally shortened, vertically thickened ductile middle crust would be capable of accommodating strain from the brittle upper crust. Mapped structures with orientations that dip away from the SAF can merge into this layer rather than severely bending its orientation back around into the SAF. Such crustal discontinuity may discount the flower structure model dominating crustal deformation in central California.



Figure 24. Photograph (looking south) of the Pliocene Varian Ranch formation. Bedding changes within the sandstone facies show clear angular unconformities within the unit, suggesting syntectonic sedimentation. Taken near the F-F' cross section line, just southwest of the numerous faults cutting the Etchegoin unit.



Scenario A:
L-Shaped Thrusts
(dextral/oblique)



Scenario B:
Slide Blocks

Figure 25. Figure illustrating two hypotheses to explain the presence of exotic granite (gr) and marble (m) blocks within the Varian Ranch formation (Tvr). The granite and marble are correlative to a southwestern source and exhibit nearly horizontal basal contacts. Scenario A shows an L-shaped fault that plucks gr/m from depth along a nearly vertical fault plane, then shallows considerably near the surface and emplaces the blocks into the Tvr by oblique slip. Scenario B shows a granitic highland with a marble roof pendant and xenoliths comprising the southwest terrain. Periodic shaking along the oversimplified SAF creates fractures and isolates blocks within the granite and marble bodies. Gravitational forces then move the blocks downward and into the lowlying Tvr unit.

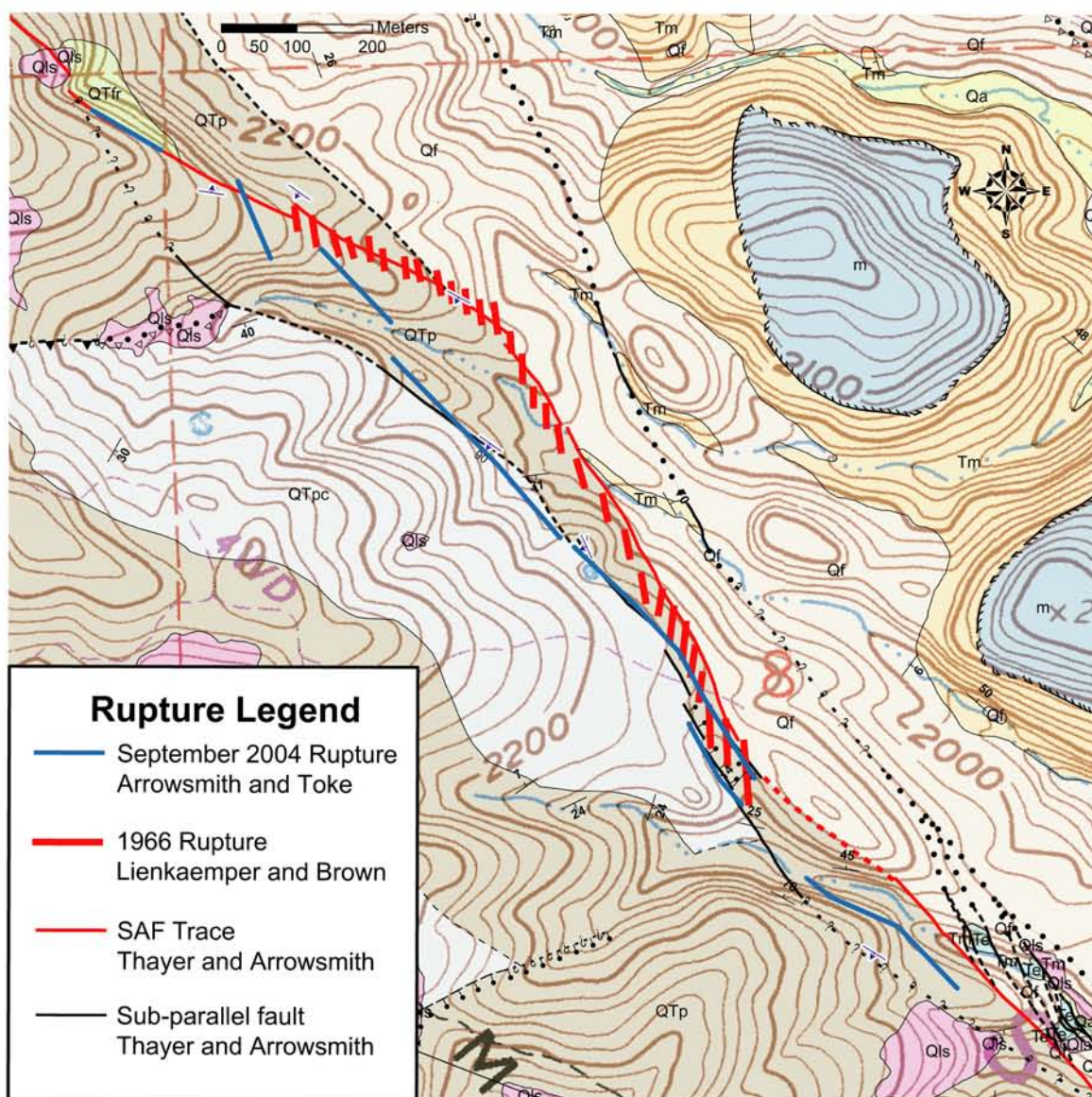


Figure 26. Figure showing rupture variations of the SAF trace over different cycles. The 1966 rupture trace was mapped by Brown et al (1967) and compiled by Lienkaemper and Brown (1985) and is denoted by the red en echelon ticks, the 2004 rupture mapping was conducted by Arrowsmith and Toke and is shown by the blue lines. Both faults were mapped by Thayer and Arrowsmith in the 2004 field season (prior to the EQ) and are denoted by the solid red and black lines. These observations suggest that the active trace may vary in location from rupture to rupture. The 2004 trace is straighter and more consistent with the regional SAF orientation. The more irregular 1966 trace may be less common due to its peculiar dogleg geometry and the 2004 trace's stronger geomorphic features. This behavior may explain the transfer of rocks from the southwestern to the northeastern side and vice versa noted elsewhere on Middle Mountain.

REFERENCES

- Allen, C. R., 1968, The tectonic environments of seismically active and inactive areas along the San Andreas Fault system *in* Proceedings of conference on geologic problems of San Andreas Fault system, (edited by W. R. Dickinson and A. Grantz), Stanford University Publications in the Geological Sciences 11, 70-82.
- Arrowsmith, J R., 1995, Chapter 4, Coupled tectonic deformation and geomorphic degradation along the San Andreas Fault System, PhD. Dissertation, Stanford University, p. 147-186.
- Atwater, Tanya, 1970, Implications of plate tectonics for the Cenozoic tectonic evolution of western North America: Geological Society of America Bulletin, v. 81, no. 12, p. 3513-3536.
- Atwater, Tanya, and Stock, Joann, 1998, Pacific-North America plate tectonics of the Neogene southwestern United States: an update: International Geology Review, v. 40, no. 5, p. 375-402.
- Bakun, W.H., and Lindh, A.G., 1985, The Parkfield, California, earthquake prediction experiment: Science, v. 229, no. 4714, p. 619-623.
- Bakun, W.H., Aagaard, B., Dost, B., Ellsworth, W.L., Hardebeck, J.L., Harris, R.A., Ji, C., Johnston, J.S., Langbein, J., Lienkaemper, J.J., Michael, A.J., Murray, J.R., Nadeau, R.M., Reasenber, P.A., Reichle, M.S., Roeloffs, E.A., Shakal, A., Simpson, R.W., and Waldhauser, F., 2005, Implications for prediction and hazard assessment from the 2004 Parkfield earthquake: Nature, v. 437, p. 969-974.
- Blake, M.C., Campbell, R.H., Dibblee, T.W., Howell, D.G., Nilsen, T.H., Normark, W.R., Vedder, J.G., and Silver, E.A., 1978, Neogene basin formation in relation to plate-tectonic evolution of San Andreas fault system, California: American Association of Petroleum Geologists Bulletin, v. 62, p. 344-372.
- Bramlette, M.N., 1946, The Monterey Formation of California and the Origin of its Siliceous Rocks, USGS Professional Paper 212
- Bridwell, R.J., 1975, Sinuosity of strike-slip fault traces, Geology, v. 3, p. 630-632.
- Brown, R.D., Vedder, J.G., Wallace, R.E., Roth, E.F., Yerkes, R.F., Castle, R.O., Waananen, A.O., Page, R.W., and Eaton, J.P., 1967, The Parkfield-Cholame California, Earthquakes of June-August 1966-Surface Geologic Effects Water-Resources Aspects, and preliminary seismic data: USGS Professional Paper 579.
- Chester, F.M., Evans, J.P., and Biegel, R.L., 1993, Internal Structure and Weakening Mechanisms of the San Andreas Fault: Journal of Geophysical Research, v. 98, p. 771-786.

- Chester, F.M., and Chester, J.S., 1998, Ultracataclasite Structure and Friction Processes of the Punchbowl Fault, San Andreas System, California: *Tectonophysics*, v. 295, p. 199-221.
- Compton, R.R., 1985, *Geology in the Field*, New York: John Wiley & Sons, 398 p.
- Davis, G.H., and Reynolds, S.J., 1996, *Structural geology of rocks and regions*, New York: John Wiley & Sons, 776 p.
- DeMets, Charles, Gordon, R.G., Stein, Seth, and Argus, D.F., 1987, A revised estimate of Pacific-North American motion and implications for western North American plate boundary zone tectonics: *Geophysical Research Letters*, v. 14, no. 9, p. 911-914.
- Dibblee, T.W., Jr., 1973, Regional geologic map of San Andreas and related faults in Carrizo Plain, Temblor, Caliente, and La Panza ranges and vicinity, California: U.S. Geological Survey Map I-757, scale 1:125,000
- Dibblee, T.W., Jr., 1973, Stratigraphy of the Southern Coast Ranges near the San Andreas Fault from Cholame to Maricopa, California: USGS Professional Paper 764.
- Dibblee, T.W., Jr., 1971, Geologic map of the Parkfield Quadrangle *in* Geologic maps of seventeen 15-minute quadrangles (1:62,500) along the San Andreas fault in the vicinity of King City, Coalinga, Panoche Valley, and Paso Robles, California, with index map: USGS Open-File Report 71-0087, 17 sheets, scale 1:62,500.
- Dickinson, W.R., 1966, Structural relationships of San Andreas fault system, Cholame Valley and Castle Mountain Range, California: *Geol. Soc. America Bull.*, v 77, p. 707-719.
- Dickinson, W.R., 1981, Plate tectonics and the continental margin of California, *in* Ernst, W.G., ed., *The geotectonic development of California* (Rubey volume 1): Englewood Cliffs, N.J., Prentice-Hall, p. 1-28.
- Dickinson, W.R., and Snyder, W.S., 1979, Geometry of triple junctions related to San Andreas transform: *Journal of Geophysical Research*, v. 84, no. B2, p. 561-572.
- Dickinson, W.R., Ducea, M., Rosenberg, L.I., Greene, H.G., Graham, S.A., Clark, J.C., Weber, G.E., Kidder, S., Ernst, W.G., Brabb, E.E., 2005, Net dextral slip, Neogene San Gregorio-Hosgri fault zone, coastal California: Geologic evidence and tectonic implications: Geological Society of America Special Paper 391.
- Ellsworth, W.L., Luetger, J.H., Oppenheimer, D.H., 2005, Borehole Array Observations of Non-Volcanic Tremor at SAFOD: *Eos Trans. AGU*, 86(52), Fall Meet Suppl., Abstract T21A-0443

- Emmons, R.C., 1969, Strike-slip rupture patterns in sand models: *Tectonophysics*, v. 7, p. 71-87.
- Evans, J.P., Moore, D.E., Kirschner, D., Solum, J.G., 2005, Lithologic Characterization of the Deep Portion of the SAFOD Drillhole: *Eos Trans. AGU*, 86(52), Fall Meet Suppl., Abstract T21A-0450.
- Galehouse, Jon S., 1967, Prevalence and Paleocurrents of the Paso Robles Formation, California: *Geological Society of America Bulletin*, v. 78, p. 951-978.
- Harding, T.P., 1976, Tectonic significance and hydrocarbon trapping consequence of sequential folding synchronous with San Andreas faulting, San Joaquin Valley, California: *American Association of Petroleum Geologists Bulletin*, v. 58 (7), p. 356-378.
- Hearn, T.M., and Clayton, R.W., 1986, Lateral velocity variations in southern California: *Seismological Society of America Bulletin*, v. 76, p. 495-520.
- Hickman, S., and M.D. Zoback (2004), Stress orientations and magnitudes in the SAFOD Pilot Hole: *Geophysical Research Letters*, 31, L15S12, doi:10.1029/2004GL020043.
- Hickman, S., Zoback, M., Ellsworth, W., 2004, Introduction to special section: Preparing for the San Andreas Fault Observatory at Depth: *Geophysical Research Letters*, vol. 31, L12S01, doi: 10.1029/2004GL020688, 2004.
- Hickman, S., Zoback, M., Ellsworth, W., 2005, Structure and Composition of the San Andreas Fault Zone at Parkfield: Initial Results from SAFOD Phases 1 and 2: *Eos Trans. AGU*, 86(52), Fall Meet. Suppl., Abstract T23E-05.
- Irwin, W.P., 1990, *Geology and Plate-Tectonic Development in* Wallace, R.E., 1990, *The San Andreas Fault System, California*, USGS Professional Paper 1515.
- Langbein, J.O., Burford, R.O., Slater, L.E., 1990, Variations in fault slip and strain accumulation at Parkfield, California: Initial results using two-color geodimeter measurements, 1984-1988: *Journal of Geophysical Research*, v. 95, no. B3, p. 2533-2552
- Lawson, A.C., chairman, 1908, *The California earthquake of April 18, 1906: Report of the State Earthquake Investigation Commission: Carnegie Institution of Washington Publication 87, 2 v.*
- Lienkaemper, J. J., and Brown, R. D., 1985, Map of faulting accompanying the 1966 Parkfield, California, earthquake, U.S. Geological Survey Open File Report, 85-661.

- Loomis, Karen B., 1989, Lithofacies and Depositional Environments of Etchegoin Group: Model for Late Neogene Sedimentation in Western San Joaquin Basin: AAPG Bulletin, vol. 73, no. 4., p 544.
- Matthews, V., III, 1973, Pinnacles-Neenach correlation; A restriction for models of the origin of the Transverse Ranges and the big bend of the San Andreas fault: Geological Society of America Bulletin, v. 84, p. 683-688.
- Matthews, Vincent, III, 1976, Correlation of Pinnacles and Neenach Volcanic Formations and their bearing on San Andreas fault problem: American Association of Petroleum Geologists Bulletin, v. 60, no. 12, p. 2128-2141.
- McClay, Ken, and Bonora, Massimo, 2001, Analog models of restraining stopovers in strike-slip fault systems: AAPG Bulletin, v. 85, no. 2, p. 233-260.
- Minster, J.B., and Jordan, T.H., 1987, Vector constraints on western U.S. deformation from space geodesy, neotectonics, and plate motions: Journal of Geophysical Research, v. 92, no. B6, p. 4798-4804.
- Murray, J., and Langbein, J., in press, Slip on the San Andreas Fault at Parkfield, California over two earthquake cycles and the implications for seismic hazards: BSSA
- Nadeau, R.M., Michelini, A., Uhrhammer, R.A., Dolenc, D., McEvilly, T.V., 2004, Detailed kinematics structure and recurrence of micro-seismicity in the SAFOD target region: Geophysical Research Letters, vol. 31, L12S08, doi: 10.1029/2003GL019409
- Page, B.M., 1981, The southern Coast Ranges, *in* Ernst, W.G., ed., The geotectonic development of California (Rubey volume 1): Englewood Cliffs, N.J., Prentice-Hall, p. 329-417.
- Page, B.M., Thompson, G.A., Coleman, R.G., 1998, Late Cenozoic tectonics of the central and southern Coast Ranges of California: Geological Society of America Bulletin, v 110, no. 7, p. 846-876.
- Park, R.G., 1997, Foundations of structural geology, London; New York: Chapman & Hall, 202 p.
- Pisciotta, K.A., Garrison, R.E., 1981, Lithofacies and depositional environments of the Monterey Formation, California *in* The Monterey Formation and related siliceous rocks of California: Society of Economic Paleontologists and Mineralogists, p. 97-112.

- Ross, D.C., 1970, Quartz Gabbro and Anorthositic Gabbro: Markers of Offset along the San Andreas Fault in the California Coast Ranges: Geological Society of America Bulletin, v. 81, p. 3647-3662.
- Ryberg, T., Fuis, G.S., Bauer, K., Hole, J.A., Bleibinhaus, F., 2005, Upper-Crustal Reflectivity of the Central California Coast Range Near the San Andreas Fault Observatory at Depth (SAFOD), USA: *Eos Trans. AGU*, 86(52), Fall Meet Suppl., Abstract T21A-0441
- Ryder, R.T., and Thomson, A., 1989, Tectonically controlled fan delta and submarine fan sedimentation of late Miocene age, Southern Temblor Range, California: USGS Professional Paper 1442.
- Rymer, M.J., Tinsley, J.C., Treiman, J.A., Arrowsmith, J.R., Clahan, K.B., Rosinski, A.M., Bryant, W.A., Snyder, H.A., Fuis, G.S., Toke, N., Bawden, G.W., in press, Surface fault slip associated with the 2004 Parkfield, California earthquake: BSSA
- Scholz, C.H., 2000, Evidence for a strong San Andreas fault: *Geology*, v.28, no.2, p. 163-166.
- Sieh, K.E., and Jahns, R.H., 1984, Holocene activity of the San Andreas fault at Wallace Creek, California: Geological Society of America Bulletin, v. 95, no. 8, p. 883-896.
- Sims, J.D., 1988, Geologic map of the San Andreas Fault in the Cholame Hills and Cholame Valley 7.5 Minute Quadrangle, Monterey County, California: USGS Miscellaneous Field Studies Map MF-1995, scale 1:24,000.
- Sims, J.D., 1990, Geologic map of the San Andreas Fault in the Parkfield 7.5-Minute Quadrangle, Monterey and Fresno Counties, California: USGS Miscellaneous Field Studies Map, scale 1:24,000.
- Sims, J.D., 1993, Chronology of displacement on the San Andreas fault in central California: Evidence from reversed positions of exotic rock bodies near Parkfield, California: Geological Society of America Memoir 178.
- Solum, J.G., Hickman, S.H., Lockner, D.A., Moore, D.E., 2005, Mineralogy of the SAFOD Main Hole: Detailed characterization of fault and country rocks: *Eos Trans. AGU*, 86(52), Fall Meet Suppl., Abstract T24B-01.
- Stone, D.S., 1995, Structure and kinematic genesis of the Quealy wrench duplex: transpressional reactivation of the Precambrian Cheyenne belt in the Laramie basin, Wyoming: AAPG Bulletin, v. 79, p. 1349-1376.
- Sylvester, A.G., Smith, R.R., 1976, Tectonic Transpression and Basement-Controlled Deformation in San Andreas Fault Zone, Salton Trough, California: American Association of Petroleum Geologists Bulletin, v. 60, no. 12, p. 2081-2102.

- Sylvester, A.G., 1979, Guide to the geology and structures of Painted Canyon, Mecca Hills: National Association of Geology Teachers, Palm Desert, California, United States (USA), p. 378-387.
- Sylvester, A.G., 1988, Strike-slip faults: Geological Society of America Bulletin, v. 100, p.1666-1703.
- Stone, E.M., 2000, Geomorphology, structure, and paleoseismology of the central Cholame segment, Carrizo Plain, California: M.S. Thesis, Arizona State University, p. 1-100.
- Thatcher, W., 1990, Present-day crustal movements and the mechanics of cyclic deformation *in* Wallace, R.E., 1990, The San Andreas Fault System, California, USGS Professional Paper 1515.
- Titus, S.J., DeMets, C., Tikoff, B., 2005, New slip rate estimates for the creeping segment of the San Andreas fault, California: *Geology*, v. 33, no. 3, p. 205-208.
- Toké, N.A., Arrowsmith, J.A., in review, Reassessment of a surface slip budget along the Parkfield segment of the San Andreas fault, BSSA.
- Turner, D.L., Curtis, G.H., Berry, F.A.F., and Jack, R.N., 1970, Age relationships between the Pinnacles and Parkfield felsites and felsite clasts in the southern Temblor Range, California; Implications for San Andreas fault displacement: Geological Society of America Abstracts with Programs, v. 2, p. 154.
- Wakabayashi, J., 1999, Distribution of displacement on and evolution of a young transform fault system: The northern San Andreas fault system, California: *Tectonics*, v. 18, no. 6, p. 1245-1274.
- Wallace, R.E., 1949, Structure of a portion of the San Andreas Rift in Southern California: Geological Society of America Bulletin, v. 60, p. 781-806.
- Wallace, R.E., 1990, The San Andreas Fault System, California: USGS Professional Paper 1515.
- Willis, B., 1938, San Andreas rift, California: *Journal of Geology*, v. 46, p. 793-827.
- Wilcox, R.E., Harding, T.P., and Seely, D.R., 1973, Basic wrench tectonics: American Association of Petroleum Geologists Bulletin, v. 57, p. 74-96.
- Wright, T.L., 1991, Structural geology and tectonic evolution of the Los Angeles basin, California *in* K.T. Biddle, ed., Active margin basins: AAPG Memoir 52, p. 35-130.

Zoback, M.D., Zoback, M.L., Mount, V., Suppe, J., Eaton, J., Healy, J., Oppenheimer, D., Reasonberg, P., Jones, L., Raleigh, B., Wong, I., Scotti, O., and Wentworth, C., 1987, New evidence on the state of stress of the San Andreas fault system: *Science*, v. 238, p. 1105-1111.

Zoback, M.D., Hickman, S.H., 2005, Preliminary Observations of Stress and fluid pressure in and near the San Andreas Fault at depth in the SAFOD boreholes: *Eos Trans. AGU*, 86(52), Fall Meet Suppl., Abstract T21A-0438.